CAE ANALYSIS, OPTIMIZATION AND FABRICATION OF TU 2014 FORMULA SAE VEHICLE STRUCTURE

A Dissertation submitted in partial fulfillment of the requirement

for the award of the degree of

MASTER OF ENGINEERING

IN

CAD/CAM ENGINEERING

Submitted By

SAHIL KAKRIA

Roll No: 801281019

Under the guidance of

Mr. DALJEET SINGH

Assistant Professor, MED

DEPARTMENT OF MECHANICAL ENGINEERING

THAPAR UNIVERSITY (TU), PATIALA

PUNJAB - 147004, INDIA

JULY 2014

This Thesis is dedicated to

My Respected Parents, Thesis Guide &

Team Fateh (TU Formula Student team)

CERTIFICATE

I hereby declare that work done in this Thesis Report entitled, **"CAE ANALYSIS, OPTIMIZATION AND FABRICATION OF TU 2014 FORMULA SAE VEHICLE STRUCTURE"** submitted towards partial fulfillment of requirement for award of **Master of Engineering** degree in **CAD/CAM Engineering** in **Mechanical Engineering Department** of **Thapar University, Patiala** is an authentic record of work carried out by me under the supervision and guidance of **Mr. DALJEET SINGH**, Assistant Professor of Mechanical Engineering Department, Thapar University, Patiala.

This matter embodied in this report has not been submitted in part or full to any other university or institute for the award of any degree.

Sahil Kakria

Date: 14/07/2014

SAHIL KAKRIA

(801281019)

This is to certify that the above statement made by the student concerned is correct to the best of my knowledge and belief.

Mr. DALJEET SINGH
Assistant Professor
Mechanical Engineering Department (MED)
Thapar University, Patiala

Countersigned by:

Dr. AJAY BATISH
Professor & Head (MED)
Thapar University, Patiala

Dr. S.K. MOHAPATRA
Dean of Academic Affairs
Thapar University, Patiala

ACKNOWLEDGEMENT

Pursuing ME in CAD/CAM Engineering and being a part of Team Fateh was one of the most valuable and exciting experiences in my education. The knowledge and practical experience gained during the study years will be beneficial throughout my life.

I take the opportunity to express my heartfelt adulation and gratitude to my Thesis supervisor, **Mr. Daljeet Singh** for his unreserved guidance, constructive suggestions and thought provoking discussions in the nurturing work. He has been very kind and patient while working on the details of this project and sharing his invaluable experience and advice.

I want to sincerely thank **Dr. Ajay Batish**, Professor and Head, Mechanical Engineering Department, Thapar University, Patiala for giving the opportunity & believing in me to work on this Thesis project and providing the adequate facilities & infrastructure required for the fabrication work. His unabashed inspiration and moral support went a long way in successful completion of the work.

I do not find enough words with which I can express my sincere gratitude to all the members of **Team Fateh** (Formula Student team of Thapar University, Patiala) for extending their whole hearted co-operation throughout the development of this work.

I am grateful to the entire faculty and staff of Mechanical Engineering Department, Thapar University, Patiala for their guidance during the course of my study.

Most importantly and with deep sense of gratitude, I am greatly indebted to my Parents for motivating and inspiring me to believe in my abilities. Their warm blessings, unconditional support & continuous encouragement fostered my confidence and proved instrumental in the successful completion of this Thesis work.

SAHIL KAKRIA

PREFACE

The development of sports cars awakened the interest of many enthusiasts and specialists in the automobile engineering area during the last few decades. Consequently, their demand motivated the competition between manufacturers from all over the world to dominate international markets. Formula SAE competition offers teams of university students to practically take part in the world competition. The key factors to compete in international sports car markets are high performance, well power/weight ratio, good drivability, maneuverability, stability, comfort and security.

To achieve a rigid and lightweight structure is the objective of a sports car design. The above mentioned vehicle performance factors are highly dependent upon a well-designed chassis. A number of factors influence the decisions that the teams make when formulating their design, these include the normal performance factors of weight, stiffness and cost. The most effective strategy should consider both the weight reduction and the increase of chassis stiffness.

The FSAE competition provides great platform to engineering students to improve their skills. Challenges faced in this series truly test the knowledge, creativity and imagination of every university race team, providing a great environment for young engineers to gain experience and wisdom. Although as the FSAE encourages students to do most of the hands on manufacturing work, if not all of the construction of the car themselves, elements such as team experience, knowledge sharing and confidence building are also the major learning during the FSAE project.

PROJECT SUMMARY

This report examines the work done during the Thesis project as a part of the M.E. course curriculum at Thapar University (TU), Patiala.

The objective of the Thesis project is to design & develop FSAE vehicle structure for the year 2014, better than the similar structures designed previously for Thapar University, Patiala as part of Team Fateh for participating in Formula student vehicle design competition held internationally. The focus is to achieve a rigid & lightweight design for TU FSAE 2014 vehicle structure with high stability.

The Thesis work started with the study & model building of various subsystems in the TU FSAE vehicle like Double wishbone push rod type Front & Rear Suspension, Rack and pinion type steering system & Space frame type tubular steel chassis. This was followed by analysis & study of the characteristics of the subsystems in the TU FSAE vehicle like roll center for suspension & stiffness/weight for chassis frame.

The MBD models of TU FSAE Front & Rear Suspension (2012 & 2014 vehicles) were prepared from the hardpoints extracted from CAD models & were used for carrying out kinematic analysis (suspension wheel travel) to calculate the respective roll centers.

The FE models of TU FSAE Chassis (2011, 2012 & 2014) were prepared using Hypermesh by meshing the frames and applying boundary conditions. The models were used for determination of mode shapes, natural frequencies by carrying out normal modes analysis and for calculating chassis stiffness by carrying out linear static analysis.

As the Roll center & Torsion stiffness are the two most important quantifiable aspects to the suspension & chassis (respectively) of any race car, their evaluation at subsystem level is essential to analyze the performance of the TU FSAE vehicles. The comparison & improvements in these characteristics of TU FSAE 2014 vehicle over 2011 & 2012 vehicles (all of them being space frame structures) has been presented.

Further, the Topology optimization carried out (using input loads from MBD analysis) on various components of TU FSAE 2014 vehicle like Front & Rear suspension Uprights and Chassis Bulkhead and the resultant weight reduction has been described.

Finally, the Fabrication of the final design of the frame has been carried out and presented as part of TU FSAE 2014 vehicle structure development.

TABLE OF CONTENTS

LIST OF FIGURES

LIST OF TABLES

LIST OF ABBREVIATIONS USED

TU	:	Thapar University
MED	:	Mechanical Engineering Department
TUFF	:	Thapar University Formula Force
FSAE	:	Formula SAE
FS	:	Formula Student
FSG	:	Formula Student Germany
FSI	:	Formula Student India
CAE	:	Computer Aided Engineering
MBD	:	Multi Body Dynamics
FEA	:	Finite Element Analysis
SPC	:	Single Point Constraint
DOF	:	Degrees of freedom
LCA	:	Lower Control arm
UCA	:	Upper Control arm

CHAPTER 1

INTRODUCTION

1.1 COMPUTER AIDED ENGINEERING (CAE)

CAE is the usage of computer software to aid in engineering tasks. CAE tools are very widely used to analyze the robustness and performance of components and assemblies. CAE systems are major providers of information to help support design teams in decision making. In fact, their use has enabled reduction in development cost and time while improving the safety, comfort and durability of the vehicles. The predictive capability of CAE tools has progressed to the point where much of the design verification is now done using computer simulations rather than physical prototype testing every time. Several iterations can be done with the help of virtual simulation to reduce the no. of prototypes and the final product can be tested physically.

Computer Aided Engineering includes the following applications:

- Stress analysis on components and assemblies using Finite Element Analysis.
- Thermal and fluid flow analysis using Computational fluid dynamics (CFD).
- Multibody dynamics (MBD) & Kinematics.
- Analysis tools for process simulation such as casting & die press forming.
- Optimization of the product or process.

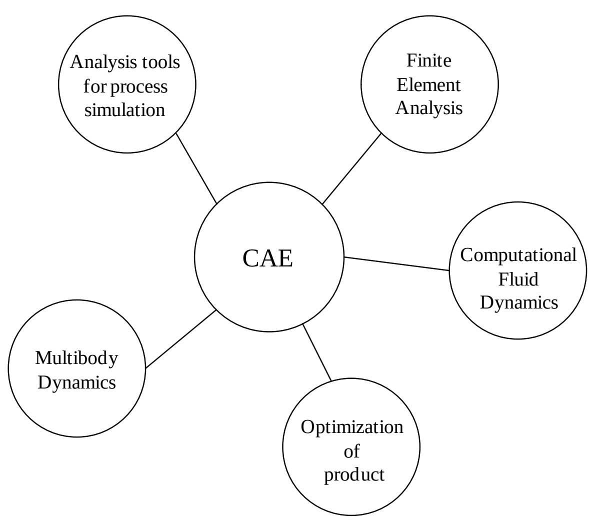

Fig 1.1: CAE Domain

1.1.1 Finite Element Method (FEM)

The Finite Element Method (FEM) (sometimes referred to as finite element analysis) is a numerical technique for finding approximate solutions of partial differential equations (PDE) as well as of integral equations. The solution approach is based either on eliminating the differential equation completely (steady state problems), or rendering the PDE into an approximating system of ordinary differential equations, which are then numerically integrated using standard techniques such as Euler's method, Runge-Kutta, etc.

In solving partial differential equations, the primary challenge is to create an equation that approximates the equation to be studied, but is numerically stable, meaning that errors in the input data and intermediate calculations do not accumulate and cause the resulting output to be meaningless.

For structures under static loading, the basic finite element equation that is solved can be expressed as,

$$\mathbf{Kd=f}$$

where **K** is the effective stiffness matrix of the structure, **d** is the displacement vector, and **f** is the load vector as applied to the structure. This equation is often referred to as the matrix equivalent form of the Bubnov-Galerkin equation, and it represents equilibrium of external and internal forces. Once the unknown nodal displacements are solved for, Hooke’s law can be used to calculate the material stresses for deformations in the elastic range. Hooke’s Law can be stated as

$$\boldsymbol{\sigma}=\mathbf{C}\boldsymbol{\varepsilon}$$

where $\boldsymbol{\sigma}$ is the stress vector, **C** is the material elasticity matrix, and $\boldsymbol{\varepsilon}$ is the strain vector.

Finite Element Analysis was first developed over 60 years ago as a method to accurately predict the reaction of complex parts to various inputs. Prior to the development of FEA the only way to validate a design or test a theory was to physically test a part. This was and still is both time consuming and expensive. Now, FEA can drastically reduce the time and money spent on intermediate stages and concepts.

FEA is comprised of three major phases explained below:

1. Pre-Processing

In which the analyst develops a finite element mesh to divide the subject geometry into sub domains for mathematical analysis, and applies material properties and boundary conditions.

2. Solution

During which the program derives the governing matrix equations from the model and solves for the primary quantities.

3. Post-Processing

In which the analyst checks the validity of the solution, examines the values of primary quantities (such as displacements and stresses) and based on the observations provides suitable countermeasures.

1.1.2 Multibody Dynamics (MBD)

A multibody dynamic (MBD) system is one that consists of solid bodies, or links, that are connected to each other by joints that restrict their relative motion. The study of MBD is the analysis of how mechanism systems move under the influence of forces, also known as forward dynamics. A study of the inverse problem, i.e. what forces are necessary to make the mechanical system move in a specific manner is known as inverse dynamics.

MBD system is used to model the dynamic behavior of interconnected rigid or flexible bodies, each of which may undergo large translational and rotational displacements. In MBD, system degrees of freedom & constraint conditions play a major role.

Motion analysis is important because product design frequently requires an understanding of how multiple moving parts interact with each other and their environment. From automobiles and aircraft to washing machines and assembly lines - moving parts generate loads that are often difficult to predict. Complex mechanical assemblies present design challenges that require a dynamic system-level analysis to be met. Motion analysis enables one to meet these challenges by quickly evaluating and improving designs for important characteristics like performance, safety and comfort.

Terminologies in MBD:

Some of the terminologies in MBD are explained below:

<u>Degree of freedom</u>:

The degrees of freedom denote the number of independent kinematical possibilities to move. A rigid body has six degrees of freedom in the case of general spatial motion, three of them translational degrees of freedom and three rotational degrees of freedom. In the case of planar motion, a body has only three degrees of freedom with only one rotational and two translational degrees of freedom.

<u>Constraint condition</u>:

A constraint condition implies a restriction in the kinematical degrees of freedom of one or more bodies. The classical constraint is usually an algebraic equation that defines the relative translation or rotation between two bodies.

These are of two types:

1. Joint constraint – applied between two bodies
2. Motion constraint – applied on a joint

A ***joint*** is the connection of two or more bodies, or a body with the ground. It is a constraint that restricts degrees of freedom between two bodies by constraining the relative motion of the bodies. It can be of following types:

1. <u>Prismatic/Translational/Sliding joint</u>: single DOF joint which allows relative displacement along one axis, constrains relative rotation; implies 5 kinematical constraints.
2. <u>Revolute joint</u>: single DOF joint which allows only one rotation about an axis; implies 5 kinematical constraints
3. <u>Cylindrical Joint</u>: 2-DOF joint which allows one rotation & one translation about an axis.

4. Spherical joint: 3-DOF joint which allows all three rotations, constrains relative displacements in one point; implies 3 kinematical constraints
5. Hooke's joint: 2-DOF joint in which relative rotation along 2 axes is allowed, 1 rotation and all displacement axes are constrained; implies 4 kinematical constraints.
6. Fixed/Lock joint: 0 DOF joint which constrains all relative displacements and rotations. It is used to ground a part or lock two parts together; implies 6 kinematical constraints.

A ***motion*** is a constraint that restricts the way joint moves. It can be following types depending on the joint on which it is applied:

1. Translational motion – applied on translational or cylindrical joint
2. Rotational motion – applied on revolute or cylindrical joint

1.2 OVERVIEW OF SOFTWARE TOOLS USED

The software used for doing the FEA and MBD analysis are mentioned as follows:

1.2.1 Altair Hypermesh

Altair HyperMesh is a part of Altair Hyperworks. It is a high-performance finite element (FE) pre and post-processor for major finite element solvers, which allows engineers to analyze design conditions in a highly interactive and visual environment. Hyper Mesh's user interface is easy to learn and supports the direct use of CAD geometry and existing finite element models, providing robust interpolation and efficiency. Advanced automation tools within Hyper Mesh allow users to optimize meshes from a set of quality criteria, change existing meshing through morphing, and generate mid-surfaces from models of varying thickness.

The application of Hypermesh in FEA is depicted in the following flowchart:

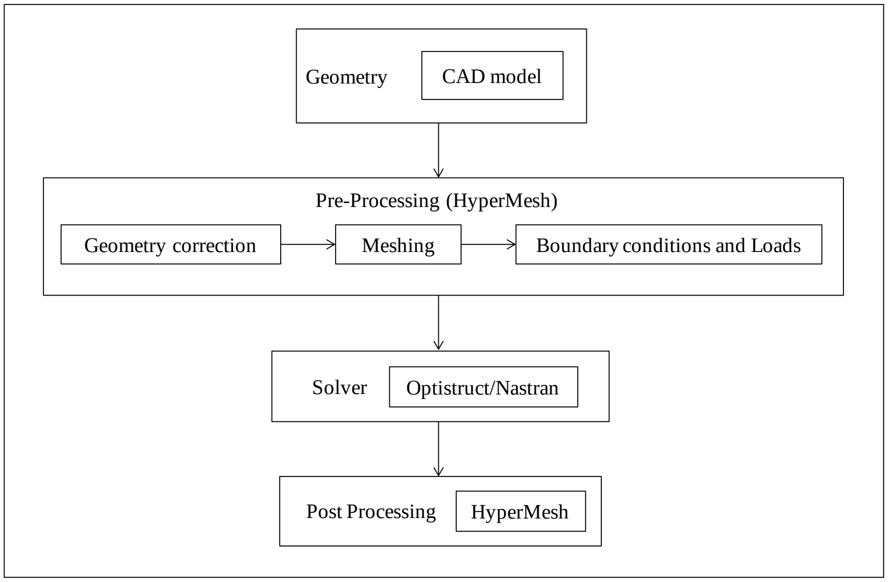

Fig 1.2: FEA Process methodology

1.2.2 Altair Optistruct

The main program used for performing finite element analyses and optimizations is the solver Optistruct from Altair Engineering. Optistruct started out as a research code at a university research lab in 1991. The only problem solved was the minimization of weighted compliance and/or eigen-frequencies using the homogenization method. In 1993 the first commercial version was marketed as Altair Optistruct 1.0. Optistruct do not have any graphical interface, the full problem formulation is made using HyperMesh and any other options are supplied via the command line. The solver was used not only for linear static & modal analysis but also to carry out structural optimization.

Summarizing the workflow in Altair Hyperworks, HyperMesh is the preprocessor which is used to discretize (mesh) a CAD model, set boundary conditions, properties and options and to set up the problem to be solved (optimization, static analysis, modal analysis etc.). From HyperMesh, a file which completely describes the problem is exported and then processed using Optistruct. The results from Optistruct can then be evaluated using the postprocessor HyperView (or Hypermesh).

As HyperMesh, Optistruct and HyperView are all part of the software suite Hyperworks, they are designed to easily integrate with each other. The workflow in Altair Hyperworks module is as shown.

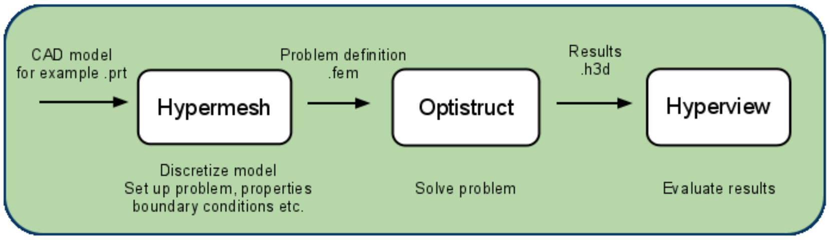

Fig 1.3: An overview of the workflow in Hyperworks

1.2.3 MSC NASTRAN

NASA Structural Analysis (NASTRAN) is a program that was originally developed for NASA in the late 1960s. Presently, Nastran source code is integrated in a number of different software packages, which are distributed by a range of companies. MSC Nastran is a powerful general purpose FEA solution for small to complex assemblies. A proven and standard tool in the field of structural analysis for over four decades, Nastran provides a wide range of modeling and analysis capabilities, including linear statics, displacement, strain, stress, vibration and heat transfer.

1.2.4 MSC ADAMS

ADAMS (Automated Dynamic Analysis of Mechanical Systems) is the most widely used multi body dynamics (MBD) and motion analysis software in the world. Adams helps to study the dynamics of moving parts, how loads and forces are distributed throughout mechanical systems, and to improve and optimize the performance of their products.

Adams multi body dynamics software enables engineers to easily create and test virtual prototypes of mechanical systems in a fraction of the time and cost required for physical build and test. Unlike most CAD embedded tools, Adams incorporates real physics by simultaneously solving equations for kinematics, statics, quasi-statics, and dynamics. Utilizing multi body dynamics solution technology, Adams also runs nonlinear dynamics in a tiny fraction of the time required by FEA solutions. Loads and forces computed by Adams simulations improve the accuracy of FEA by providing better assessment of how they vary throughout a full range of motion and operating environments.

1.3 INTRODUCTION TO FSAE COMPETITION

SAE International, formerly the Society of Automotive Engineers is a U.S based globally active professional association and standards organization for engineering professionals in various industries. Principal emphasis is placed on automotive, aerospace and commercial vehicles. Also, the SAE Collegiate Design Series provides an opportunity for college students to go beyond textbook theory and replicates the process of engineering design and manufacturing through various competitions which include Formula SAE, Formula Hybrid, Baja SAE, SAE Aero Design etc.

The Formula SAE (FSAE) is a design competition for University students organized by the SAE International that started in 1978 and was originally called Mini Indy. The concept behind the competition is that a design team has been contracted by a manufacturing company to design and build a formula style racing car. A formula car is an open wheeled vehicle with only one seat, typically in the middle of the vehicle. Each team has to design, build and test a prototype based on a set of rules laid out by the governing body. The competition is held internationally and currently includes the United States, Australasia, Brazil, Italy, Germany, Austria and United Kingdom.

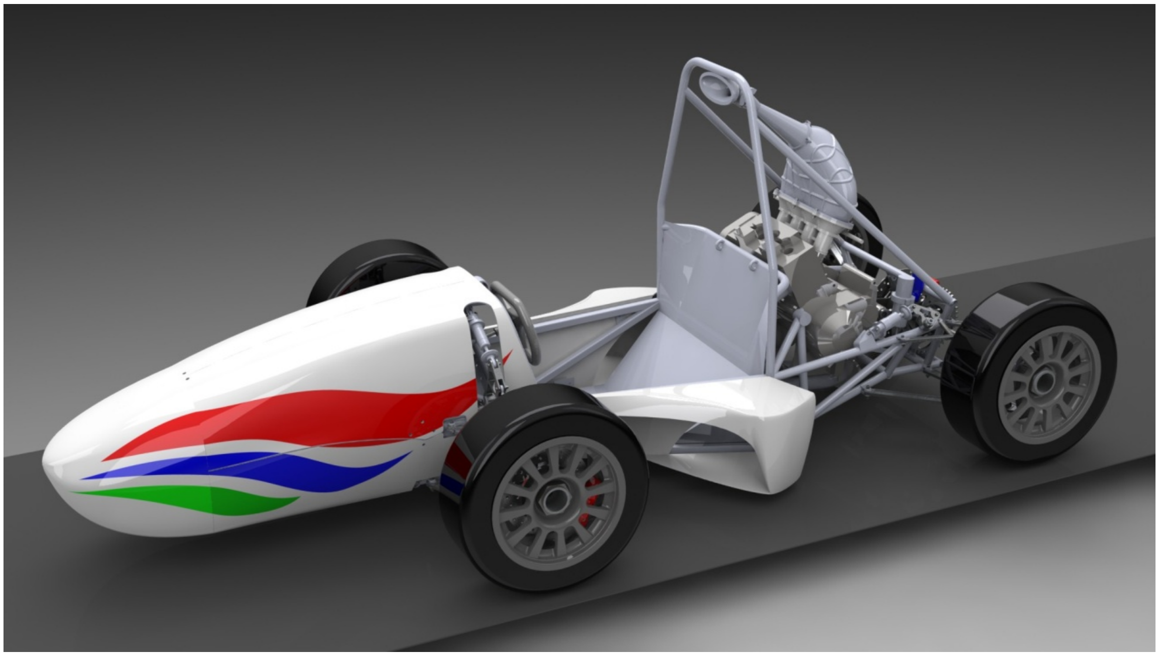

Fig 1.4: Formula SAE Race Car (Thapar University - 2011)

1.4 HISTORY OF FS TEAM FATEH @ THAPAR UNIVERSITY

The **Team Fateh** Formula Student Racing Team represents Thapar University's entry into the Formula SAE collegiate design series, a competition sanctioned by Society of Automotive Engineers. Every year, the team designs, develops and builds an open-wheel, open-cockpit race vehicle for Formula Student vehicle competition held internationally. The team has participated in Formula Student UK (held at Silverstone), Formula Student Germany (held at paddock of the Hockenheimring), and Formula Student Czech Republic (held at Czech Ring race track, Hradec Kralove) events till now.

Team Fateh gets its name from the word Fateh which means "Victory". Formed in 2008 with the aim of being the best collegiate team in India, the team now approaches its 7th outing. The team, for the year 2014-15, is participating in two competitions - Formula Student Germany (FSG) 2014 & Formula Student India (FSI) 2015.

(a) Team Fateh - Thapar University

(b) Formula Student Germany

(c) Formula Student India

Fig 1.5: Team & Event logos

Formula Student Germany will take place at Hockenhiemring in Germany during July-August, 2014. This competition has 115 teams participating from all over the world, and this year has a record maximum number of Indian teams.

The Inaugural Formula Student India is set to take place during January, 2015. This is the first registered Formula SAE event to take place in India and will have participation from the 44 Indian teams now active on the Formula SAE circuit.

Below listed is a summary of Formula student vehicles, the team Fateh has built so far:

1. TUFF 01: Participated in Formula Student UK for the First time in 2008. The vehicle got its name from the abbreviation **T**hapar **U**niversity **F**ormula **F**orce (TUFF). In the first attempt, it was the First Indian car to complete endurance event at Formula Student UK and also received Toyota Best Endeavour award & First prize for fuel economy.

Fig 1.6: TU FSAE vehicle 2008

2. TUFF 02: Participated in Formula Student UK for the Second time in 2009. The key highlights of the vehicle include indigenously developed fuel injection system (MPFI) & use of 599 cc four cylinder Kawasaki Ninja engine instead of previously used 500 cc Royal Enfield engine. The vehicle successfully completed endurance event.

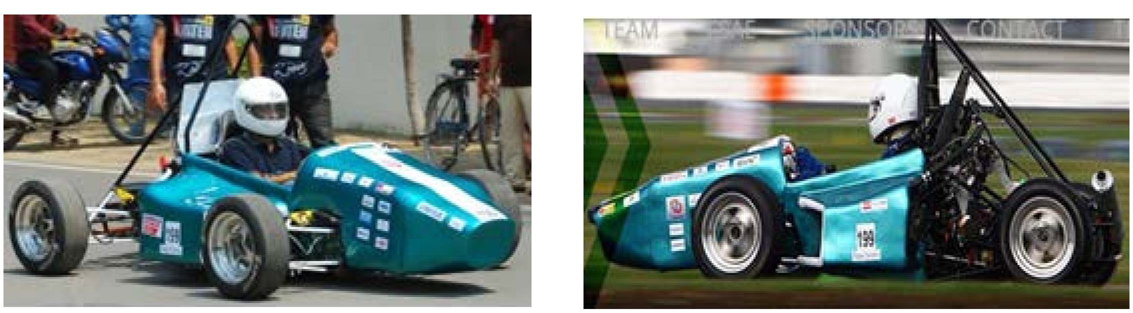

Fig 1.7: TU FSAE vehicle 2009

3. Falcon: Participated in Formula Student UK for the Third time in 2010. The key highlights of the vehicle include the use of rapid prototype Engine intake manifold.

Fig 1.8: TU FSAE vehicle 2010

4. Tarkshya: Participated in Formula Student UK for the Fourth time in 2011. The key highlights of the vehicle include the use of CBR 600 cc Engine & student developed solenoid shifter mechanism. The team was able to achieve the 42nd overall position (out of 117 teams) and was the best performance by the team.

Fig 1.9: TU FSAE vehicle 2011

5. Astra: Participated in Formula Student UK for the Fifth time in 2012. The key highlights of the vehicle include the use of DAQ systems & the Rear Aluminium Chassis.

Fig 1.10: TU FSAE vehicle 2012

6. Garuda: Participated in Formula Student Germany & Formula Student Czech Republic for the First time in 2013. The key highlight of the vehicle was the Semi-monocoque chassis prepared for the First time by an Indian team.

Fig 1.11: TU FSAE vehicle 2013

The journey of Team Fateh so far…

Fig 1.12: TU FSAE vehicles 2008-2013

The Current vehicle…

7. Jäger/Jager: Participating in Formula Student Germany for the Second time in 2014 & Formula Student India organized for the First time in 2014-15. The key highlights of the vehicle include the use of carbon fiber control arms and bodyworks for the first time.

Fig 1.13: TU FSAE vehicle 2014

The journey of the efforts put in by the team to improve continues with every new vehicle prepared. This project work is contribution to the efforts put in to improve the current vehicle performance as compared to previous vehicles developed. The work aims to improve the vehicle chassis stiffness using CAE analysis & reduce the mass of suspension components through Topology optimization.

1.5 FSAE CHASSIS AND SUSPENSION COMPONENTS

All the components are designed for minimal weight, very good strength and ease of manufacture. Also, care is taken to ensure the center of mass of the vehicle is kept centered and low to the ground. Designs must adhere to the rules outlined in the FSAE rulebook. An experienced designer will optimize the design using virtual simulation approach and then the final prototype will be tested physically.

These components must accommodate all of the required suspension points (upper ball joint, lower ball joint, steering linkage) and handle all of the loads that the vehicle will see without failing, keeping deflection to a minimum. The FSAE Chassis and Suspension components are described below:

1. Chassis

The chassis is the skeleton of the vehicle. It provides all of the mounting points for all subsystems. It must be light in weight, while withstanding all forces/stresses experienced in a race. There are many rules which the chassis design must adhere to, such as specific tube sizes, meeting template clearances and maintaining minimum angles between certain locations of the chassis structure.

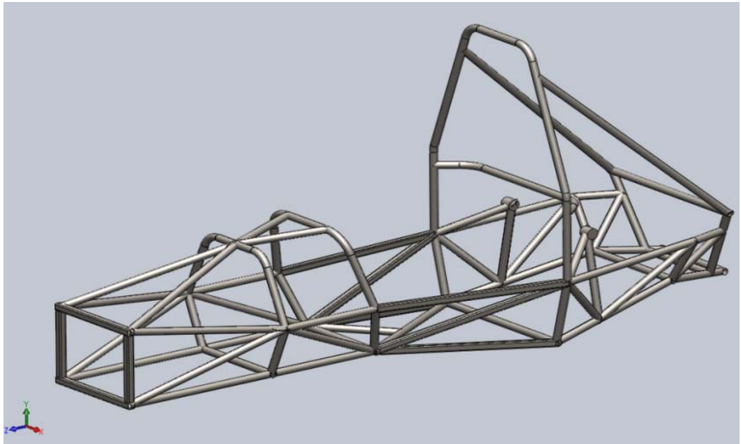

Fig 1.14: Chassis

2. Control Arms

Unequal A-arms are most commonly used for FSAE racing suspension and most suited for stiff racing independent suspension. The control arms are reliable with predictable and calculable motions and forces throughout travel.

The most commonly used set up in racing is the non-parallel arm design. In this design, it allows even better camber control of the wheels and allows the designer to locate the roll center wherever deemed appropriate.

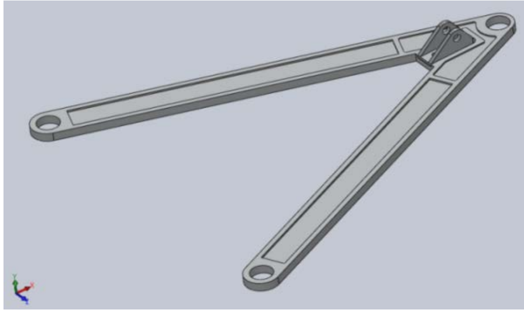

(a) Lower Control Arm (LCA)

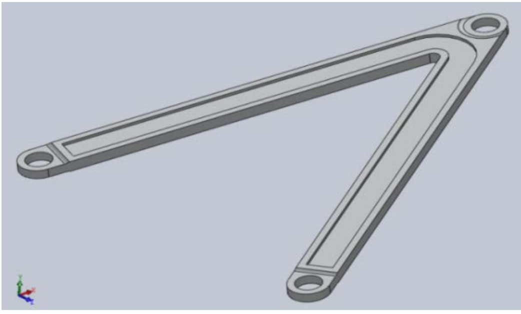

(b) Upper Control Arm (UCA)

Fig 1.15: Control Arm

3. Upright

The upright connects the suspension and steering linkages to the wheels, they typically house the brake disks/calipers. The upright provide a link between the upper and lower ball joints. The weight of the uprights must be minimized. During a bump the weight of the upright is controlled by the shock absorber.

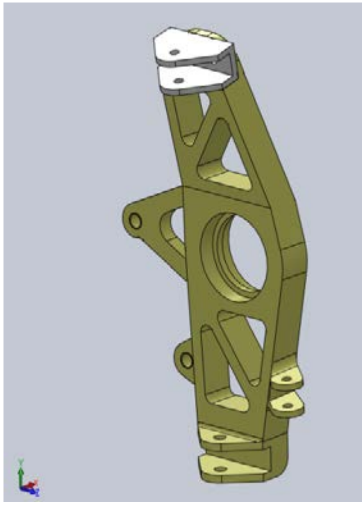

Fig 1.16: Upright

4. Push Rod

Push rod helps in transferring the load coming from the ground to shocks. One end of the pushrod is mounted on the lower A-arm while the other end is connected to the bell crank. It is usually constructed of carbon fiber rods with glued aluminium inserts that hold the rod ends.

Mounting the pushrod on the lower A-arm will introduce a bending moment on it. These rods are very strong and stiff in compression and tension, but cannot endure bending. If the orientation of a pushrod is chosen such that the center line (force line) goes through the tire contact patch, no moments are created that try to change camber and caster angles. It results in a suspension system that creates better loading conditions for the connection rods.

Fig 1.17: Pushrod

5. Bell Crank

A bell crank is a type of crank that changes motion through an angle. It has four mounting points. First end is connected to pushrod, second end is connected to spring damper system, third end is connected to the anti roll bar and the fourth end is connected to the chassis. The bell crank transfers the loads from the pushrod to the spring damper system.

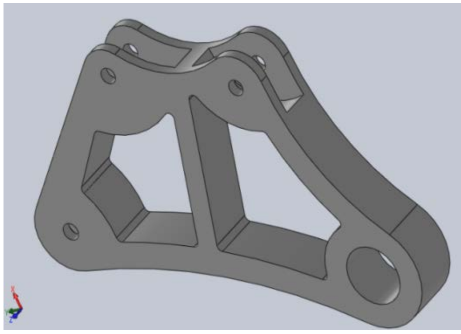

Fig 1.18: Bell Crank

6. Anti roll bar

There is only a certain amount that the springs of a vehicle can resist roll as the coils can only be made strong to a specific limit where manufacture or design integration becomes impossible. To compensate this, anti roll bar can be used to improve the vehicle's stiffness without altering the springs excessively. The first step in the bar selection and design process is to decide where the bars will be placed in relation to the overall vehicle layout. Considerations when positioning the bars will include clearing the driver's legs, gearbox and other key components in the vicinity, the ability to mount on rigid, low friction locations, accessibility for adjustment and to avoid fouling on any other parts of the vehicle.

Stiffness adjustability can be achieved by changing lever arm length. Once the required stiffness is known, the designer can move on to select appropriate bar geometry to achieve this required stiffness. Key dimensions for the bar will include the diameter and wall thickness.

Fig 1.19: Anti roll bar

CHAPTER 2

LITERATURE SURVEY

In the recent past there has been a lot of focus on research of Formula SAE vehicles. With the increasing competition, the need to prepare better vehicle in given time & cost has increased. To achieve this, the application of CAE in the FSAE vehicle design plays a very important role. Some of the research carried out by various researchers has been discussed below in brief:

Edmund F. Gaffney III and Anthony R. Salinas [1] presented an introduction to Formula SAE® (FSAE) suspension and frame design based on the experience of the design team at UM-Rolla's 1996 FSAE race car. The basic theories and methodologies for designing these systems were described so that new teams will have a baseline for their first FSAE design.

Lonny L. Thompson et al. [2] performed a study to understand the influence of the various structural members on the torsion stiffness of a race car chassis. A sensitivity study was carried out of individual structural members on the torsion stiffness of a baseline chassis. Results from the sensitivity analysis were used as a guide to modify the baseline chassis with the goal of increased torsion stiffness with minimum increase in weight and low center of gravity placement.

William B. Riley and Albert R. George [3] discussed analytical and experimental aspects of the frame design, with an emphasis on their applicability to FSAE. The different loading conditions such as Longitudinal Torsion, Vertical Bending, Lateral Bending, Horizontal Lozenging and requirements of the vehicle frame were first discussed, focusing on road inputs and load paths within the structure. Then a simple spring model was developed to determine targets for frame and overall chassis stiffness relative to the suspension spring and anti-roll bar rates. After that, a finite element model was developed to enable the analysis of different frame concepts. Some modeling techniques were followed for both frames in isolation as well as the assembled vehicle including suspension. Finally, different experimental techniques were presented to determine the stiffness actually achieved from a constructed vehicle and a comparison of frames tested in isolation versus whole vehicle testing was done.

Badih A. Jawad and Brian D. Polega [4] performed finite element analysis on control arms, uprights, spindles, hubs, pullrods, and rockers for increasing the strength with least deflection. The forces were calculated analytically and applied on these components for various loadcases. The weight of hub was reduced to decrease rotating and unsprung mass. The analyses were performed to increase vehicle safety, durability and to reduce vehicle weight.

Badih A. Jawad and Jason Baumann [5] performed a study on the safety, durability and maintainability of the FSAE car. Quick camber adjustment mechanism was incorporated in upper control arm for good camber adjustment. In lower control arm, toe link was incorporated for tow adjustment. Loads were calculated analytically for worst case conditions. FEA was done on upright, spindle, hub and pullrods. The purpose was to make the components light weight and good in strength.

Lucas V. Fornace [6] performed a topology optimization study as a means to determine the optimum material distribution within a component for a given set of loading and boundary conditions. The topology optimization techniques were applied in the design of a rear suspension bell crank component of 2006 UC San Diego Formula SAE vehicle. This was compared to that of the 2005 model bell crank component, which was designed using more traditional techniques. A hydraulic load cell system was created to simulate the vehicle suspension forces and was used to physically test the original and optimized parts to failure. Through the use of Altair OptiStruct® topology optimization software, weight savings coupled with an increase in yield strength was realized in the optimized design of the 2006 bell crank.

R Andrew Jen Wong [7] presented an approach to design, optimize and manufacture the Formula SAE Vehicle Front and Rear Upright Assemblies. Various constraints were imposed on the upright for various load cases while performing the analyses. This was done to optimize the upright as well as improving the suspension characteristics. For high performance of the vehicle, the design objective for the upright was to provide a stiff, compliance-free design and installation, as well as achieving lower weight to maximize the performance to weight ratio of the vehicle.

Derek Silsby and Francis Song [8] performed a study on the optimization of control arm under various loading conditions such as acceleration and braking. A Design of Experiment (DOE) study was conducted for making several possible models of the control arm. Finite Element Analysis was performed using ABAQUS software with the criteria of minimizing the stress as well as the weight of the control arm.

Abrams and Ryan [9] performed a study to determine the methods and validate results for using an engine as a structural member of a Formula SAE race car chassis. Modal analysis was used with a beam mesh of the chassis to validate an increase of chassis stiffness. Results confirmed that providing structural support at engine mounting points of the chassis increased the stiffness and changed the first elastic mode of vibration from bending to torsion. Additionally a static analysis was performed to measure chassis deflection so as to decrease chassis deflection when structural support was provided at the engine mounting points of the chassis.

Lane Thomas Borg [10] proposed the changes that occur in suspension member load calculations under a variety of loading scenarios. For determining the suspension member loads, a finite element (FE) model of the entire suspension system was prepared. In first stage, FE model replicated the suspension with all of the current assumptions and the member loads were compared to the hand calculations. This truss-element-based FE model resulted in member loads identical to the hand calculations. The second stage of the FE model development converted the truss model to beam elements. This step was performed to determine if the assumption that bending loads are insignificant is a valid approach for calculating member loads. The third stage of model development incorporated the steer angle for load cases that involve some level of cornering. Finally, the FE model was further enhanced to account for vertical movement of the suspension as allowed by the spring and damper assembly. The quasi-static loading scenarios were used to determine any member loading change due to vertical movement. The FE model was also used to predict the amount of vertical movement expected at the wheel center.

C. Ozturk [11] performed a study to investigate the kinematic characteristics of the rear suspension of the URE05 FSAE vehicle. The challenge was to satisfy the compromising demands from the suspension system. A higher camber gain for the outer wheel during cornering was the essential aim of the design while keeping the structural stiffness high and the centre of the gravity low. In order to obtain an optimal suspension system, a double-wishbone suspension was proposed. After many iterations, the optimum configuration was obtained.

Anton Olason and Daniel Tidman [12] performed a study to investigate how and when structural optimization should be applied in the design process. The optimization methods were used to generate a design concept early in the design process by using Altair HyperWorks tools. Topology optimization was used to reduce mass with maintained mechanical properties as a constraint. This was used to develop a sensible methodology. The importance of structural optimization in the design process was highlighted.

Jock Allen Farrington [13] presented an approach for the redesign of the steering and suspension system for the University of Southern Queensland's 2008 FSAE vehicle. The problems with the suspension and steering system of 2008 vehicle were uncovered and then these findings, coupled with appropriate research, were used to create a new & revised steering and suspension system that possessed improved performance. Completion of the project saw the design of geometry for the suspension arms, suspension actuation mechanisms, uprights as well as the steering rack and arms. Additionally, concepts in the way of 3d models were established for the suspension and steering systems.

Brendan. J. Waterman [14] analyzed and presented a new configuration for 2011 REV FSAE car which required an entirely new chassis design. The FSAE car was powered by four electric motors with one mounted to each wheel's upright, as opposed to the more conventional internal combustion engine mounted within the frame. The frame was supposed to not only support the loads placed on it but also weigh as little as possible. The chassis design implemented structural battery boxes which had the dual purpose of protecting the driver from the batteries and adding strength to the frame. This was not used previously in any other FSAE car. Using these stressed battery boxes gave the chassis excellent torsion stiffness, yet the entire frame still weighed just over 40 kg.

William Davis et al. [15] discussed the improvement of the chassis, front suspension components, continuously variable transmission (CVT), air intake, exhaust system, engine mounting, fuel tank and the brake components. Various load cases like Braking, Headrest and torsion test were performed for checking the strength of the chassis. Also vertical travel, cornering and braking analysis were performed for checking the strength of the knuckle and hub. Various countermeasures were taken for reducing the weight and making the vehicle more efficient.

Liman Jiang et al. [16] performed a study on the stiffness and modal analysis for a FSC (Formula Student China) racing car frame. The design parameters of optimal tubular space frame were determined through the sensitivity analysis. Sensitivity analysis is an effective way for light weighting of frame, which can provide feasible foundation for realization of lightweight. The thickness of tubes was modified meeting the stiffness & modal performance requirements minimizing the weight of the chassis.

P.K. Ajeet Babu and M.R. Saraf [17] performed a study on the design, analysis and validation of the primary structure of the race car which includes chassis and impact attenuator. Based on the rules of Supra SAE India, the chassis was modeled using cad tool and simulated for longitudinal acceleration, lateral acceleration, braking condition, braking with one circuit failure, bending stiffness and torsion stiffness using finite element analysis. The chassis was then fabricated and validated in actual condition using data acquisition tools. The impact attenuator mounted on the front bulkhead of the car increases impact time and thus protects the driver during frontal crash. It was made of aluminium honeycomb structure and designed such that during crash, the average deceleration of the vehicle does not exceed 20g. It was then fabricated and tested using drop test method.

Jacob I. Salter [18] performed a study on Torsion stiffness and weight, the two most important quantifiable aspects to the chassis of any race car. The aim of this project was to design a chassis of which the trade-off between high torsion stiffness and low weight is balanced so as to achieve high vehicle performance across the various competition events. Then finite element analysis was used to calculate the mechanical chassis properties of weight and torsion stiffness for comparing them against values measured from the fully fabricated chassis. To eliminate possible sources of error in the modeled values, mechanical testing of materials used in the construction was conducted.

Syed Naveed Hasan [19] performed a study on optimization of chassis to reduce weight without sacrificing strength requirements. First, the chassis was checked for static analysis using FEM as per the SAE guidelines. Then, Torsion stiffness of the structure was calculated by applying loads on suspension attachment points. The differences in the results were observed using 1D Beam and 2D Shell Elements. Finally, an optimization study was carried out in order to maximize the torsion stiffness and minimize the chassis weight by minimizing tube thicknesses for different frame members avoiding failure in any loading condition.

Liew Zhen Hui [20] investigated various subjects of chassis with specific emphasis on FSAE application using CAE tools. The design and analysis of the chassis was conducted with a parametric approach, which was performed in a systematic and systemic manner. Every progression of design was assessed and interpreted in detail. Data of accelerations, which the chassis experienced during the operation of the race car, was also collected using accelerometers. Data acquired was interpreted and related back to assumptions used in the design analysis. Stressed skin construction for the chassis was also researched and presented in the thesis, with physical tests carried out to compare the performance of stressed skin frame and the bare space frame.

GAPS FOUND DURING LITERATURE SURVEY

- In the studied literature, it has been observed that a lot of importance has been given to analyze the FSAE chassis torsion stiffness. This is because it has significant effect during the lateral weight transfer during cornering. But it is observed that the work has not been reported for the calculation of the torsion stiffness at various sections along the length of the chassis. This study is important to provide design related feedback to improve the chassis structure over its complete length.

- In the papers reviewed, the loads have been calculated analytically. It has been observed that it is very difficult to analytically calculate the loads coming on the suspension attachment points for large translational and rotational displacements. This needs to be done using the MBD software by building the FSAE suspension system. This will act as input for Topology optimization of suspension components.

CHAPTER 3

PROJECT OBJECTIVE

OBJECTIVE/ SCOPE/ PROBLEM DEFINITION

The objective of this Thesis project is to design & develop FSAE vehicle structure for the year 2014, better than similar structures designed previously for Thapar University, Patiala as part of Team Fateh for participating in Formula student vehicle design competition held internationally. The focus is to achieve a rigid & lightweight design for TU FSAE 2014 vehicle structure with high stability.

To fulfill the above objective, the different steps described below will be discussed in subsequent sections.

- Prepare the MBD models of TU FSAE 2012 & 2014 Front & Rear suspension system; Analyze the systems by carrying out kinematic analysis (suspension wheel travel) to calculate the respective roll centers and Compare the roll center characteristics of TU FSAE 2014 suspension system with that of 2012 suspension system. **[Chapter 4]**
- Prepare the FE models of TU FSAE 2011, 2012 & 2014 Chassis structures; Analyze the structures for Torsion, Lateral & Bending stiffness along with stiffness-to-mass ratios, normal mode shapes & natural frequencies and Compare these characteristics of TU FSAE 2014 chassis structure with that of 2011 & 2012 structures. **[Chapter 6]**
- Determine the Torsion stiffness at various sections along the length of the chassis and Compare the same for 2011, 2012 & 2014 TU FSAE vehicles. **[Chapter 6]**
- Calculate the loads coming on suspension/body attachment points by using the MBD software and Carry out the Topology optimization on various components of TU FSAE 2014 vehicle like Front & Rear suspension Uprights and Chassis Bulkhead to make them lightweight. **[Chapter 4 &7]**
- Carry out the Fabrication of final designed chassis as part of TU FSAE 2014 vehicle structure development. **[Chapter 8]**

CHAPTER 4

TU FSAE SUSPENSION – MBD MODELING & ANALYSIS

In order to achieve better roll center characteristics and to obtain input loads for component optimization, the suspension subsystems modeled and analyzed using Adams/Car are discussed below:

4.1 FSAE SUSPENSION SYSTEM - MBD MODELING: The FSAE Suspension system comprises of following major subsystems as explained below:-

4.1.1 Front Suspension Subsystem

Most commonly used in the front of FSAE vehicles is the Double Wishbone Push/Pull rod type suspension. A double wishbone (or upper and lower A-arm) suspension is an independent suspension design using two wishbone-shaped arms to locate the wheel [10]. Each wishbone or arm has two mounting points to the chassis and one joint at the upright. The shock absorber and coil spring are mounted to the Bell crank to control vertical movement.

It mainly consists of following general parts:-

1. Lower Control arm (LCA)
2. Upper Control arm (UCA)
3. Bell Crank
4. Upright
5. Hub
6. Pushrod
7. Tierod

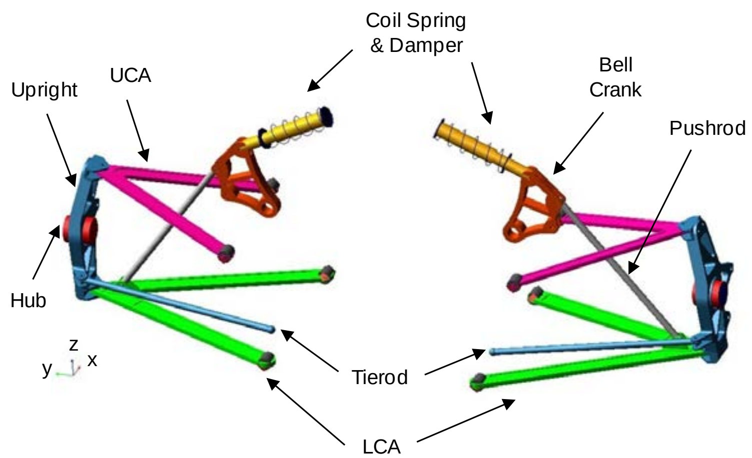

Fig 4.1: MBD Model of TU FSAE Front Suspension Subsystem

The upper arm is usually shorter to induce negative camber as the suspension jounces (rises), and often this arrangement is titled an "SLA" or "short long arms" suspension. This helps to avoid rollover when the vehicle takes a turn.

The function of the front suspension subsystem is to control the independent motion of each front wheel relative to the chassis. The wheels are allowed to precess (controlled by the steering subsystem) and spin independently (controlled by the braking system). The overall layout and individual part descriptions are shown in Figure 4.1 with the wheel/tire subsystem excluded for clarity. The front suspension subsystem design for this vehicle is symmetric about the x-z plane. Part mass and inertia properties are defined in the model.

The front suspension design used on the FSAE racecar is described as an independent SLA type with push rod actuated coil-over shock. Each side of the suspension forms a three-dimensional version of a four-bar linkage in order to control the four DOF (three translations, one rotation) of each front upright with a desired amount of stiffness and damping. The hub allows the spin DOF of the wheel with respect to the upright.

The coil-over shock is a damper and coil spring combination. The shock is actuated by a bell crank, or rocker, that transfers the relative motion of wheel and chassis from the push rod attached to the lower control arm. The final linkage is a steering link attaching the steering subsystem to the suspension.

The MBD model of Front Suspension was prepared from the hardpoints extracted from the CAD model. Hardpoints define the performance characteristics of the Suspension. They are the parametric locations that define where to place the joints and offer the ability to adjust suspension geometry very quickly and easily. The number of joints and the number of hardpoints are not usually equal because some joints share hardpoint locations or are pre-defined relative to other suspension geometry.

4.1.2 Rear Suspension Subsystem

The suspension used in the rear of FSAE vehicle is the Double Wishbone suspension. The suspension includes upper and lower control arms, knuckle, strut, driveshaft having spring and damper systems. The parameters like moment of inertia, center of gravity and mass of the parts have been obtained from the FE model. It mainly consists of following general parts:-

1. Lower Control arm (LCA)
2. Upper Control arm (UCA)
3. Bell Crank
4. Upright
5. Hub
6. Pushrod
7. Tierod
8. Driveshaft

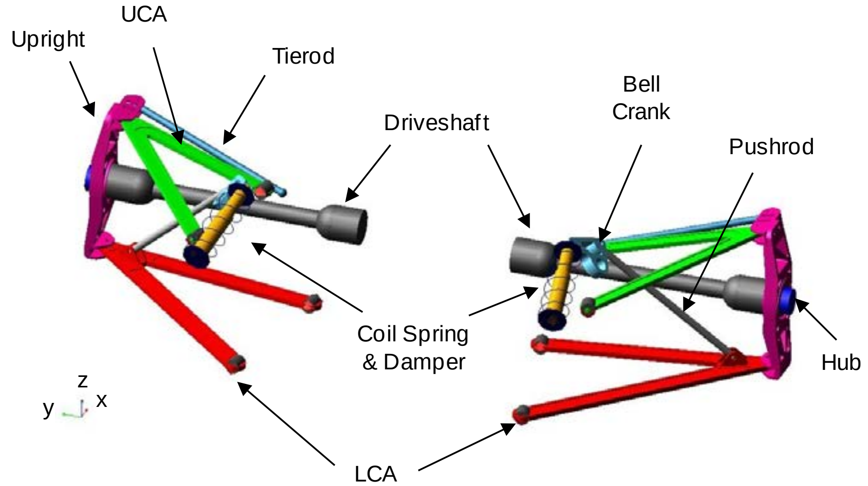

Fig 4.2: MBD Model of TU FSAE Rear Suspension Subsystem

Figure 4.2 displays the rear suspension subsystem, which is quite similar to the front suspension subsystem. In the FSAE racecar design, the rear suspension adopts the same SLA with push rod actuated coil-over shock concept as the front suspension with some changes to the geometry. The spin DOF for the rear wheels is no longer free as this is a rear wheel-driven racecar and has drive shafts transferring the torque between the powertrain subsystem and the wheels. The wheel precession is no longer controlled by a steering subsystem since what was a steering link is now a tie rod that links the upright to the chassis. The wheel has all six DOF determined by the rear suspension subsystem linkages and drive shafts.

The driveshaft assembly is composed of three parts: tripod, driveshaft, and spindle. Connected by the appropriate kinematic joints, the outboard end (spindle) moves along with the upright through any suspension travel while the inboard end (tripod) remains constrained relative to the chassis. The spindle is fixed to the wheel subsystem and has a single rotational DOF within the upright. The tripod is fixed to the powertrain subsystem with the axial translation DOF free to allow for axial plunge of the driveshaft.

4.1.3 Steering Subsystem

Rack and pinion steering is the most common type of steering used in FSAE vehicle. A rack and pinion gearset is enclosed in a metal tube, with each end of the rack protruding from the tube. A rod, called a tie rod, connects to each end of the rack. The pinion gear is attached to the steering shaft. When the steering wheel is rotated, the gear spins, moving the rack. The tie rod at each end of the rack connects to the steering arm on the spindle.

The rack-and-pinion gearset performs two functions:

- It converts the rotational motion of the steering wheel into the linear motion needed to turn the wheels.
- It provides a gear reduction, making it easier to turn the wheels.

Steering Subsystem is rack and pinion type and consists of following general parts:-

1. Steering wheel
2. Steering column
3. Intermediate shaft
4. Steering shaft
5. Steering rack
6. Steering rack housing
7. Pinion

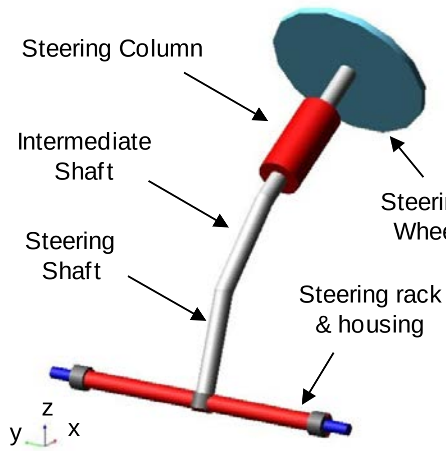

Fig 4.3: MBD Model of TU FSAE Steering Subsystem

Recalling the description of the front suspension subsystem, a rotational DOF is left free for the wheel to precess and steer the vehicle in the desired heading.

The function of the steering subsystem is to link the driver's control input to the orientation of the front wheels via the front suspension subsystem. Input from the driver turns the steering wheel in the desired heading.

The location of the steering wheel usually does not lend itself to using a straight shaft to the rest of the subsystem because of driver ergonomics. The FSAE steering (Figure 4.3) has three shafts connected by two Hooke's joints to accommodate most configurations. The shafts connect the steering wheel to the rack and pinion assembly transferring the rotation of the shafts and pinion to linear translation of the geared rack. The tie rods, or steering links, discussed earlier in the front suspension subsystem are attached to the ends of the rack. As the rack travels, the steering links push (or pull) on the corresponding upright to steer the front wheels.

4.2 FSAE SUSPENSION ASSEMBLY

4.2.1 Front Suspension Assembly

The Front Suspension assembly consisting of Front Suspension subsystem and Steering subsystem is as shown below:

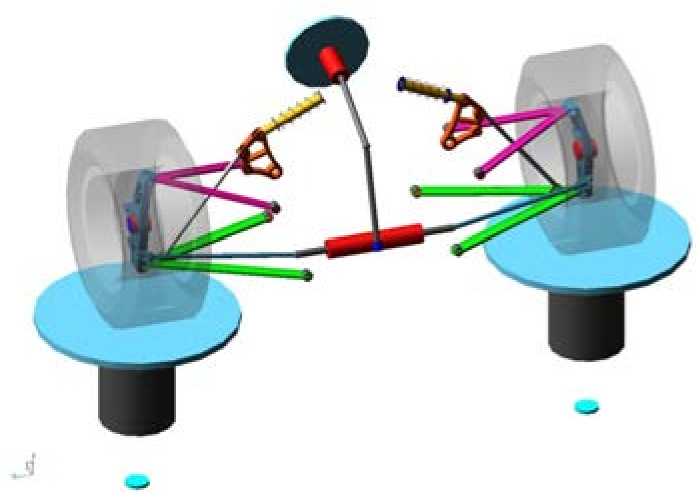

Fig 4.4: MBD Model of TU FSAE Front Suspension Assembly

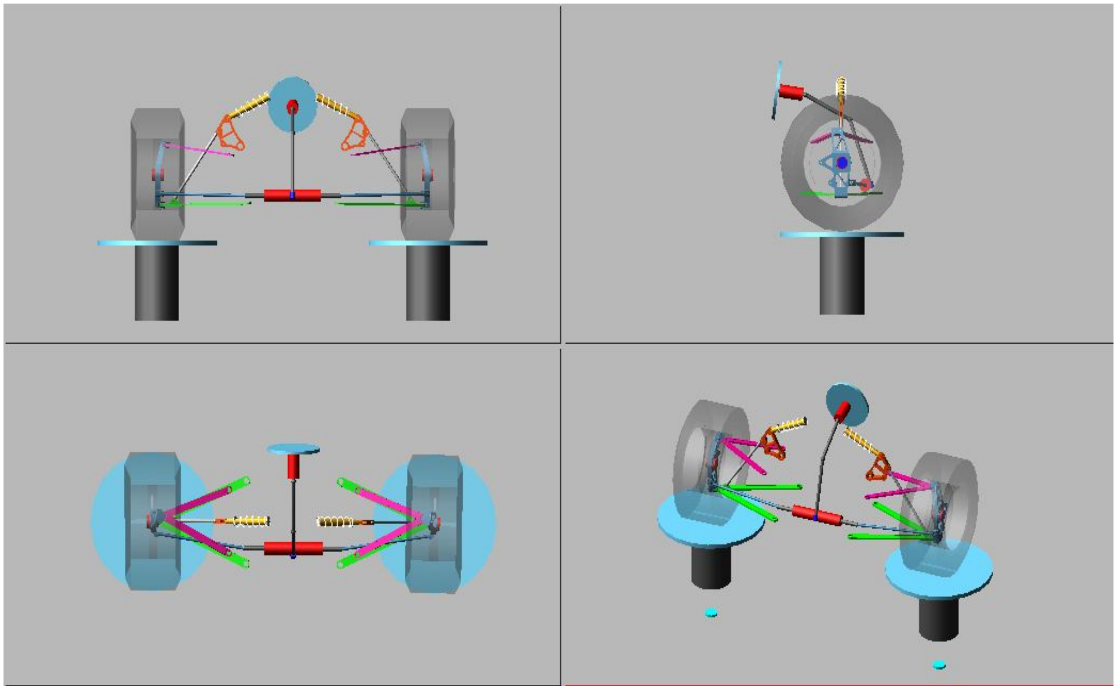

Fig 4.5: TU FSAE Front Suspension Assembly (MBD Model Views)

4.2.2 Rear Suspension Assembly

The Rear Suspension assembly consisting of Rear Suspension subsystem is as shown below:

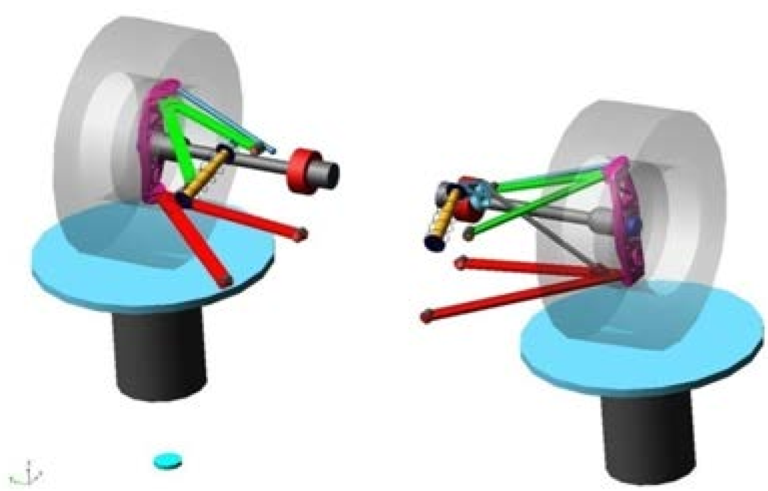

Fig 4.6: MBD Model of TU FSAE Rear Suspension Assembly

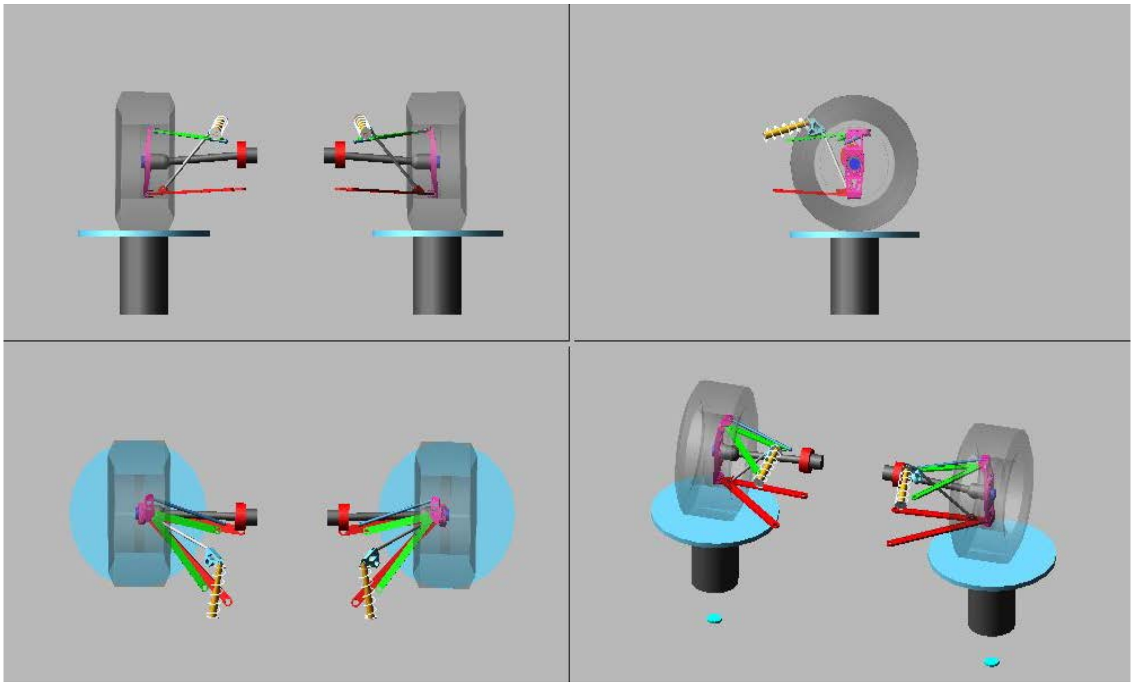

Fig 4.7: TU FSAE Rear Suspension Assembly (MBD Model Views)

4.3 ROLL CENTER CONCEPT

The roll center position is a position where the lateral forces developed at the wheels are transmitted to the vehicle sprung mass. This point will affect the behavior of both the sprung and unsprung mass and thus effects the vehicles cornering characteristics. The roll center is defined as the point in the transverse vertical plane where the lateral forces may be applied to the sprung mass without producing any suspension roll.

When a car experiences centrifugal cornering forces the sprung mass between both the front and rear axles will tend to rotate around a center which is also located in a transverse plane to the axles. These points are called the roll centers and are the locations at which lateral forces generated by the tires on the road will act upon the chassis.

4.3.1 Determination of Roll Center

The roll center position is calculated differently for each type of suspension system. The procedure for calculating the roll center position for the double A-arm type of suspension is as follows:

i. The first step is to locate the instant center. This is accomplished by drawing a line that passes through each of the A-Arms when looking at the vehicle in the front view. The intersection of these lines represents the instantaneous center.
ii. The second step is to draw a line from the center of the tire's contact patch to the instant center. The point where the line drawn in step two intersects the center line of the vehicle represents the roll center position (Figure 4.8).

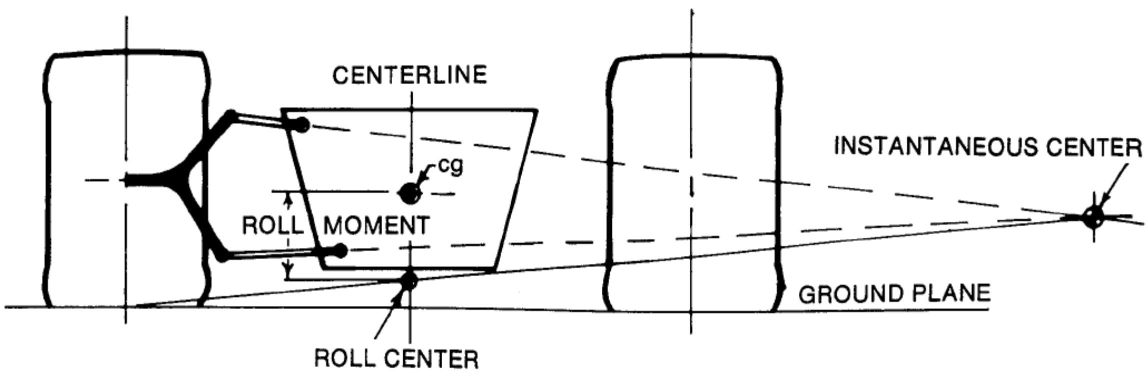

Fig 4.8: Roll center position and moment arm of a double A-arm type of suspension [13]

Figure 4.8 details the process of finding the roll center for the widely used four bar independent suspension system.

4.3.2 Roll Axis

The roll axis (Figure 4.9) is the line that would connect the roll center at the front axle to roll center at the rear axle. Building on the fact that front and rear roll centers will not always be at the same point at the front or rear of the vehicle, the roll axis will usually not be parallel to the ground plane [24].

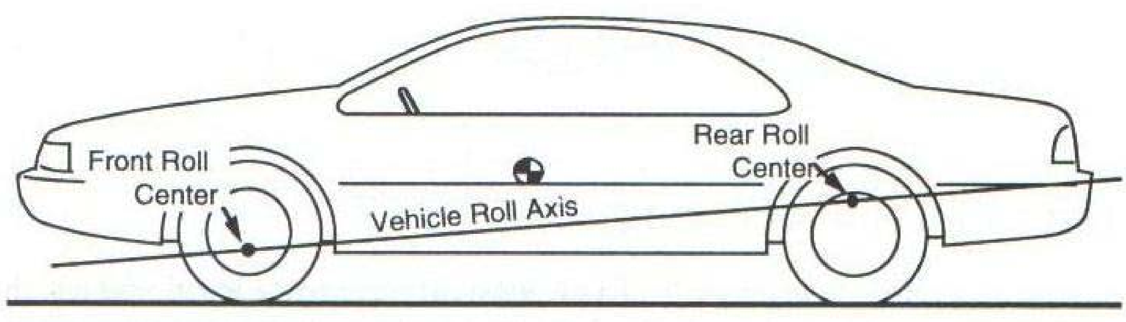

Fig 4.9: The roll axis of the vehicle [25]

The roll center is the intersection of the roll axis with the vertical plane at the front and rear of the vehicle.

4.3.3 Movement of Roll Center

According to Carroll Smith [24], the front roll center should always be lower than the rear. Smith [24] also recommends that the front and rear roll center movements should be approximately equal and in the same direction. On top of this, Staniforth suggests that the movement of the roll centers should be restricted so that handling feel does not dramatically change as the vehicle goes through its various movements. Pat Clarke is another expert supporting the need to keep the roll centers from moving around excessively where he mentions that "*A mobile roll axis will send confusing feedback to the driver, making accurate control difficult*".

4.4 ROLL CENTER ANALYSIS

The front and rear suspension systems geometry were evaluated by considering each system separately, however, it is important to make sure that the front and rear suspension characteristics are consistent with each other in order to optimize the full vehicle's suspension performance. The vehicle is designed with a roll axis that is inclined towards the front for exhibiting oversteer characteristics.

4.4.1 Vertical Wheel travel analysis

4.4.1.1 MBD Analysis Setup

The test rig setup of Parallel wheel travel analysis for Front & Rear suspension is as shown in Fig 4.10. A vertical input is given from 1 inch rebound to 1 inch jounce at the wheel center. The analysis is carried out for suspension of TU FSAE 2012 and 2014 vehicles and the variation of Front & Rear Roll centers during wheel vertical travel is observed and compared during the evaluation.

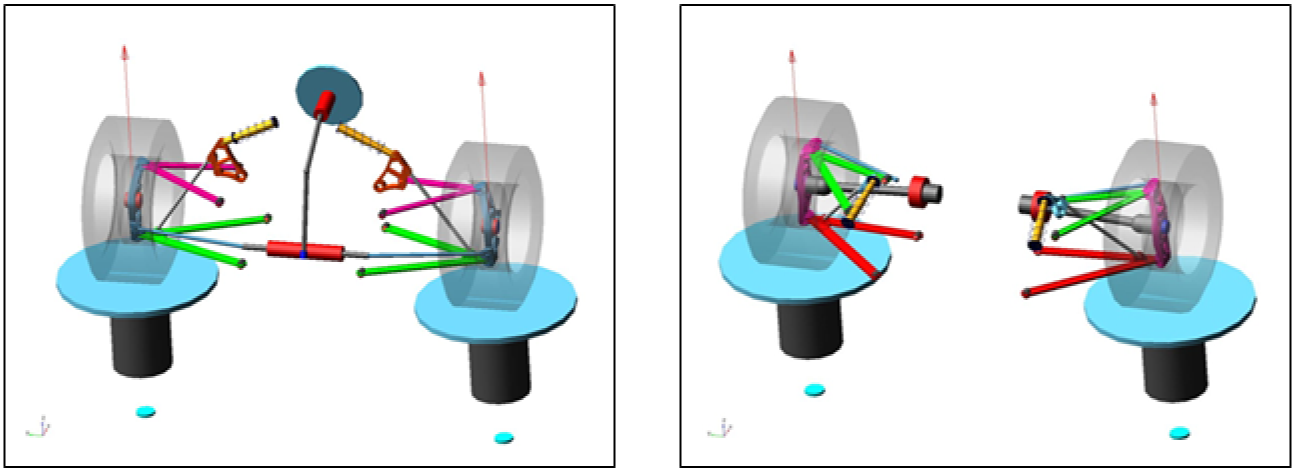

(a) Front suspension test rig (b) Rear suspension test rig

Fig 4.10: Parallel Wheel Travel Suspension Test rig - MBD Model

4.4.1.2 Results

The variation in position of Front & Rear Roll centers during wheel vertical travel of TU FSAE 2012 and 2014 vehicle is shown below:

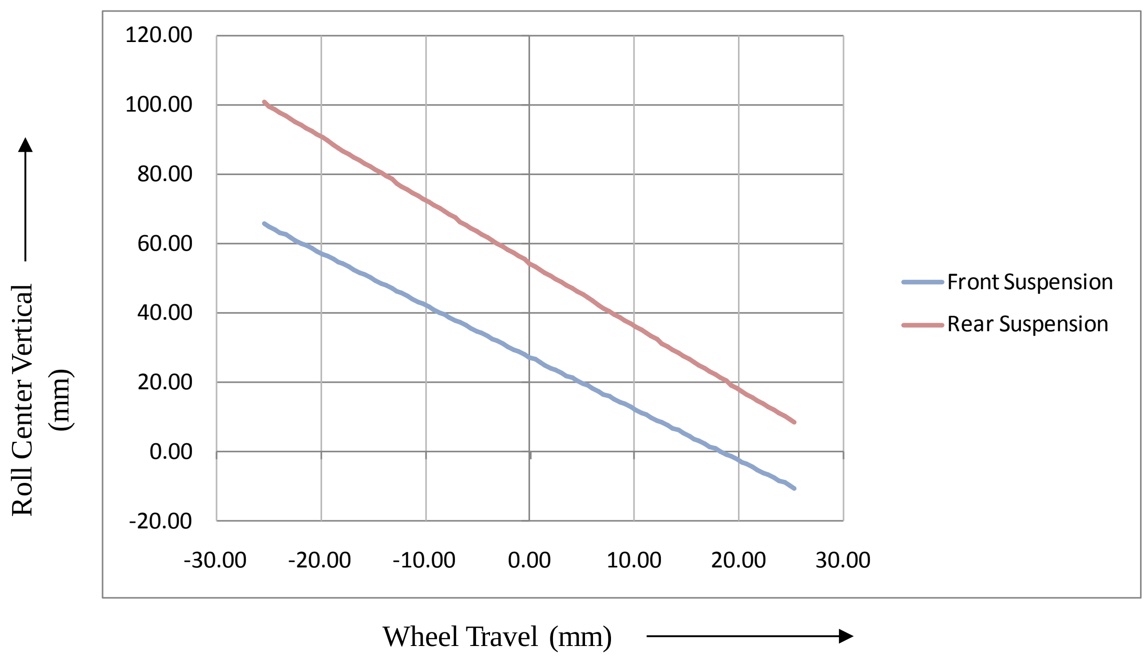

Fig 4.11: Variation in Roll Center Vertical Position (Front & Rear) vs. Wheel Travel (TU FSAE vehicle 2012)

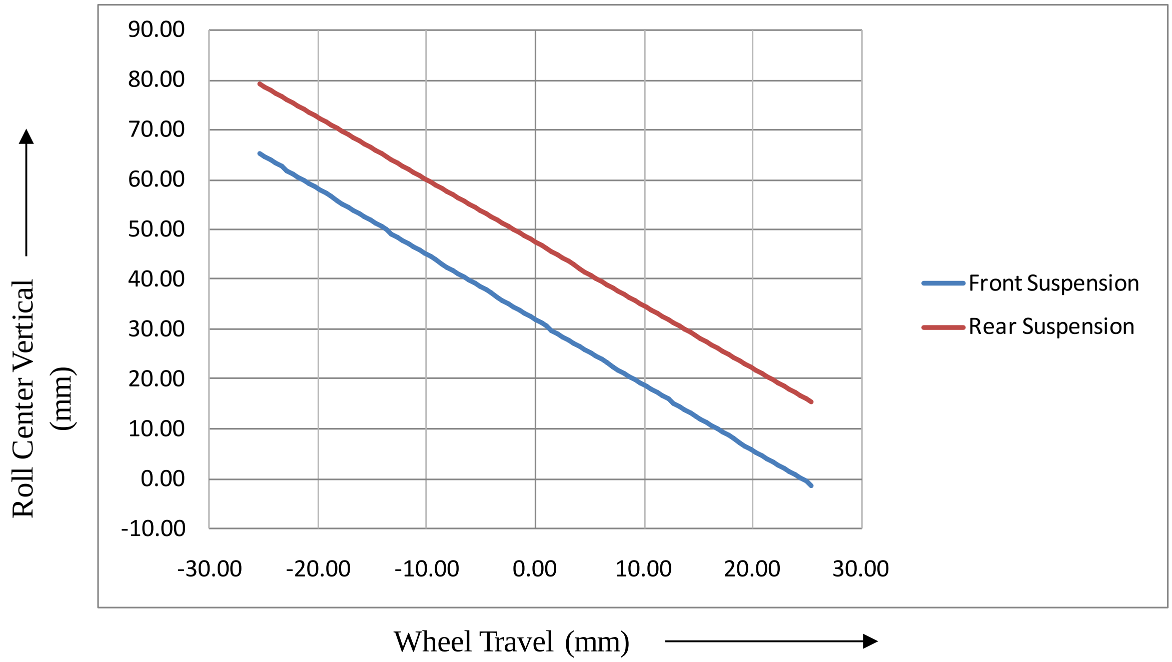

Fig 4.12: Variation in Roll Center Vertical Position (Front & Rear) vs. Wheel Travel (TU FSAE vehicle 2014)

The comparison of Roll center movement with respect to Wheel travel (Front & Rear suspension) between 2012 & 2014 vehicle was carried out as shown below.

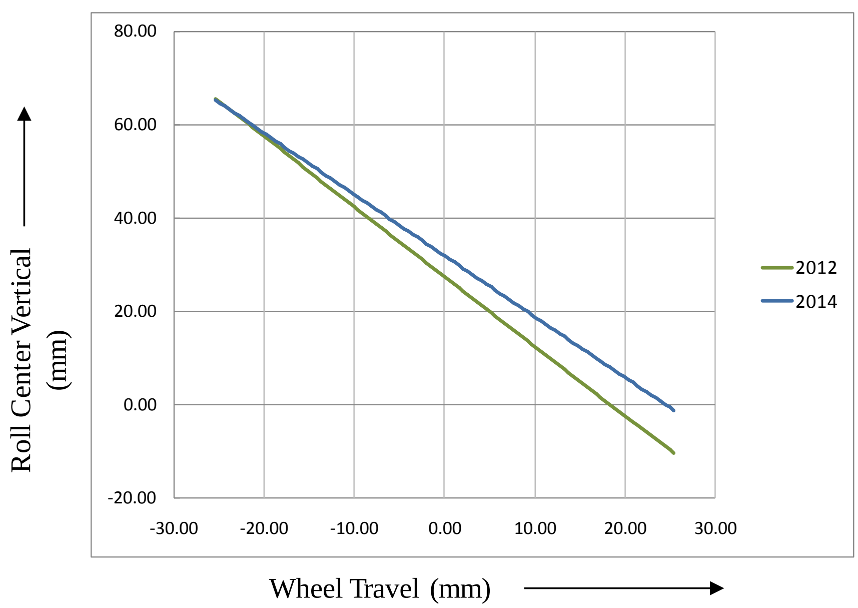

(a) Front Suspension

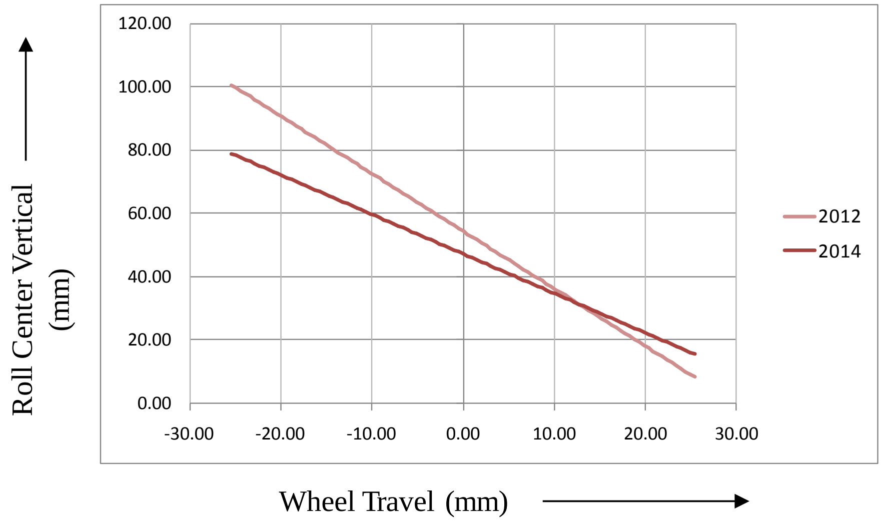

(b) Rear Suspension

Fig 4.13: Roll Center movement comparison – 2012 & 2014 Suspension

4.4.1.3 Remarks

1. Both the TU FSAE 2012 and 2014 vehicle exhibit oversteer characteristics (roll center of front suspension is lower than rear suspension) which is helpful for reducing driver's effort during cornering. Further, the roll center movement due to vertical wheel travel is same for front and rear suspension of 2014 vehicle (fig. 4.12) which is not the case in 2012 vehicle (fig. 4.11). Thus the roll axis of 2014 vehicle is more stable than 2012 vehicle.
2. Roll center movement in 2014 suspension (front & rear) is lesser than that of 2012 for the same Wheel travel (fig. 4.13). Lesser the roll center movement, lesser is the variation in roll axis, lesser will be the change in handling feel to the driver, better will be the control on the vehicle as it goes through various movements.

   Thus, it signifies that the TU FSAE 2014 vehicle has better roll center characteristics as compared to 2012 vehicle

4.5 DETERMINATION OF LOADS AT SUSPENSION/BODY ATTACHMENT POINTS

The objective is to calculate the loads coming at suspension/body attachment points during vertical travel, braking/acceleration and cornering condition. These loads were utilized later for Topology optimization of components.

4.5.1 Types of MBD static load analysis: For MBD static load analysis, three load cases are considered as follows:

4.5.1.1 Vertical Static Load Test

In this test, the suspension is subjected to a displacement of 50.8 mm (2”) in vertical Z direction at wheel center.

4.5.1.2 Braking/Acceleration Static Load Test

In Braking/Acceleration Static Load test, load is applied on the front and rear wheels at the contact patch to simulate the condition. The load applied on the front and rear wheel is calculated as follows:

Total Force coming on all tires, F = 280×9.81 = 2746.8 N

Force coming on front tires during braking, F_{xmf} = 0.74×2746.8 = 2032.632 N

Force coming on rear tires during acceleration, F_{xmr} = 0.79×2746.8 = 2169.972 N

4.5.1.3 Cornering Static Load Test

In Cornering Static Load test, cornering load is applied on the inner and outer wheels to simulate the cornering condition. The load applied on the inner and outer wheels is calculated as shown below:

When the vehicle is taking a turn, the force coming on the outer tire is given by:

$$\boxed{R_o = \frac{W}{2} + W \times \left(\frac{h}{t}\right) \times \left(\frac{a_y}{g}\right)} \qquad \text{(i)}$$

The force coming on the inner tire is given by,

$$\boxed{R_i = \frac{W}{2} - W \times \left(\frac{h}{t}\right) \times \left(\frac{a_y}{g}\right)} \qquad \text{(ii)}$$

where $R_o \rightarrow$ Reaction force on outer tire

$W \rightarrow$ Vehicle Weight

$h \rightarrow$ CG height

$t \rightarrow$ Wheel Track

$a_y \rightarrow$ Lateral Acceleration

$g \rightarrow$ Acc. due to gravity

Substituting values in Eq. (i), the force coming on outer tires is,

R_o = 2097.26 N

Substituting values in Eq. (ii), the force coming on the inner tires is given by,

R_i = 604.296 N

4.5.2 Results: The results for vertical, braking/acceleration and cornering static load test are presented below:

4.5.2.1 Vertical Static Load Test: The forces coming on the front suspension-body attachment points during front vertical static load test are tabulated below:

Table 4.1: Forces on body attachment points during front suspension vertical static load test

Sr. No.	Attachment Points	Force (N)		
		X-direction	Y-direction	Z-direction
1	LCA Outer	-24.30	-518.75	57.63
2	UCA Outer	-28.25	80.00	-26.64
3	Tierod Outer	3.94	90.50	-9.85
4	Pushrod Outer	0.00	-348.25	-465.09

The forces coming on rear suspension-body attachment points during rear vertical static load test are tabulated below:

Table 4.2: Forces on body attachment points during rear suspension vertical static load test

Sr. No.	Attachment Points	Force (N)		
		X-direction	Y-direction	Z-direction
1	LCA Outer	103.16	-16.20	474.86
2	UCA Outer	-119.01	90.61	-30.36
3	Tierod Outer	15.85	-74.41	10.48
4	LCA Inner	-103.16	566.48	-64.46

5	UCA Inner	119.01	-90.61	33.83
6	Tierod Inner	-15.85	74.41	-7.09
7	Bell Crank Pivot	0.00	139.99	-411.81
8	Damper to Chassis Mount	0.00	-690.27	12.95

4.5.2.2 Braking/Acceleration Static Load Test: The forces coming on the front suspension-body attachment points during braking static load test are tabulated below:

Table 4.3: Forces on body attachment points during front suspension braking load test

Sr. No.	Attachment Points	Force (N)		
		X-direction	Y-direction	Z-direction
1	LCA Outer	1600.02	881.64	-101.00
2	UCA Outer	-518.78	240.37	-86.56
3	Tierod Outer	-65.08	-1491.03	214.21
4	Pushrod Outer	0.00	-386.75	-509.26

The forces coming on rear suspension-body attachment points during rear braking static load test are tabulated below:

Table 4.4: Forces on body attachment points during rear suspension acceleration load test

Sr. No.	Attachment Points	Force (N)		
		X-direction	Y-direction	Z-direction
1	LCA Outer	-1708.14	79.68	598.26
2	UCA Outer	581.67	114.19	-42.95
3	Tierod Outer	41.49	-194.03	29.97
4	LCA Inner	1708.14	712.60	-105.03
5	UCA Inner	-581.67	-114.19	46.42
6	Tierod Inner	-41.49	194.03	-26.58
7	Bell Crank Pivot	0.00	178.41	-486.36
8	Damper to Chassis Mount	0.00	-874.94	5.50

4.5.2.3 Cornering Static Load Test: The forces coming on the front suspension-body attachment points during cornering static load test are tabulated below:

Table 4.5: Forces on body attachment points during front suspension cornering load test

Sr. No.	Attachment Points	Force (N)		
		X-direction	Y-direction	Z-direction
1	LCA Outer	26.85	-2575.26	300.44
2	UCA Outer	-43.41	441.01	-158.64
3	Tierod Outer	34.27	785.44	-108.35
4	Pushrod Outer	0.00	-386.56	-509.04

The forces coming on rear suspension-body attachment points during rear cornering static load test are tabulated below:

Table 4.6: Forces on body attachment points during rear suspension cornering load test

Sr. No.	Attachment Points	Force (N)		
		X-direction	Y-direction	Z-direction
1	LCA Outer	128.41	-936.98	716.42
2	UCA Outer	-148.80	793.98	-285.76
3	Tierod Outer	202.89	-948.85	140.74
4	LCA Inner	-128.42	1613.98	-233.54
5	UCA Inner	148.80	-793.98	289.23
6	Tierod Inner	-202.89	948.85	-137.35
7	Bell Crank Pivot	0.00	178.41	-486.36
8	Damper to Chassis Mount	0.00	-874.94	5.21

4.6 CONCLUSION

- The MBD analysis (parallel wheel travel) of the Front & Rear suspension of TU FSAE 2012 & 2014 vehicles was carried out to calculate their respective roll centers. The vertical front and rear roll center positions follow the same pattern throughout wheel travel with the rear roll center being always higher than the front. Roll center movement in TU FSAE 2014 suspension is lesser than that of 2012 for the same Wheel travel which signifies more stability in 2014 suspension.
- The loads coming at suspension/body attachment points during vertical travel, braking/acceleration and cornering condition have been calculated. These loads were utilized later for Topology optimization of components in 2014 vehicle.

CHAPTER 5

FSAE CHASSIS OVERVIEW

Frame is one of the most important parts in a vehicle. It is the main structure in order to create a car. The purpose of the frame is to rigidly connect the front and rear suspension while providing attachment points for supporting the different systems of the car. Relative motion between the front and rear suspension attachment points can cause inconsistent handling. The frame must also provide attachment points which will not yield within the car’s performance envelope. A frame for competitive car would have high rigidity and lightweight which are important factors in every frame of vehicles.

5.1 FSAE CHASSIS TYPES USED

There are two most common types of chassis or frame styles used in the FSAE vehicles, these being a space frame and a monocoque, teams make decisions based on their design criteria and restriction to what type of chassis they will use.

5.1.1 Tubular Space Frame Chassis

The space frame design is a very popular option for chassis type in the FSAE, as it is a low cost, simple to design and easy to construct. A space frame or space structure is a truss-like, lightweight rigid structure constructed from interlocking struts in a geometric pattern. Space frames are series of tubes which are joined together to form a structure that connects all the necessary components together. The design is governed by the FSAE rules, although they leave enough freedom to see a wide variety of spaceframe shapes, sizes and design techniques. Generally there are two main options for the material used in the space frame, these are plain carbon steel and AS 4130, commonly known as chrome – moly because of its chromium and molybdenum content. One of the main advantages of using the space frame design is its easy and logical construction process, of which can be performed by student with intermediate knowledge and experience using basic welding and metal working equipment.

5.1.2 Stressed Skin/Monocoque Chassis

The other popular choice is a monocoque which is made usually from a composite material, with carbon fiber composite being the most popular of these choice. Monocoque is a construction technique that supports structural load by using an object's exterior. It is generally made as one piece. The use of composite materials in monocoque skins allows strength, stiffness and flexibility to be controlled in different directions [20]. The construction of a monocoque is relatively difficult and allows no room for error as once the 'tub' is set, there is no going back. The rules require that the main roll hoop is to be made from steel tubing and attached to the monocoque structure. The greater cost and experience required to create a composite monocoque chassis outweighs the possible mechanical advantages, of which can be replicated by a spaceframe through smart material selection and effective triangulation.

5.1.3 Selection of Chassis

The combination of budget requirements, team experience and the time constraints for construction ruled out the use of a monocoque for the TU FSAE chassis, thus leaving a simple spaceframe as the best option. Space frame style was chosen for the study purpose due to the ease and accuracy in analyzing and manufacturing. Further, modifications can be easily done in case of spaceframe as compared to monocoque chassis during structural design change at a later stage during manufacturing process.

5.2 FSAE CHASSIS NOMENCLATURE & RULES

The definitions of various parts in the Space frame as shown in figure 5.1 & 5.2 are as follows:

1. Main Hoop – A roll bar located alongside or just behind the driver's torso.
2. Front Hoop – A roll bar located above the driver's legs, in proximity to the steering wheel.
3. Roll Hoops – Both the Front Hoop and the Main Hoop are classified as "Roll Hoops".
4. Roll Hoop Bracing Supports – The structure from the lower end of the Roll Hoop Bracing back to the Roll Hoop(s).
5. Frame Member – A minimum representative single piece of uncut, continuous tubing.

6. Frame – The “Frame” is the fabricated structural assembly that supports all functional vehicle systems. This assembly may be a single welded structure, multiple welded structures or a combination of composite and welded structures.
7. Front Bulkhead – A planar structure that defines the forward plane of the Major Structure of the Frame and functions to provide protection for the driver’s feet.
8. Side Impact Zone – The area of the side of the car extending from the top of the floor to 350 mm above the ground and from the Front Hoop back to the Main Hoop.

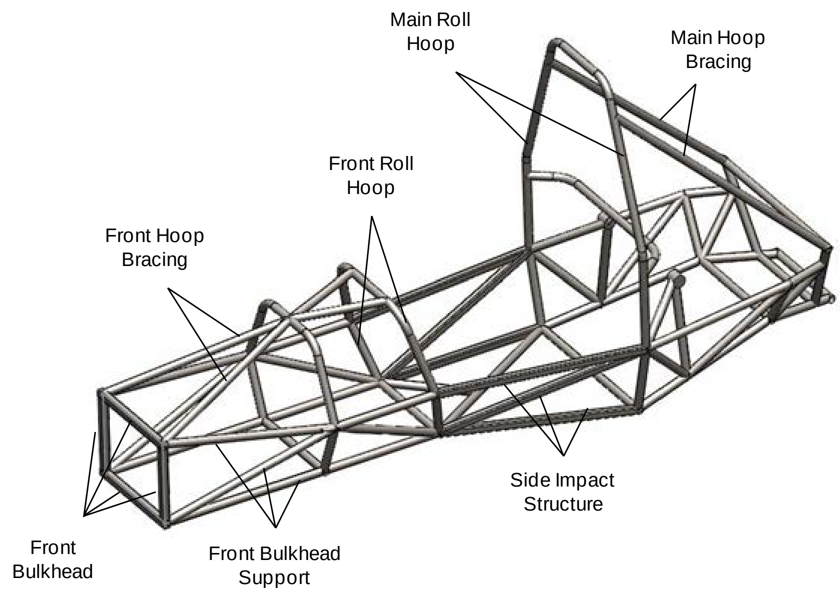

Fig 5.1: Definitions of frame’s parts (TU FSAE 2011 chassis)

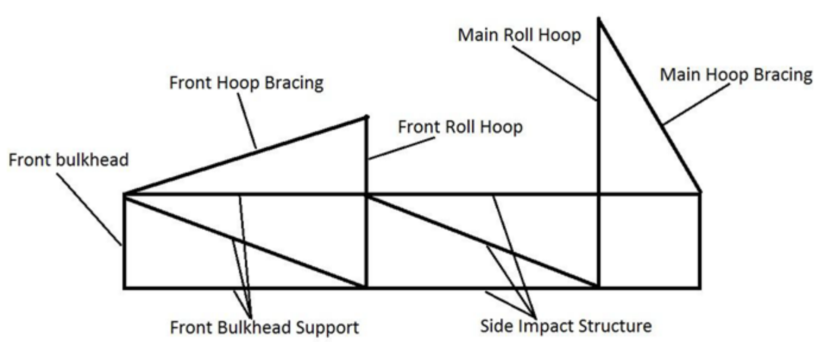

Fig 5.2: Pictorial representation of the members required by the FSAE rules [21]

The FSAE rules define a minimum size for all the chassis members shown in Table 5.1 and for some other members not shown. To avoid adding un-necessary weight, the chassis design should make best use of the required members so that as few possible additional members are needed. This is where much of the design work needs to be done because the rules limit many of the chassis members.

Table 5.1: 2011 Formula SAE Rules for Member size [21]

Item or Application	Outside Dimension X Wall Thickness
Main & Front Hoops, Shoulder Harness Mounting Bar	Round 1.0 inch (25.4 mm) x 0.095 inch (2.4 mm) or Round 25.0 mm x 2.50 mm metric
Side Impact Structure, Front Bulkhead, Roll Hoop Bracing, Driver's Restraint Harness Attachment (except as noted above)	Round 1.0 inch (25.4 mm) x 0.065 inch (1.65 mm) or Round 25.0 mm x 1.75 mm metric or Round 25.4 mm x 1.60 mm metric or Square 1.0 inch x 1.0 inch x 0.049 inch or Square 25.0 mm x 25.0 mm x 1.25 mm metric or Square 26.0 mm x 26.0 mm x 1.2 mm metric
Front Bulkhead Support, Main Hoop Bracing Supports	Round 1.0 inch (25.4 mm) x 0.049 inch (1.25 mm) or Round 25.0 mm x 1.5 mm metric or Round 26.0 mm x 1.2 mm metric

The FSAE rules also require the chassis to provide sufficient space for cockpit entry, where the driver enters the cockpit. The rules require a template shown in figure 5.3 be able to pass vertically through the cockpit opening until it reaches the height of the top bar in the side impact structure. Further template shown in figure 5.4 must be able to pass horizontally internally through the cockpit as mentioned in FSAE rules.

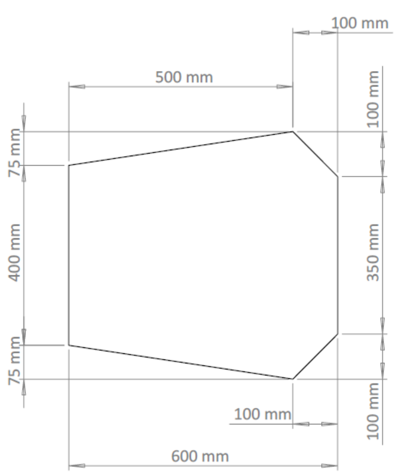

Fig 5.3: Cockpit entry template [21]

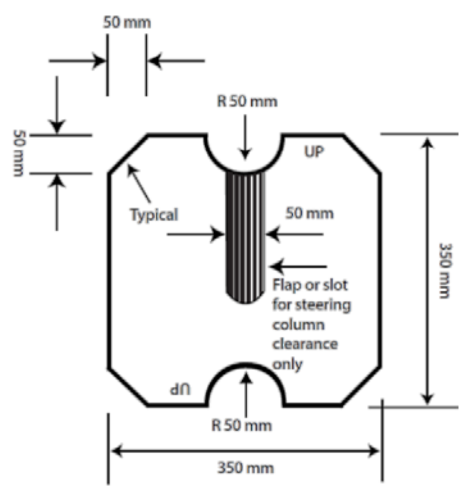

Fig 5.4: Cockpit internal cross-section template [21]

The chassis model for TU FSAE 2011 vehicle complies with the FSAE 2011 rules mentioned above. The various Model views of the chassis are as shown below:

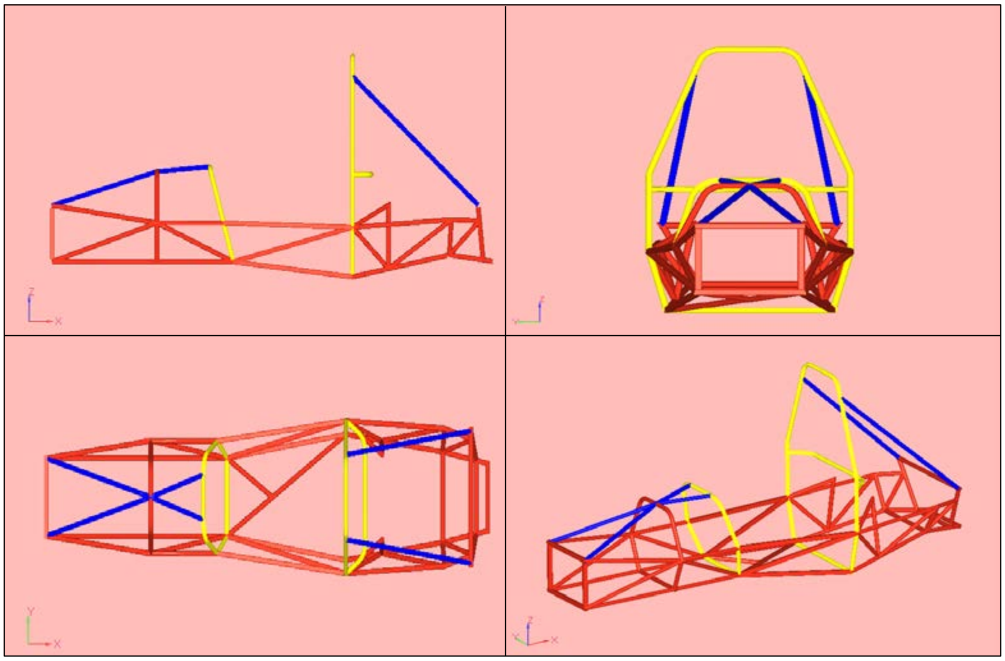

Fig 5.5: TU FSAE Chassis 2011 Views

Following types of sections were used for the TU FSAE 2011 chassis structure:

1) Round tube with OD 1”, Wall Thickness 0.095” (2.4 mm)

2) Round tube with OD 1”, Wall Thickness 0.049” (1.25 mm)

3) Round tube with OD 1”, Wall Thickness 0.063” (1.6 mm)

4) Square tube of size 1”, Wall Thickness 0.049” (1.25 mm)

First type is used primarily for the cockpit of the chassis where high strength is required for driver’s safety as shown by yellow color in figure 5.5. Second type of tube is usually used to create remaining frame members except the connecting members for triangulation as shown by red color in figure 5.5. Third type of tube is used to create connecting members for triangulation of the frame as shown by blue color in figure 5.5.

5.3 CHASSIS FE MODELING

It is important to touch on the type of mesh used for finite element modeling of the chassis structure. There are several options available for meshing. Some basic element types available in Hypermesh that could be used for the chassis modeling are shown in figure 5.6.

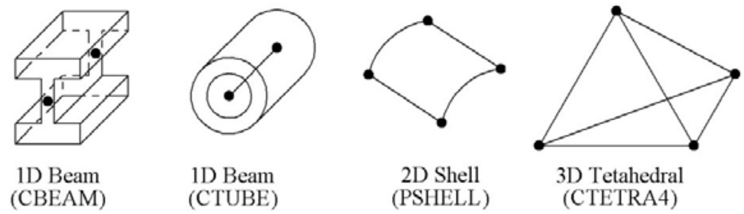

Fig 5.6: Some of the available element types in Hypermesh [19]

The chassis is a structure composed of many thin tubes and complex geometries near the corners. Therefore, it is not recommended to use a solid element mesh type. In addition, the 3D elements are not convenient to use due to small thickness of the tube section (less than 3 mm).

1D Beam elements produce models at reduced meshing time & effort, but may significantly affect the result accuracy. The beam element has just two nodes and uses only the wire frame geometry without taking into account the actual surface.

2D Shell element CQUAD4 with PSHELL physical properties has four nodes with six degrees of freedom at each node (three translations and three rotations). Although it needs more modeling effort than 1D element, it represents the joint connections in a more realistic manner. Since it can describe the physical problem better than the beam model, it leads to produce more accurate results. Moreover, 2D shell elements approximate a curved beam or any curved surface better than 1D beam element. A Shell mesh, therefore, becomes a good choice for the structural analysis of the chassis.

5.4 CHASSIS LOADING

Frame is defined as a fabricated structural assembly that supports all functional vehicle systems. This assembly may be a single welded structure, multiple welded structures or a combination of composite and welded structures. Depending upon application of loads and their direction, chassis is deformed in respective manner briefed as follows:

1. Longitudinal Torsion
2. Vertical Bending
3. Lateral Bending

5.4.1 Longitudinal Torsion

Application of equal and opposite forces at a certain distance from an axis tends to rotate the body about the same axis. Automobiles also experience torsion while moving on road subjected to forces of different magnitudes acting on one or two corners of the cars as shown in Figure 5.7. The frame can be thought as a torsion spring connecting the two ends where suspension loads act. Torsion loading and resultant momentary elastic or permanent plastic deformation and subsequent unwanted deflections of suspension springs can affect the handling as well as performance of car. The resistance to torsion deformation is called as torsion stiffness and it is expressed in Nm/degree in SI units. Torsion rigidity is a foremost and primary determinant of frame performance of cars.

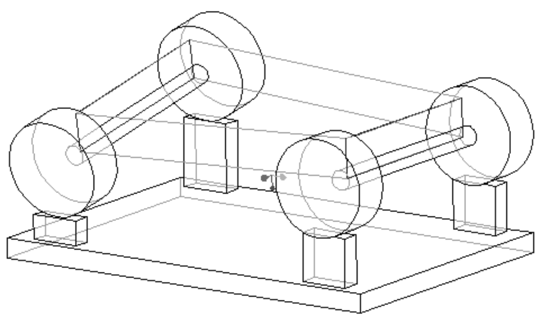

Fig 5.7: Longitudinal Torsion

5.4.2 Vertical Bending

Weight of driver, engine, drive-train, radiator and shell etc. under an effect of gravity produce sag in the frame as shown in Figure 5.8. Frame is assumed to act as simply supported beam and four wheels as supports tend to produce reactions vertically upward at the axles. Vertical dynamic forces due to acceleration/deceleration further increase the vertical deflections, hence stresses in chassis.

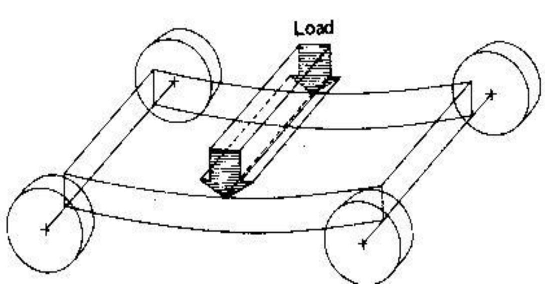

Fig 5.8: Vertical Bending

5.4.3 Lateral Bending

Lateral bending deformation occurs mainly due to the centrifugal forces caused during cornering and wind forces to some extent. Lateral forces act along the width of chassis and is resisted by axles, tires and frame members viz. hoops, side impact members and diagonal hoops etc as shown in Figure 5.9.

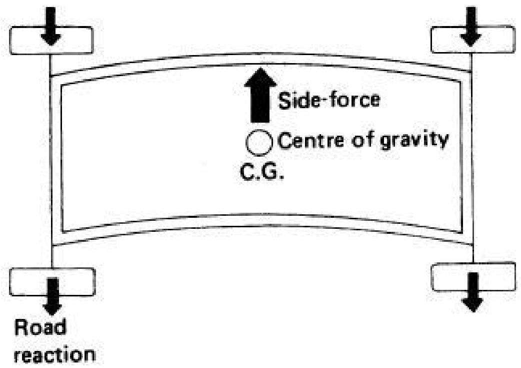

Fig 5.9: Lateral Bending

<u>Weight Transfer concept</u>:

Weight transfer is name given to the effect that lateral and longitudinal acceleration have on the load being supported by each wheel of the car, with lateral weight transfer occurring during cornering and longitudinal weight transfer present during acceleration and braking.

1. Lateral Weight Transfer

A chassis' stiffness determines how well the vehicle deals with weight transfer around corners. Lower chassis stiffness decreases the amount of weight transfer for a given stiffness fraction. As traction during cornering is the function of this lateral weight transfer [2], it is desirable to design a chassis with maximum torsion rigidity. This allows the suspension to do their job correctly.

2. Longitudinal Weight Transfer

Acceleration and braking cause longitudinal weight transfer due to the longitudinal acceleration these actions induce, by having a chassis that is of sufficient stiffness the vehicle’s suspension can be allowed to deal with the weight transfer correctly, which will increase the car’s performance during acceleration and braking [26].

5.5 CHASSIS STIFFNESS

There are two main classes of structural stiffness of chassis, namely structural torsion stiffness and structural bending stiffness. Both contribute to the structural stiffness of the chassis. Defining the system’s axis, a stiff chassis opposes rotation about the y-axis (lateral) in bending, and twisting about the x-axis (longitudinal) in torsion.

5.5.1 Torsion Stiffness

In order to design a car of maximum torsion stiffness, the basis or generalized equation for torsion must be examined. Figure 5.10 below is a basic shaft constrained at one end and an applied torque T at the other, with Φ denoting the resultant twist of the shaft.

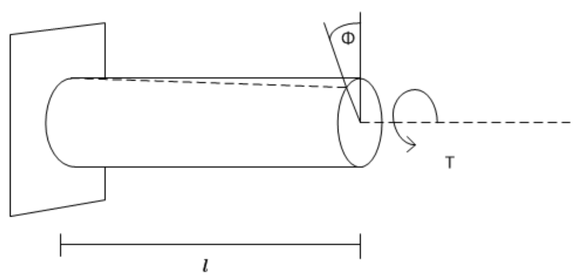

Fig 5.10: Simple Torsion of Shaft

Equation 5.1 is the simple formula that relates this angle of twist to the applied torque, with J representing the shafts polar moment of inertia, G representing the shear modulus of the material and *l* being the length of the shaft.

$$T = \frac{\phi JG}{l} \tag{5.1}$$

This equation can then be rearranged to express torsion stiffness,

$$\frac{T}{\phi} = \frac{JG}{l} \tag{5.2}$$

This expression displays that torsion stiffness is proportional to both the polar moment of inertia and material shear modulus, whilst being inversely proportional to the length. The stiffness of the chassis can be helped to be maximized, by using these key relationships and placing them in the context of the chassis. This can be achieved by making the chassis more compact, reducing its length.

The significance of the structural torsion stiffness lies primarily in its influence towards the capability of the suspension in effectively controlling the race car's handling characteristic. The suspension controls the handling characteristic through managing the distribution of the race car's wheel loads during cornering, in which the front-to-rear distribution of the lateral load transfer of the race car is controlled in proportion to the roll stiffness of the suspension.

Being the platform of which the suspension is mounted to, the chassis plays a very significant role in this aspect. The relationship between the chassis and suspension can be shown through visualizing the chassis as the torsion spring that connects the front and rear suspension. Together, the chassis and the suspensions form a system of torsion springs in series as depicted below.

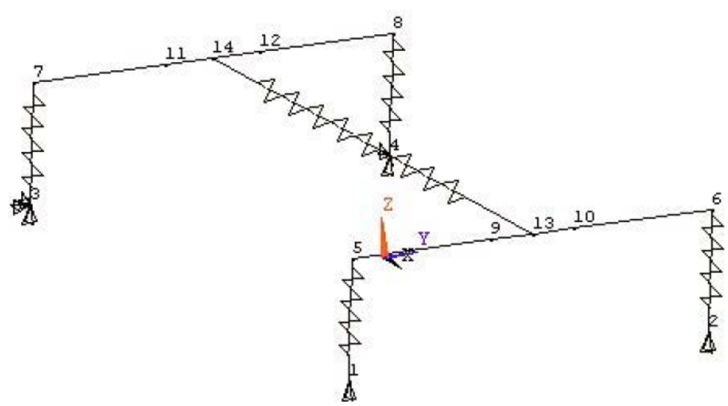

Fig 5.11: Idealized model of chassis and suspensions – representation as springs

From this idealized model, we can see that if the chassis is torsionally soft, almost all attempts to control the front-to-rear distribution of the lateral load transfer of the race car are ineffective. All setups configured to the race car through the suspension become insignificant and result only in baffling outcomes. If there is considerable twisting, the chassis will vibrate, complicating the system of the vehicle and sacrificing the handling performance. Therefore, predictable handling is best achieved when the chassis is stiff enough to be approximated as a rigid structure. In order to have the race car to be of high competence in races, the suspension must be able to control the handling characteristic of the race car and it is intuitive that this is only possible with a chassis that has the satisfactory structural torsion stiffness.

There are numerous reasons for high chassis stiffness. A chassis that flexes is more susceptible to fatigue and subsequent failure, and also the suspension compliance may be affected by deformation of the chassis.

Torsion stiffness' range from a small FSAE race car to a Formula 1 car is tabulated below:

Table 5.2: Torsion Stiffness of different vehicles [26]

Vehicle	Chassis Torsion Stiffness [Nm/deg]
Formula SAE car	1000-5000
Passenger car	5000-20000
Winston cup racing car	15000-30000
Sports car	15000-40000
Formula one car	10000-100000

5.5.2 Bending Stiffness

In the perspective of the chassis of the formula race car, the structural bending stiffness is not as important as the structural torsion stiffness. This is because the wheel loads of the race car, the primary parameter that influences the performance, are not significantly affected by the bending of the chassis. In static bending, the wheel loads and their distribution deviate only slightly.

Such relative importance is further enhanced by a past research, in which it had shown that the structural torsion stiffness is not only more important, but is also more dominant in the structural stiffness of the chassis. The research had proven and shown that the structural bending stiffness can be adequately achieved through obtaining satisfactory structural torsion stiffness of the chassis. Therefore, the structural torsion stiffness is of higher significance, thus becomes the main interest in the development of the chassis, especially in the arena of racing.

Thus, if a chassis is well designed to handle torsion loads, bending should not be an issue.

5.6 INTRODUCTION TO MODAL ANALYSIS

When perturbed, any solid body will vibrate at a certain frequency, known as its natural frequency. When a body vibrates at a resonant frequency, it will oscillate at larger amplitude than other frequencies, even those that may be larger than the natural frequency. The body will oscillate with more and more amplitude in an attempt to dissipate the energy stored within it. Since any real object has a certain amount of damping, the amount of amplitude is limited. However, it may be large enough to still cause damage to the part.

In the context of the chassis, each member has its own set of resonant frequencies. If the member is allowed to oscillate at one of its resonant frequencies, it may displace itself enough to cause a failure in one of the welds holding the frame together. As a truss structure, the primary source of vibrations in the chassis is from the excitations due to engine and suspension. Among all the resonant frequencies of the frame structure, the most dangerous one is of low frequency. *Therefore, the first natural frequency should be higher than the excitation of suspension and engine in order to prevent the low frequency resonances.*

Thus, modal frequency analysis of the chassis to find its resonant frequencies becomes important. The lower elastic modes of vibration result in lower natural frequencies. This means the first elastic mode of vibration demonstrates the shape that the chassis is most susceptible to deform because it has a lower natural frequency and hence, lower stiffness. Therefore it is desired to have a chassis with a relatively high natural frequency in the first elastic mode of vibration.

In the context of improving the performance of the FSAE frame design, the most pertinent mode shapes correspond to the first three normal modes of vibration which are characterized by frame torsion & bending. *As Torsion stiffness of the chassis plays more significant role, the torsion mode of the chassis must be improved for better performance.*

CHAPTER 6

TU FSAE CHASSIS – FE MODELING & ANALYSIS

6.1 TU FSAE CHASSIS 2014 DESIGN: The chassis of Thapar University FSAE 2014 vehicle has been designed in accordance with FSAE 2014 rules and is shown below:

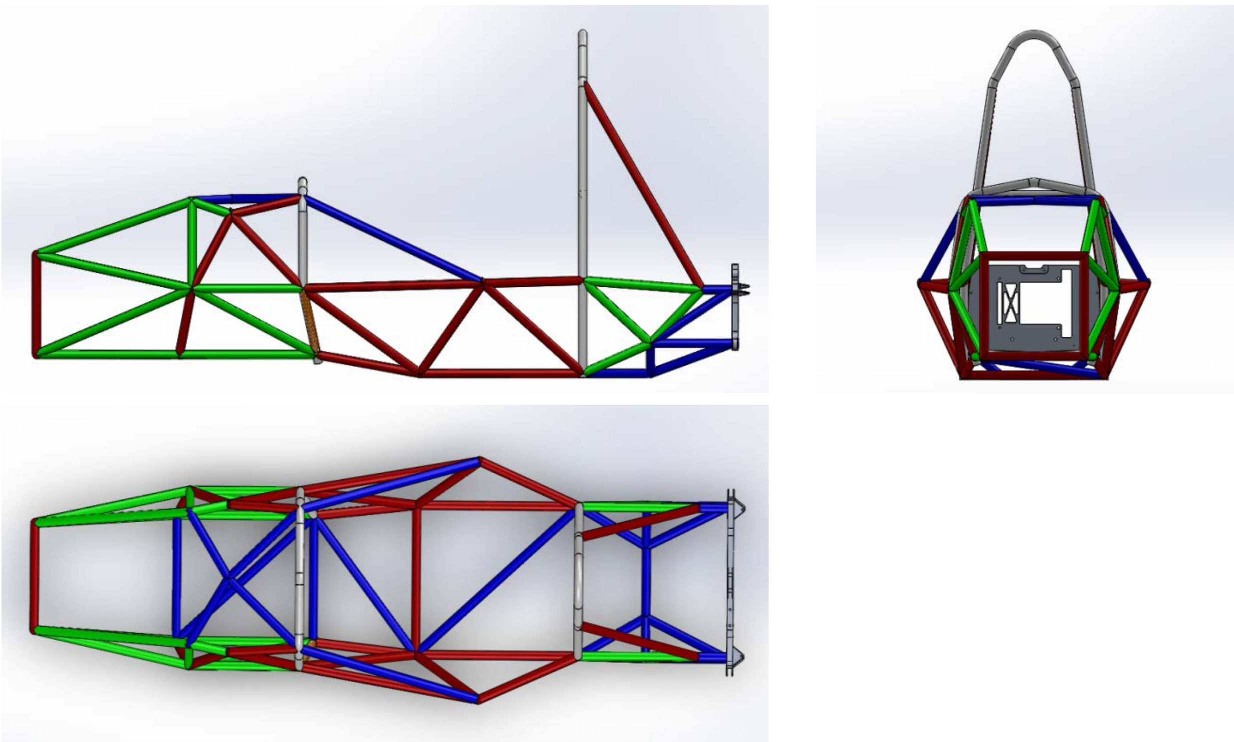

(a) Orthographic views

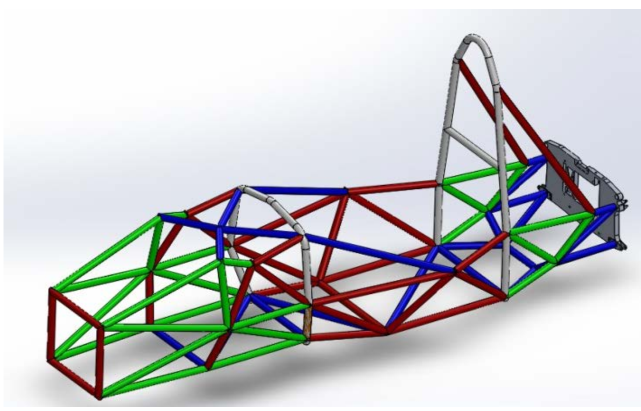

(b) Isometric view

Fig 6.1: TU FSAE Chassis 2014 design

6.2 TU FSAE CHASSIS MODEL COMPARISON

The TU FSAE Chassis models for the year 2011, 2012 & 2014 under study comply with the FSAE standard rules and are shown below:

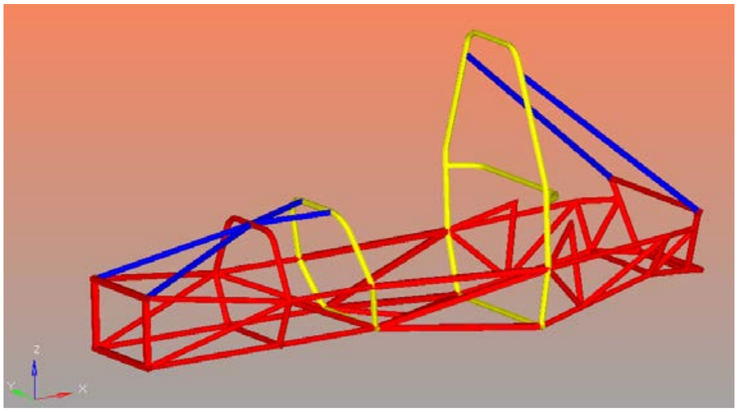

Fig 6.2: TU FSAE Chassis 2011

Table 6.1: 2011 Chassis color coding

Color	Thickness (mm)
	1.25
	1.6
	2.4

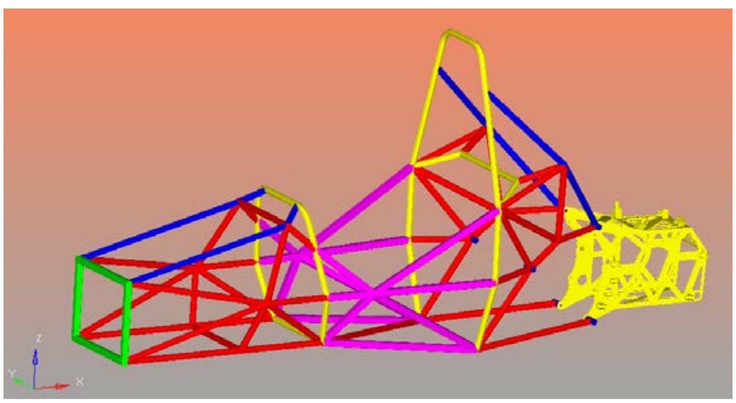

Fig 6.3: TU FSAE Chassis 2012

Table 6.2: 2012 Chassis color coding

Color	Thickness (mm)
	1.2
	1.2
	1.25
	1.6
	2.4

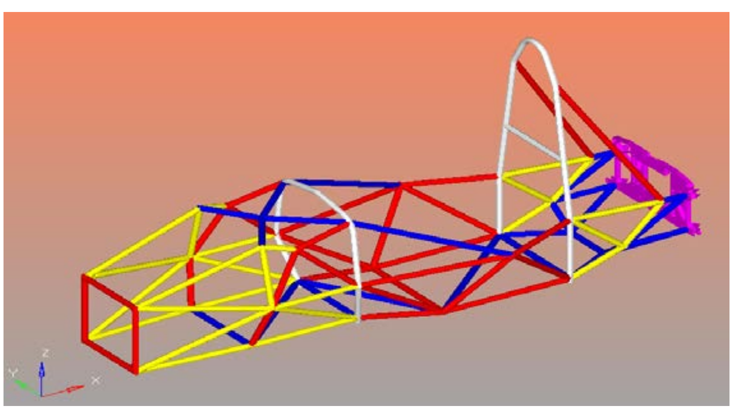

Fig 6.4: TU FSAE Chassis 2014

Table 6.3: 2014 Chassis color coding

Color	Thickness (mm)
	1.0
	1.25
	1.6
	2.4

The chassis comparison of 2011, 2012 & 2014 TU FSAE vehicles is as shown in fig 6.5. The 2014 vehicle chassis is designed to be a compact structure as compared to previous ones. It features a simple space frame with rear aluminium bulkhead. Proper triangulation and use of diagonal members helps in maintaining high stiffness at critical locations. Further ergonomics of the driver is also considered due to which the driver room (space between front hoop & main hoop) is more spacious. Also, since the 2014 vehicle features a lighter & compact engine, which can be accommodated in lesser space at the rear of the chassis, the overhang of the main hoop bracing has been significantly reduced. All in all, the overall length of the chassis in 2014 vehicle is reduced to the minimum. The length details of all the chassis have been shown in table 6.5.

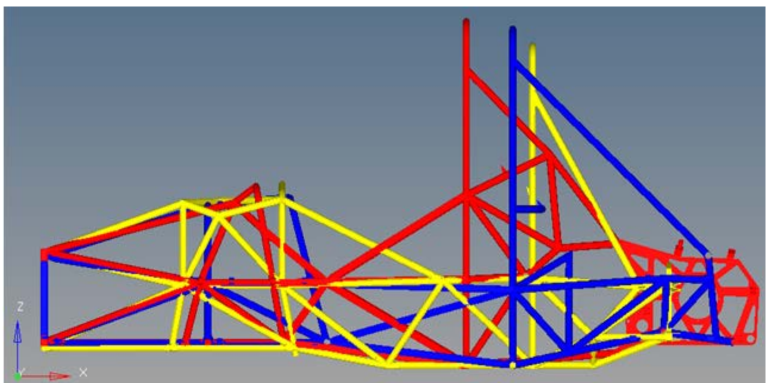

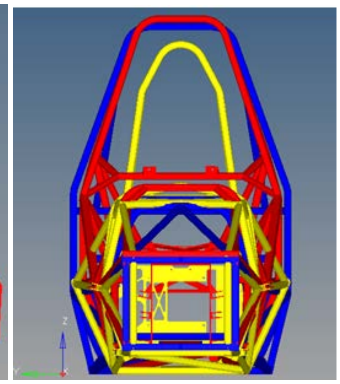

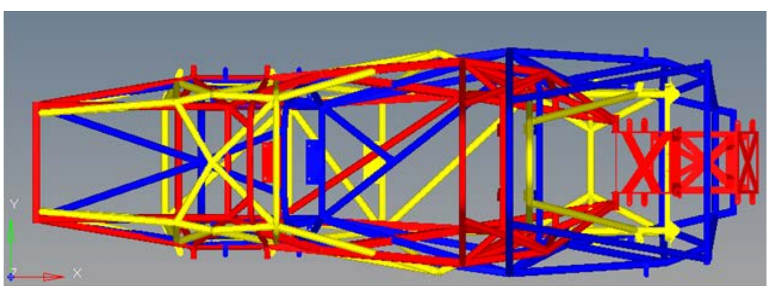

Table 6.4: 2011, 2012 & 2014 Chassis color coding

Color	Chassis
(blue)	2011
(red)	2012
(yellow)	2014

Fig 6.5: TU FSAE Chassis 2011, 2012 & 2014

Table 6.5: 2011, 2012 & 2014 Chassis length comparison

Sr. No.	Chassis	Length (mm)	Difference w.r.t 2014
1	2011	2344.1	+ 189.8
2	2012	2416.5	+ 262.2
3	2014	2154.3	0

Chassis lengths of all vehicles and difference in length of 2011 & 2012 vehicle chassis as compared to 2014 chassis (being of minimum length) are shown in table 6.5.

6.3 TU FSAE CHASSIS FE MODELING

The CAD model of the chassis was imported into Hypermesh. Firstly, the geometry cleaning was done in Hypermesh required to achieve proper quality of the elements in the meshing process. All the broken edges were repaired and the pipes were properly connected to each other at the joint locations for ensuring proper mesh connectivity.

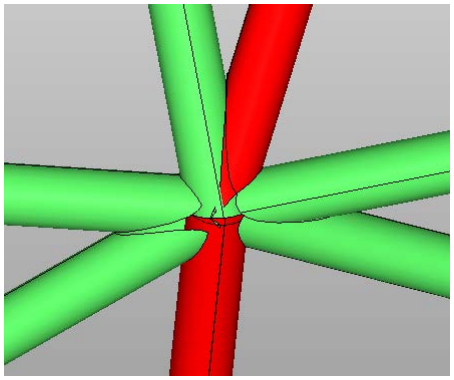

(a) Before Geometry Cleanup

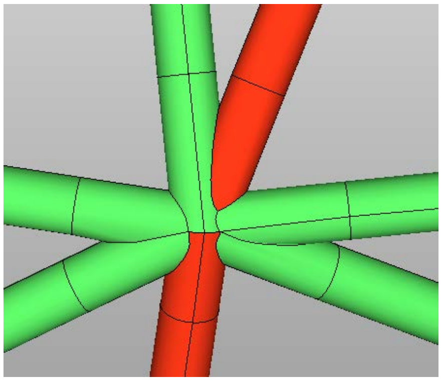

(b) After Geometry Cleanup

Fig 6.6: Chassis Geometry Editing

After geometry cleanup, the pipes in the chassis model were meshed using 2d shell elements. PSHELL property cards with different thickness were assigned to the elements with a MAT1 material card with the properties of steel. The rear bulkhead of the 2012 & 2014 chassis was meshed using 3d tetramesh elements.

Following criteria for element quality has been maintained in order to obtain the best optimized mesh.

Table 6.6: Element Quality check criteria

(a) For 2D elements

Warpage	<	25^0
Jacobian	>	0.7
Length	>	3 mm
Max % of trias	<	3%
Min quad angle	>	45^0
Max quad angle	<	135^0
Min tria angle	>	25^0
Max tria angle	<	130^0

(b) For 3D elements

Tetra collapse	>	0.2

6.3.1 FE Model for 2011 Chassis

The FE model of TU FSAE 2011 Chassis prepared using Hypermesh is shown in fig 6.7. The detailed views of various sections of the chassis are also shown.

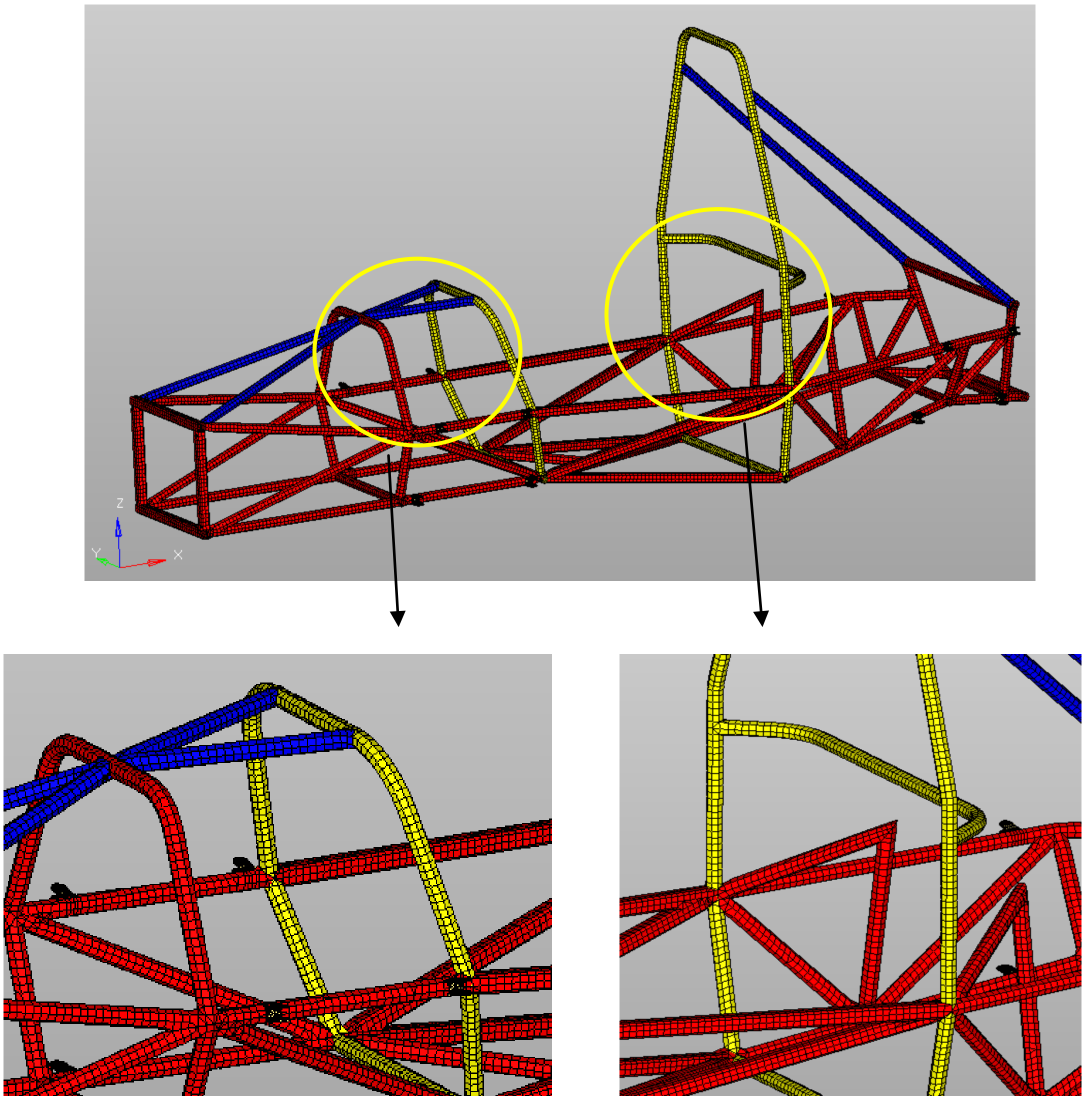

Fig 6.7: FE model of TU FSAE 2011 Chassis

6.3.2 FE Model for 2012 Chassis

The FE model of TU FSAE 2012 Chassis prepared using Hypermesh is shown in fig 6.8. The detailed views of various sections of the chassis are also shown.

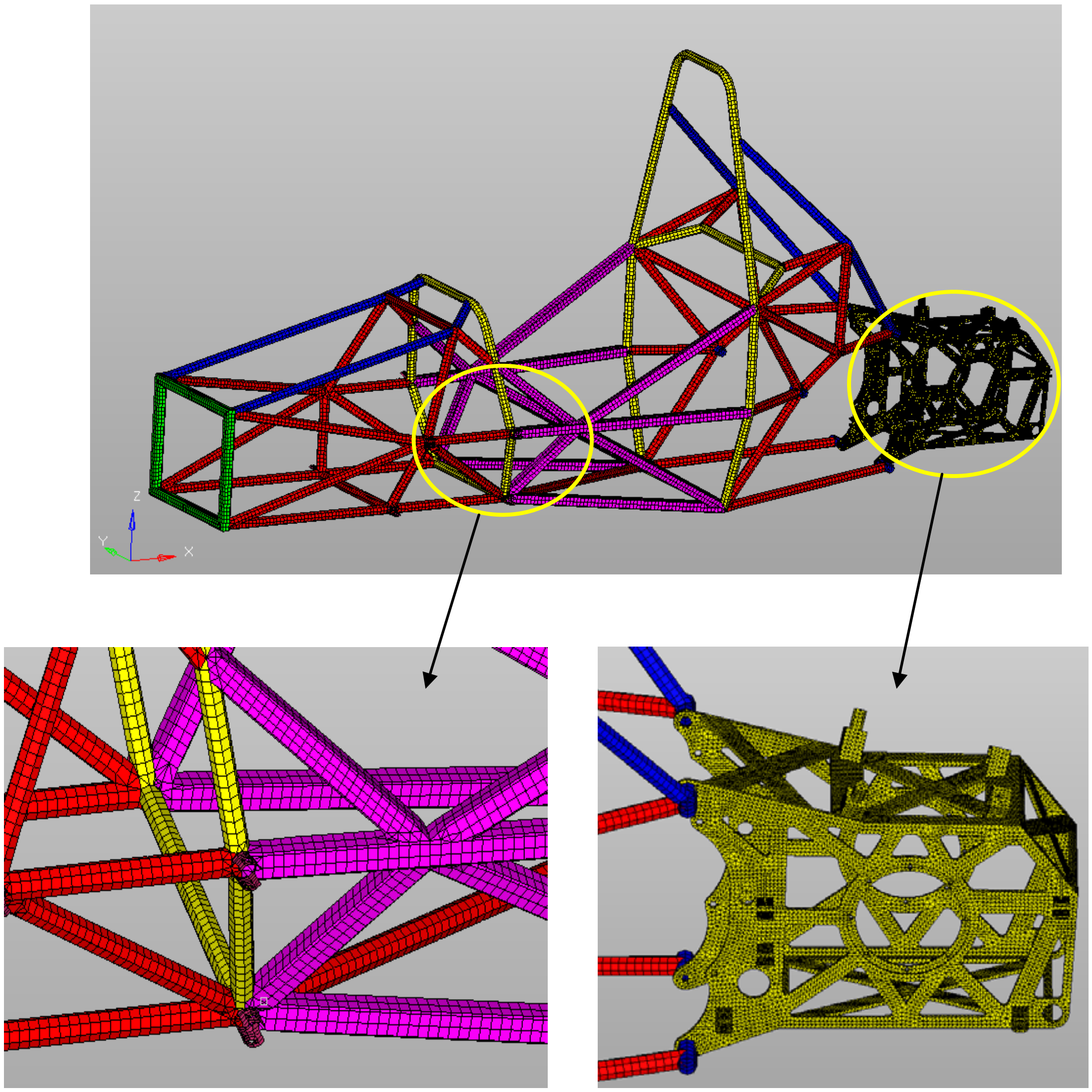

Fig 6.8: FE model of TU FSAE 2012 Chassis

6.3.3 FE Model for 2014 Chassis

The FE model of TU FSAE 2014 Chassis prepared using Hypermesh is shown in fig 6.9. The detailed views of various sections of the chassis are also shown.

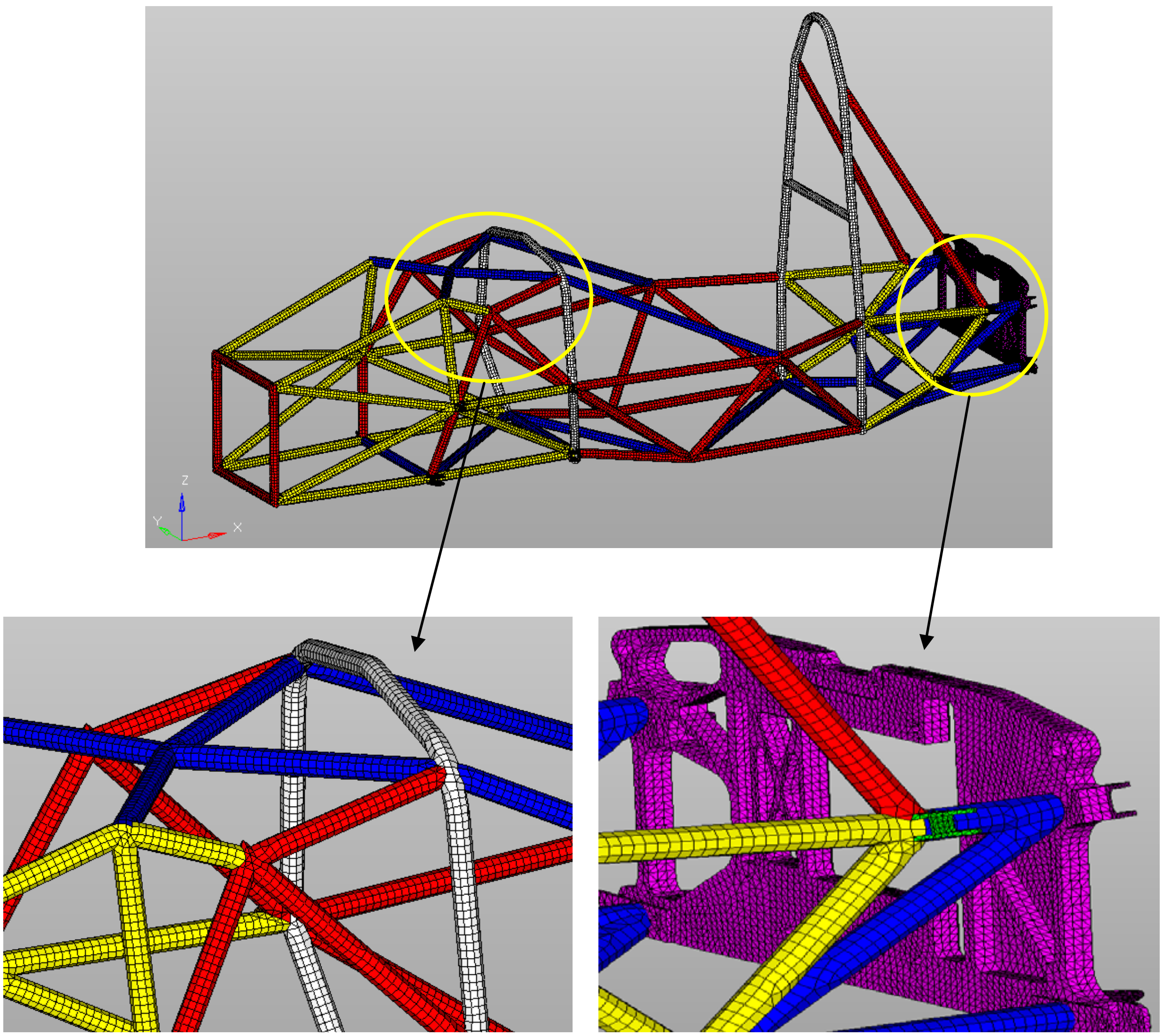

Fig 6.9: FE model of TU FSAE 2014 Chassis

6.4 TU FSAE CHASSIS STIFFNESS COMPARISON

The chassis under investigation for stiffness is of TU Formula SAE 2014 vehicle whose stiffness has been compared with chassis of TU Formula SAE 2011 & 2012 vehicles.

6.4.1 Torsion Stiffness Analysis: The chassis torsion stiffness is the average value of two sub cases - front & rear torsion stiffness. The front torsion stiffness is obtained by constraining the chassis at the rear and applying equal & opposite force of 1N at the front. Similarly, the rear torsion stiffness is obtained by constraining the chassis at the front and applying equal & opposite force of 1N at the rear.

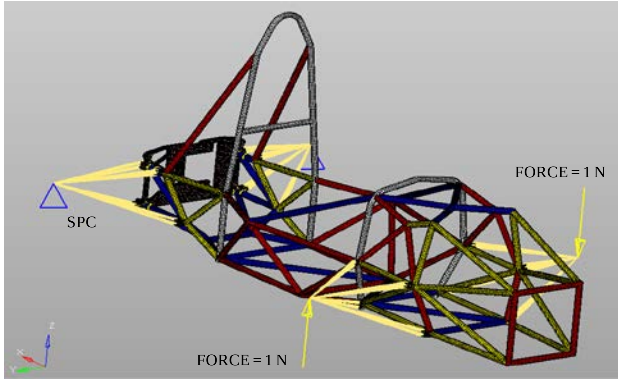

(a) Front Torsion Stiffness

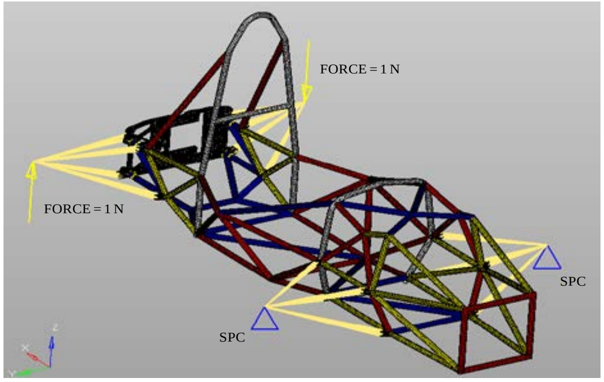

(b) Rear Torsion Stiffness

Fig 6.10: FE Model for Torsion Stiffness of Chassis 2014

The result of torsion stiffness comparison of TU FSAE 2011, 2012 & 2014 chassis is as shown below:

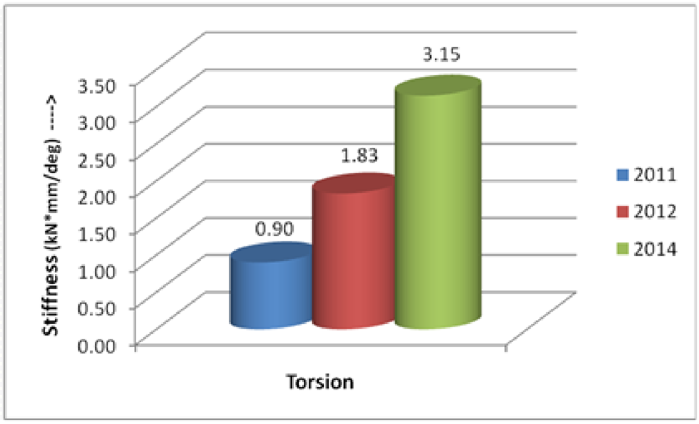

Fig 6.11: TU FSAE Chassis Torsion Stiffness comparison result

6.4.2 Lateral Stiffness Analysis: The chassis lateral stiffness is the average value of front & rear lateral stiffness. First, the chassis is constrained at the rear & unit lateral force is applied at the front (on left & right, one by one). The average value of left & right sub-cases gives the front lateral stiffness. Similarly, the rear lateral stiffness is obtained by constraining the chassis at the front & applying unit lateral force at the rear.

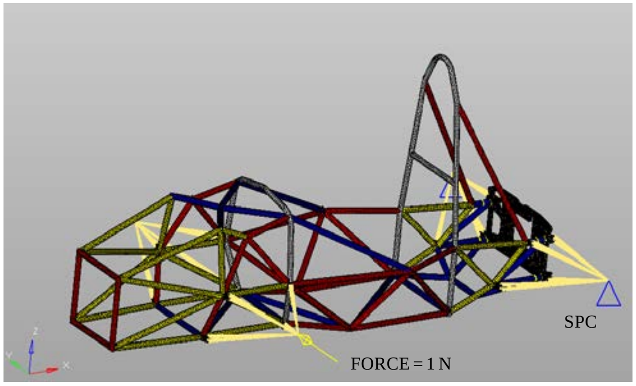

(a) Front Lateral Stiffness

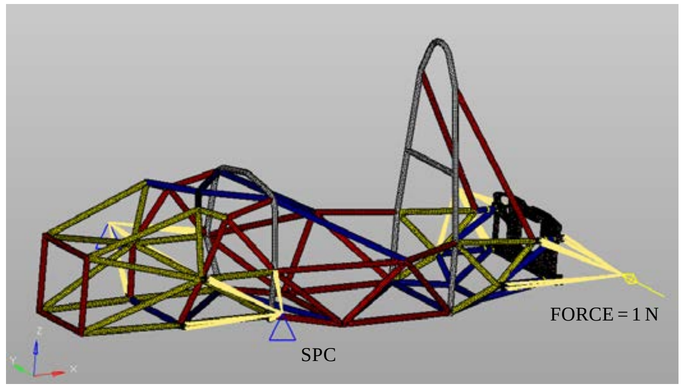

(b) Rear Lateral Stiffness

Fig 6.12: FE Model for Lateral Stiffness of Chassis 2014

The result of lateral bending stiffness comparison of TU FSAE 2011, 2012 & 2014 chassis is as shown below:

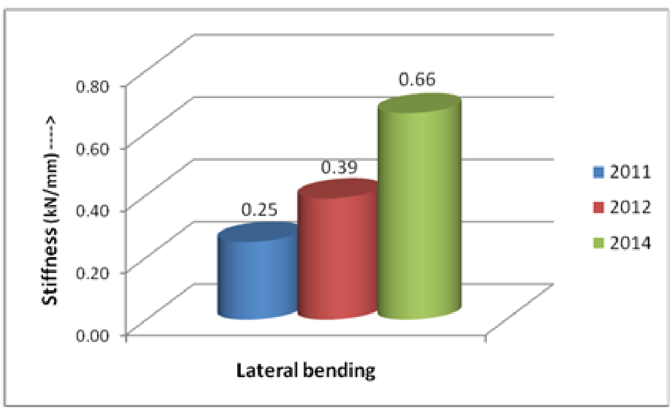

Fig 6.13: TU FSAE Chassis Lateral Stiffness comparison result

6.4.3 Vertical Bending Stiffness Analysis: The vertical bending stiffness of the chassis is obtained by applying a unit load on the center of gravity of the driver (attached to structure through seat mounting locations) and calculating the vertical displacement. The inverse of this displacement gives the vertical bending stiffness (measured in kN/mm).

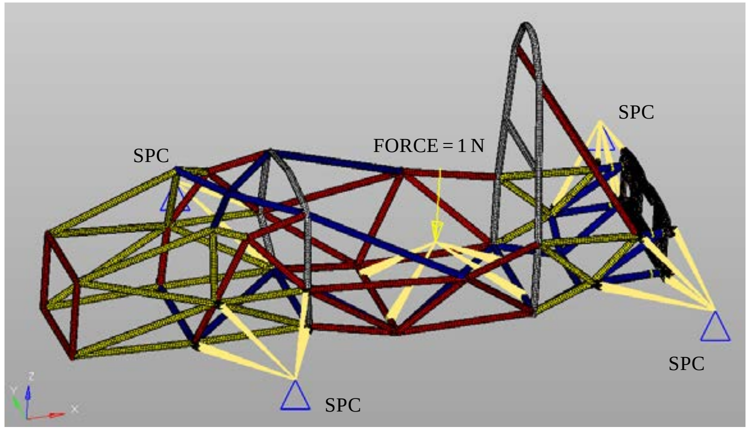

Fig 6.14: FE Model for Vertical Bending Stiffness of Chassis 2014

The result of lateral bending stiffness comparison of TU FSAE 2011, 2012 & 2014 chassis is as shown below:

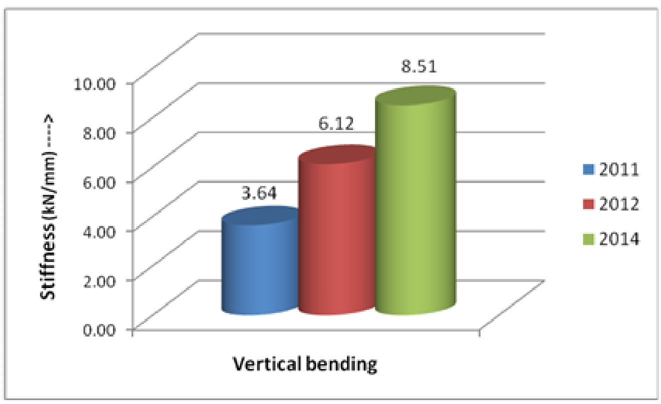

Fig 6.15: TU FSAE Chassis Vertical Bending Stiffness comparison result

6.4.4 Stiffness comparison summary:

There is significant improvement in stiffness of TU FSAE 2014 Chassis as compared to 2011 & 2012 chassis. The stiffness results are as tabulated below:

Table 6.7: TU FSAE Chassis Stiffness Comparison 2011, 2012 & 2014

Sr. No.	Stiffness	Units	Year of Make		
			2011	**2012**	**2014**
1	Torsion	kN*mm/deg	0.90	1.83	3.15
2	Lateral bending	kN/mm	0.25	0.39	0.66
3	Vertical bending	kN/mm	3.64	6.12	8.51

The comparison results are graphically depicted as shown below:

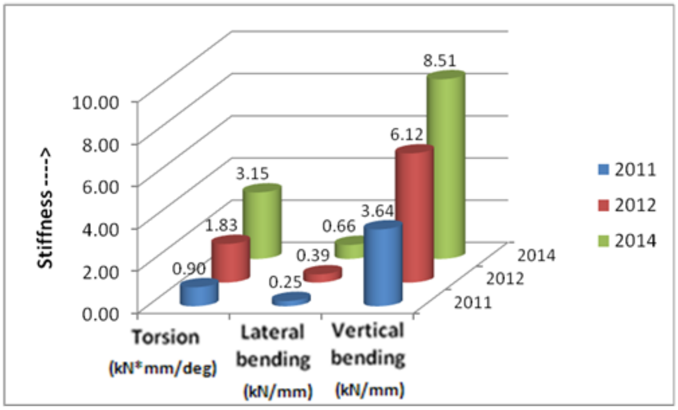

Fig 6.16: TU FSAE Chassis Stiffness Comparison 2011, 2012 & 2014

The stiffness increase of TU FSAE 2012 & 2014 chassis as compared to their respective previous year chassis is tabulated below:

Table 6.8: Stiffness Increase w.r.t previous year car

Sr. No.	Stiffness	Units	Year of Make		
			2011	**2012**	**2014**
1	Torsion	kN*mm/deg	-	0.93	1.32
2	Lateral bending	kN/mm	-	0.14	0.27
3	Vertical bending	kN/mm	-	2.48	2.39

The percentage stiffness increase of TU FSAE 2012 & 2014 chassis as compared to their respective previous year chassis is tabulated below:

Table 6.9: % Stiffness Increase w.r.t previous year car

Sr. No.	Stiffness	Units	Year of Make		
			2011	**2012**	**2014**
1	Torsion	kN*mm/deg	-	103.33	72.01
2	Lateral bending	kN/mm	-	55.76	70.20
3	Vertical bending	kN/mm	-	68.03	39.09

The mass comparison of TU FSAE 2011, 2012 & 2014 chassis is shown as follows:

Table 6.10: Mass Comparison – TU FSAE chassis

Sr. No.	**Mass**	**Units**	Year of Make		
			2011	**2012**	**2014**
1	Chassis	kg	28.34	30.26	29.48

Stiffness to Mass Ratio

One of the primary requirements defined for the chassis is a high stiffness to weight ratio. This figure is very useful for designing the chassis, and dictates a design that both maximizes stiffness and reduces weight. High stiffness improves the responsiveness of the vehicle and allows for more driver feedback, and lighter weight improves handling and overall performance. Thus, a high stiffness to weight ratio indicates that the frame will perform well.

The conventional method used for evaluating the stiffness to weight ratio is to both measure the weight of the bare frame, and calculate the stiffness, either in flexure or torsion. The ratio of these two numbers will then give the stiffness to weight ratio.

Table 6.11: Stiffness to mass ratio comparison

Sr. No.	**Stiffness/Mass**	**Units**	Year of Make		
			2011	**2012**	**2014**
1	Torsion	N*mm/deg/kg	31.8	60.5	106.9
2	Lateral bending	N/mm/kg	8.8	12.9	22.4
3	Vertical bending	N/mm/kg	128.4	202.2	288.7

6.4.5 Remarks:

1. TU FSAE 2011 Chassis has least stiffness. Although with least mass, stiffness to mass ratios are minimum.

2. TU FSAE 2012 Chassis is much stiffer than 2011 chassis. Although mass has also increased, stiffness to mass ratios in 2012 chassis are still much higher than 2011.

3. TU FSAE 2014 Chassis is even stiffer than 2012 chassis. As mass of 2014 chassis has been kept almost in between 2011 and 2012 chassis, stiffness to mass ratios are highest.

6.5 TORSION STIFFNESS ALONG CHASSIS LENGTH

Since the Torsion stiffness is most significant to the structure design of any chassis, it has been studied in more detail. This is discussed as follows:

6.5.1 FE Model & Boundary conditions

The finite element model of the TU FSAE 2011, 2012 & 2014 Chassis along with the loading and boundary conditions to determine stiffness is shown below:

Load Case Description: Rear suspension mounting points are fixed in all directions. An equal & opposite force of 1N is applied at the front (left & right) generating the torsion in the chassis. Deflections are noted at the point of application of load. The torsion stiffness at a particular section along the length of chassis is obtained from the ratio of torque applied to the angular deflection caused at that section.

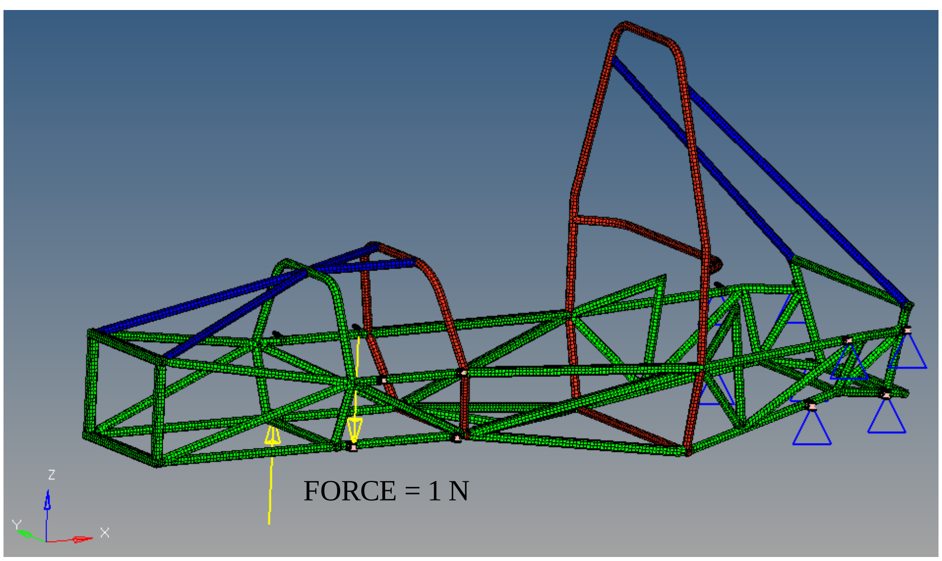

Fig 6.17: FE Model for Torsion Stiffness along length of TU FSAE Chassis 2011

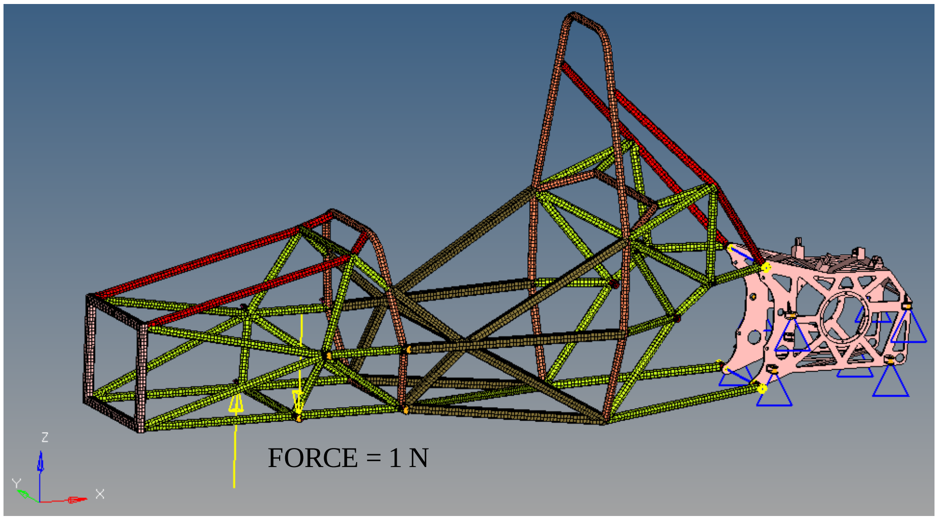

Fig 6.18: FE Model for Torsion Stiffness along length of TU FSAE Chassis 2012

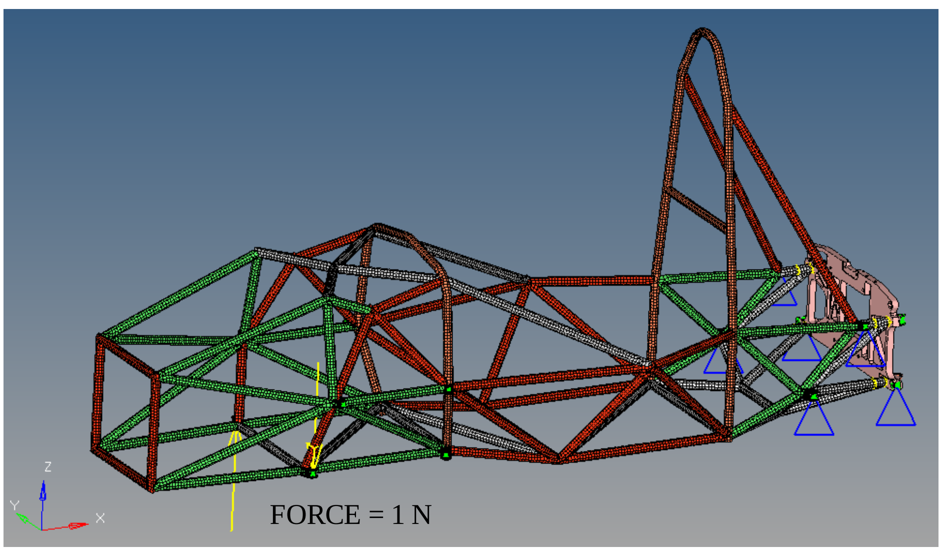

Fig 6.19: FE Model for Torsion Stiffness along length of TU FSAE Chassis 2014

6.5.2 Results

6.5.2.1 TU FSAE Chassis 2011: The stiffness of 2011 Chassis was determined at various sections/locations (mentioned 1 to 4) along the length. The stiffness value of these main locations has been highlighted in the table shown below. The stiffness was also calculated at 3 intermediate locations between the adjacent main locations. These locations are numbered in roman numerals as shown in table. The graph shows the variation of stiffness along the length of the chassis.

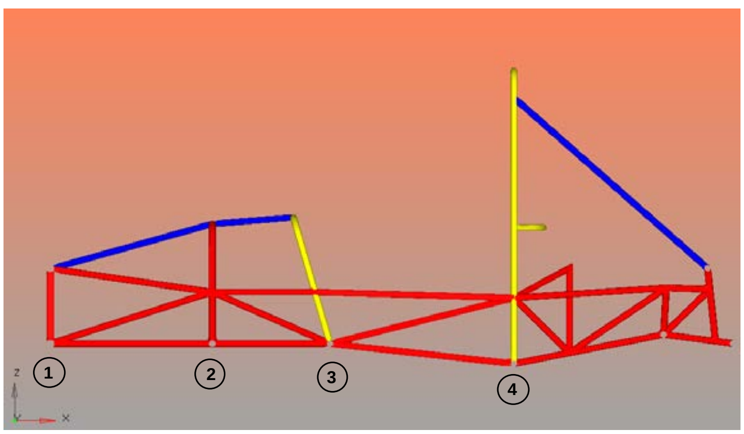

Fig 6.20: TU FSAE 2011 Chassis sections

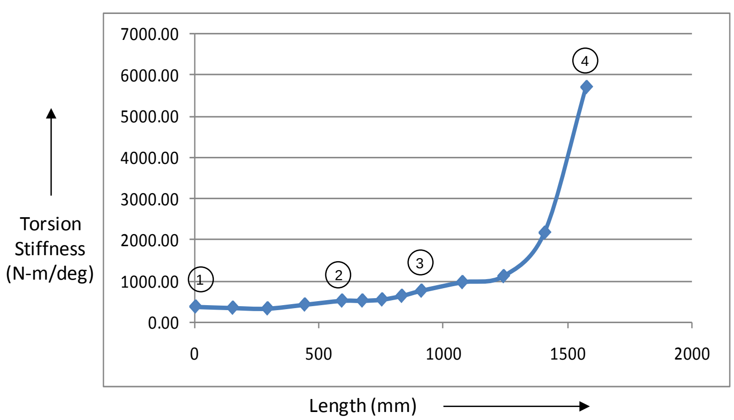

Fig 6.21: Variation of Torsion Stiffness in 2011 Chassis

Sr. No.	Distance from Front bulkhead (mm)	Torsion Stiffness (N-m/deg)
1	**0.00**	**383.27**
(i)	149.99	355.34
(ii)	289.97	339.10
(iii)	439.95	432.56
2	**590.00**	**529.19**
(iv)	671.94	530.40
(v)	751.39	556.62
(vi)	830.83	644.11
3	**910.00**	**770.12**
(vii)	1074.98	978.35
(viii)	1241.00	1123.50
(ix)	1407.01	2183.94
4	**1575.18**	**5729.04**

Table 6.12: Torsion Stiffness of 2011 Chassis

6.5.2.2 TU FSAE Chassis 2012: The stiffness of 2012 Chassis was determined at various sections/locations (mentioned 1 to 4) along the length. The stiffness value of these main locations has been highlighted in the table shown below. The stiffness was also calculated at 3 intermediate locations between the adjacent main locations. These locations are numbered in roman numerals as shown in table. The graph shows the variation of stiffness along the length of the chassis.

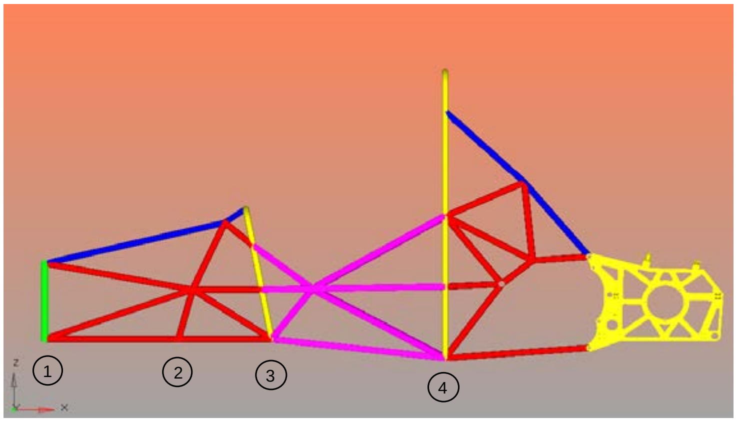

Fig 6.22: TU FSAE 2012 Chassis sections

Sr. No.	Distance from Front bulkhead (mm)	Torsion Stiffness (N-m/deg)
1	**0.00**	**554.85**
(i)	116.57	551.29
(ii)	235.79	526.64
(iii)	355.00	637.71
2	**474.22**	**811.28**
(iv)	553.05	827.72
(v)	641.75	841.77
(vi)	720.58	946.38
3	**804.22**	**1051.99**
(vii)	962.27	935.36
(viii)	1111.04	878.46
(ix)	1269.73	1245.83
4	**1419.12**	**1707.81**

Table 6.13: Torsion Stiffness of 2012 Chassis

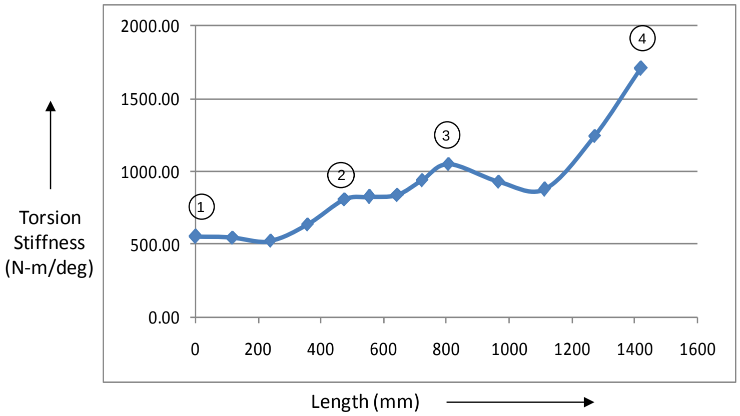

Fig 6.23: Variation of Torsion Stiffness in 2012 Chassis

6.5.2.3 TU FSAE Chassis 2014: The stiffness of 2014 Chassis was determined at various sections/locations (mentioned 1 to 5) along the length. The stiffness value of these main locations has been highlighted in the table shown below. The stiffness was also calculated at 3 intermediate locations between the adjacent main locations. These locations are numbered in roman numerals as shown in table. The graph shows the variation of stiffness along the length of the chassis.

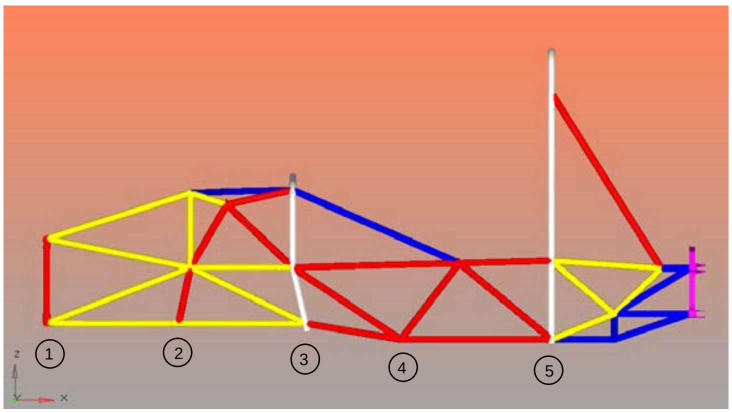

Fig 6.24: TU FSAE 2014 Chassis sections

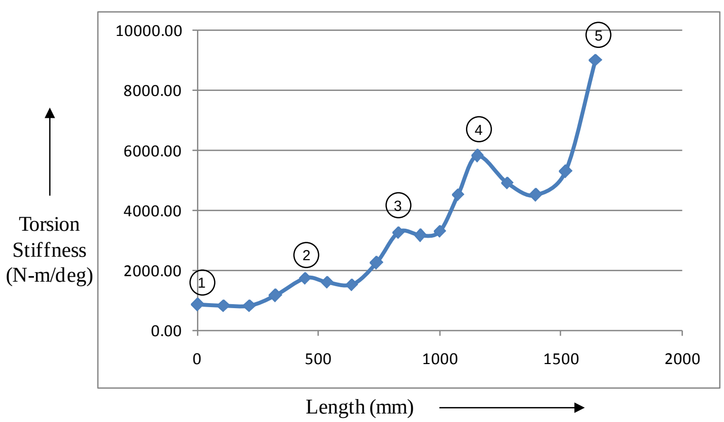

Fig 6.25: Variation of Torsion Stiffness in 2014 Chassis

Sr. No.	Distance from Front bulkhead (mm)	Torsion Stiffness (N-m/deg)
1	**0.00**	**869.90**
(i)	107.48	850.34
(ii)	214.69	841.29
(iii)	321.91	1169.35
2	**439.96**	**1759.39**
(iv)	531.92	1617.53
(v)	634.97	1549.41
(vi)	738.01	2250.02
3	**825.06**	**3286.38**
(vii)	918.65	3176.18
(viii)	996.24	3329.10
(ix)	1073.83	4547.90
4	**1151.43**	**5827.64**
(x)	1274.08	4935.73
(xi)	1396.73	4524.19
(xii)	1519.38	5296.04
5	**1642.04**	**9013.97**

Table 6.14: Torsion Stiffness of 2014 Chassis

The comparison of Torsion stiffness of the 2011, 2012 & 2014 TU FSAE Chassis along the length is shown in graph below:

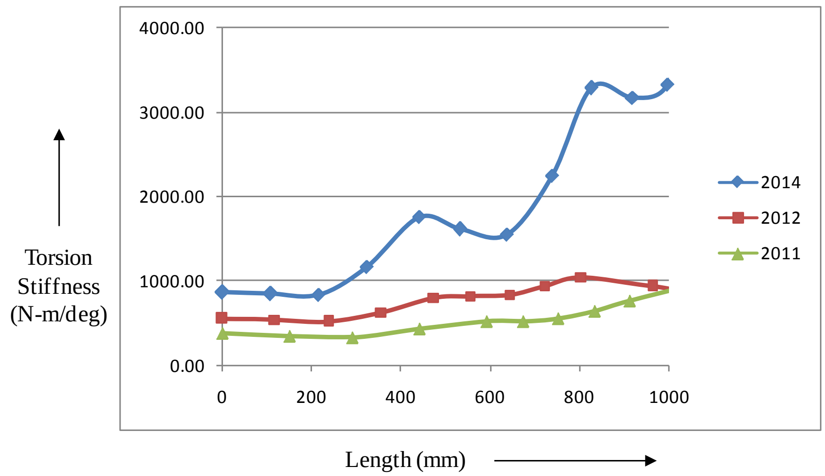

Fig 6.26: Comparison of Chassis torsion stiffness along length

6.5.3 Remarks: As observed from above graph, the torsion stiffness increases while moving towards the rear constrained suspension attachment points on chassis. This is due to the decrease in length factor affecting the torsion stiffness calculation. Further, the torsion stiffness of 2014 chassis is greater than 2011 & 2012 throughout the length.

6.6 MODAL ANALYSIS - TU FSAE CHASSIS

The finite element model for modal frequency analysis remained the same as the model in the stiffness analysis above, except for the boundary conditions changed (No loads or restraints applied) & extra masses added (corresponding to Driver & Engine).

In the free vibration modal analysis of the frame, the first to tenth natural frequencies and mode shapes were calculated. The first six harmonics of the frame structure come out to be approximately zero. This outcome is reached because the motion of the frame is completely unconstrained, allowing for 6 degrees of freedom and thus six rigid body movements (3 translational and 3 rotational). For further harmonics, the frequencies are large enough to be appreciable.

The seventh, eighth and ninth modes of vibration (first three normal modes) are of particular interest for analysis as these are first order modes in torsion and bending and representing the weakest modes of the chassis structure. Thus, the modal study shows the various prominent deformation modes of the chassis along with their natural frequency.

6.6.1 Modal Analysis of TU FSAE Chassis 2011

The FE model for the modal analysis of TU FSAE Chassis 2011 and its major normal modes of vibration along with the corresponding natural frequencies are as shown below:

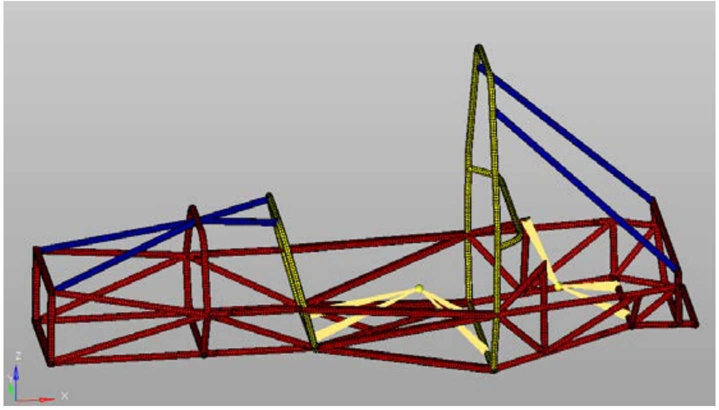

Fig 6.27: FE Model for Modal Analysis of TU FSAE Chassis 2011

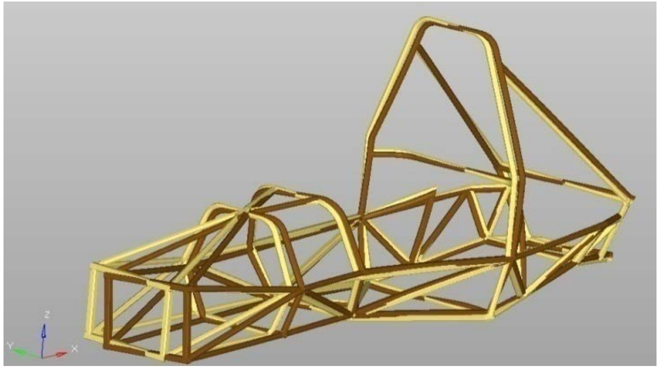

(a) Mode 7- Lateral Bending (35.3 Hz)

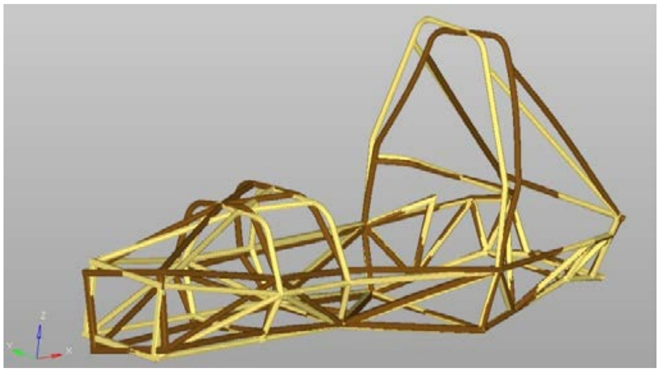

(b) Mode 8- Torsion (54.25 Hz)

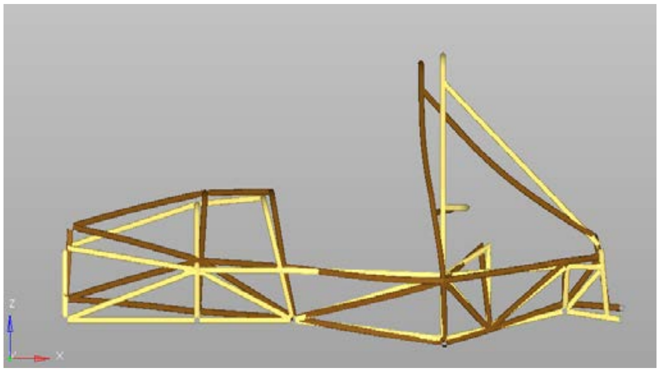

(c) Mode 9- Vertical Bending (71.88 Hz)

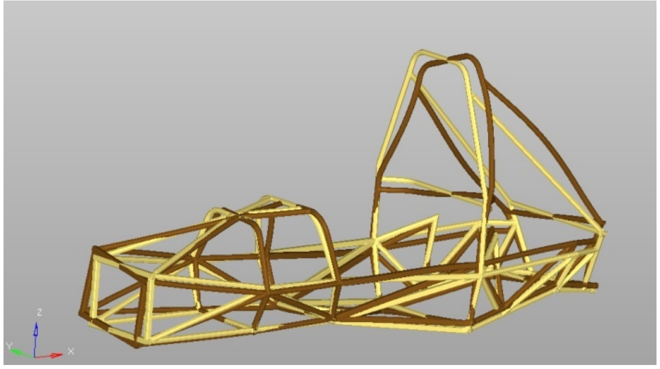

(d) Mode 10- Torsion 2nd order (79.69 Hz)

Fig 6.28: TU FSAE 2011 Chassis normal modes

6.6.2 Modal Analysis of TU FSAE Chassis 2012

The FE model for the modal analysis of TU FSAE Chassis 2012 and its major normal modes of vibration along with the corresponding natural frequencies are as shown below:

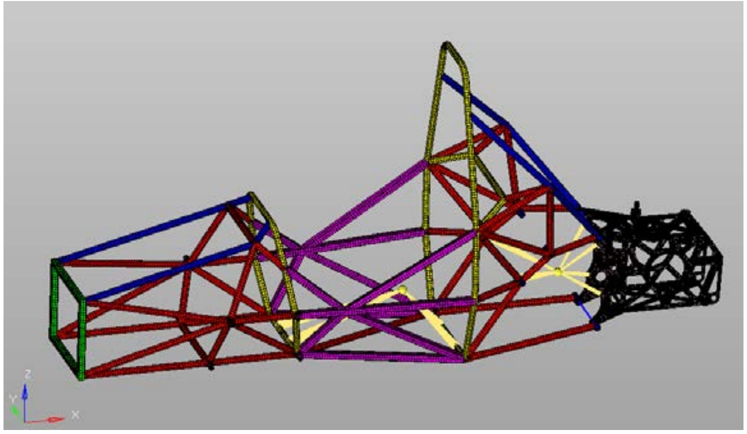

Fig 6.29: FE Model for Modal Analysis of TU FSAE Chassis 2012

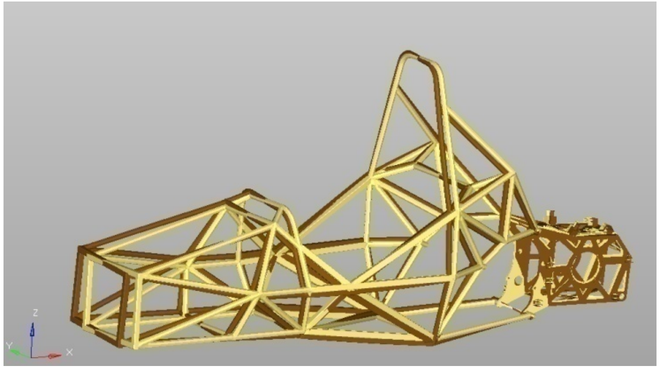

(a) Mode 7- Lateral Bending (43.87 Hz)

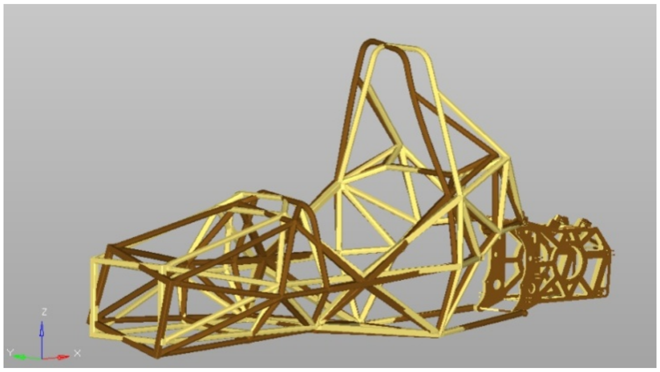

(b) Mode 8- Torsion (62.46 Hz)

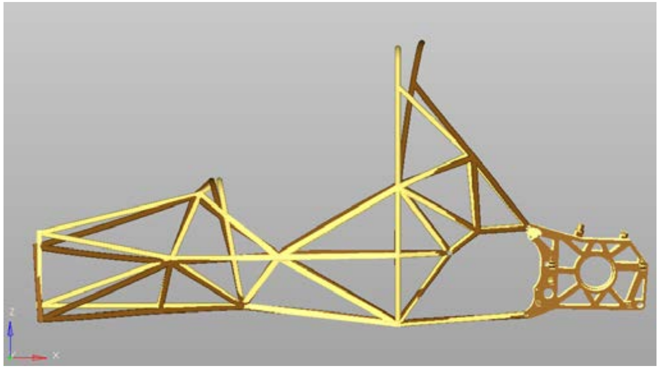

(c) Mode 9- Vertical Bending (97.78 Hz)

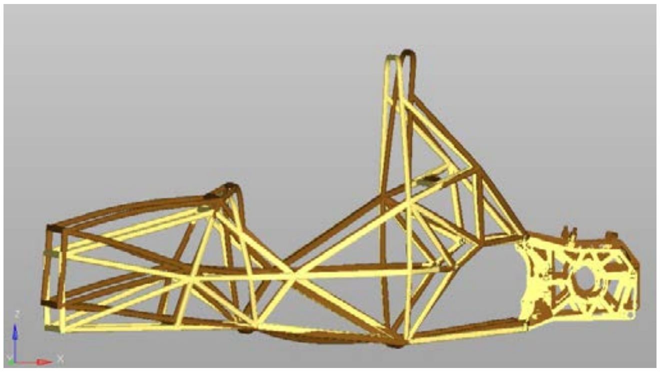

(d) Mode 10- Vertical Bending 2nd order (108.56 Hz)

Fig 6.30: TU FSAE 2012 Chassis normal modes

6.6.3 Modal Analysis of TU FSAE Chassis 2014

The FE model for the modal analysis of TU FSAE Chassis 2014 and its major normal modes of vibration along with the corresponding natural frequencies are as shown below:

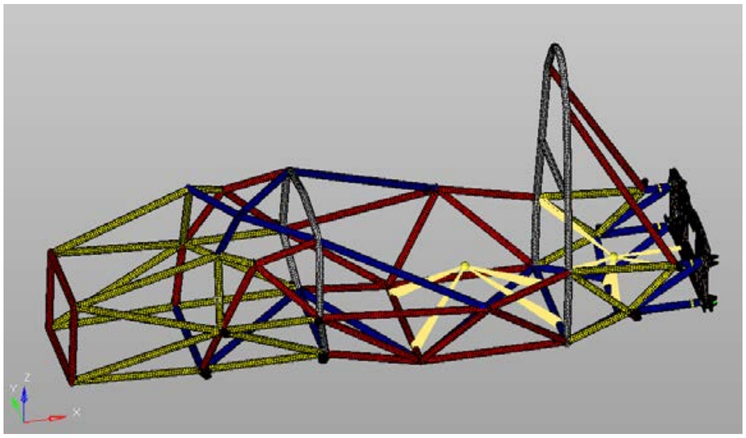

Fig 6.31: FE Model for Modal Analysis of TU FSAE Chassis 2014

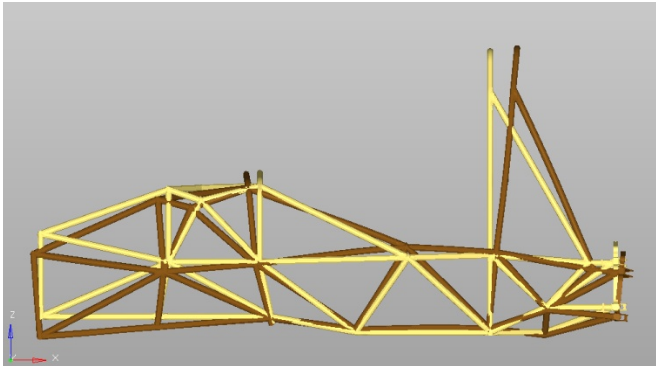

(a) Mode 7- Vertical Bending (58.01 Hz)

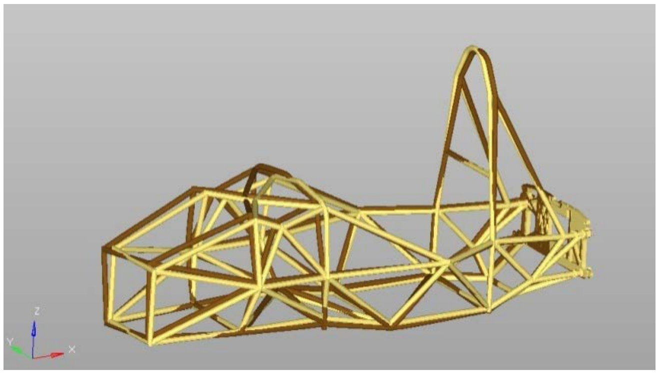

(b) Mode 8- Lateral Bending (73.88 Hz)

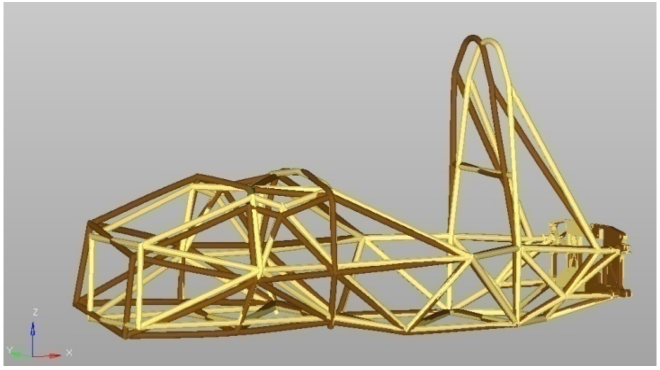

(c) Mode 9- Torsion (86.86 Hz)

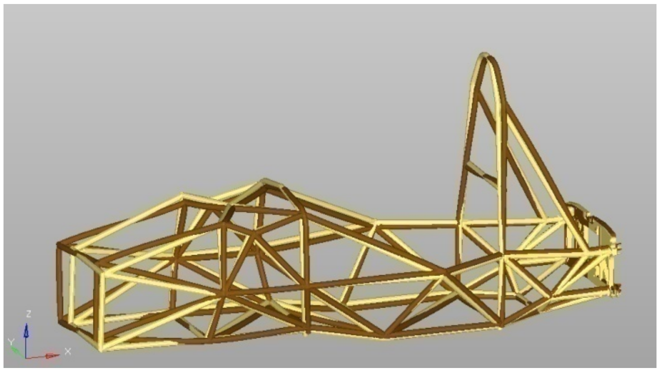

(d) Mode 10- Lateral Bending 2nd order (126.05 Hz)

Fig 6.32: TU FSAE 2014 Chassis normal modes

6.6.4 Results Summary

The result of modal analysis of TU FSAE 2011, 2012 & 2014 chassis is summarized below:

Table 6.15: Modal analysis result summary

Chassis (Year)	Normal Modes of Vibration (Hz)			
	1st mode	**2nd mode**	**3rd mode**	**4th mode**
2011	**35.3**	**54.25**	**71.88**	**79.69**
	Lateral Bending	Torsion	Vertical Bending	Torsion 2nd order
2012	**43.87**	**62.46**	**97.78**	**108.56**
	Lateral Bending	Torsion	Vertical Bending	Vertical Bending 2nd order
2014	**58.01**	**73.88**	**86.86**	**126.05**
	Vertical Bending	Lateral Bending	Torsion	Lateral Bending 2nd order

6.6.5 Remarks

The modal analysis result shows that the natural frequency of first normal mode of vibration has significantly improved in TU FSAE 2014 chassis as compared to 2011 & 2012 chassis. Further, the torsion mode frequency has been increased to 86.8 Hz in 2014 chassis which is much higher than the same in 2011 & 2012 chassis.

6.7 CONCLUSION

The FE analysis of TU FSAE 2011, 2012 & 2014 chassis has been carried out for determining their normal modes as well as chassis stiffness.

- The modal study shows the significant increase in natural frequency of first normal mode of 2014 chassis than that of 2011 & 2012 chassis reducing the possibility of resonance due to input excitations from engine & suspension.
- The stiffness study shows that torsion, lateral & vertical bending stiffness & stiffness to weight ratio of TU FSAE 2014 chassis is significantly higher than that of 2011 & 2012 chassis.

CHAPTER 7

TOPOLOGY OPTIMIZATION

7.1 INTRODUCTION

Structural design problems require the fulfillment of specific objectives while satisfying a set of performance constraints. In the automotive and aerospace worlds, this traditionally requires numerous iterations using finite element analysis results that drive design changes, and the final design is often arrived at via a trial and error approach. This iteration process can prove to be a very time-consuming and thus costly endeavor. While this technique has obviously been effective in meeting design requirements, the final solution does not necessarily represent the best solution - only one that has successfully met the objective. Furthermore, the quality of the final design relies heavily on the quality and potential of the initial design attempts. This is due to the fact that, as the design progresses, the freedom to make significant changes diminishes over time. Therefore, in the interest of time and quality, it is very important to have a good initial design solution early in the process.

Another drawback of the traditional design method is the fact that engineers tend to think intuitively. Sometimes the optimum solution can be quite counterintuitive, and thus a great solution can go justifiably overlooked because it does not seem plausible or reasonable. On the contrary, a design can include an overly complicated network of reinforcing ribs, for example, that were deemed necessary by the design engineer, when the ideal optimized solution is actually much simpler.

Topology optimization is a method used to determine the optimum shape and distribution of material within a given design space for a given set of design constraints based on responses obtained from a finite element analysis.

7.2 THEORY OF OPTIMIZATION

The basic principle of optimization is to find the best possible solution under given circumstances. One example of optimization is finding the quickest route when using the public transportation system or, as in the case of structural optimization, finding the optimal distribution of material that satisfies some given requirements. This is most often done by decisions made by the passenger or the engineer from their own experience and knowledge about the subject.

The objective of the optimization problem is often some sort of maximization or minimization, for example minimization of required time or maximization of stiffness. To be able to find the optimum solution the `goodness' of a solution depending on a particular set of design variables needs to be expressed with a numerical value. This is typically done with a function of the design variables known as the objective function.

The OptiStruct® topology optimization algorithm solves a structural optimization problem in which the goal is to minimize an objective function subject to constraint functions comprised of finite element responses. Formally, the problem can be written as follows:

Objective:	Minimize $W(x)$	(7.1)
Constraints:	$g(x)-g^{upper} \leq 0$	(7.2)
Design Variables:	$x^{lower} \leq x \leq x^{upper}$	(7.3)

where the objective function **W** and the constraint functions **g** are structural responses. Typical structural responses used to define the objective and constraint functions include mass, volume fraction, compliance, frequency and displacement. Commonly, the objective for a topology optimization study is to minimize the weighted compliance with element density as the design variable. By allowing the normalized element density to vary between 0 and 1, the end result of the topology optimization should be a mesh in which the elements take on a density value of either 0 or 1. A low density value represents a void, and a high density value indicates solid material. By masking elements of low density, the shape of the optimized structure is revealed. Overall, the optimization algorithm involves discretizing the design space into a finite element mesh, calculating the elemental material properties, and iteratively altering the material distribution (element density) and re-calculating until convergence is reached at a solution that best meets the objective function.

This technique can be used very early in the design stage to ensure that the final design of the structure not only meets the requirements, but represents the mathematically best solution based on the design constraints. Today the method is widely accepted for bracket-type structures and has already proven to be a huge benefit to many of the large aerospace and automotive corporations.

7.3 OPTIMIZATION PROCEDURE

Concept generation

The process of Concept generation is an iterative process where the problem formulation and design domain is incrementally improved until the best possible solution is found. A flow chart for the Concept generation is presented followed by the description of each step.

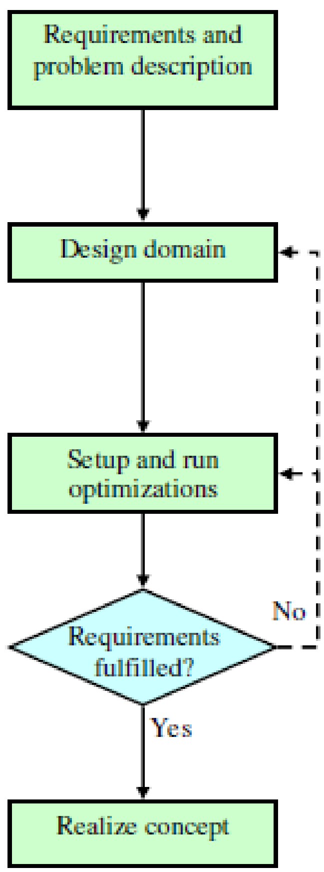

Fig 7.1: Concept generation [12]

The Concept generation process is explained in following steps:

- The objective of the optimization work and all requirements for the final product are presented and translated to numerical requirements. Requirements on geometrical interface, loads, mechanical responses, manufacturability etc. are specified.
- A design domain is generated from geometrical requirements. The idea is to start with a simple domain leaving much for the optimization to do and successively refine it after optimizations. This step needs to be redone for further iterations.
- The design is discretized using FE mesh. Loads and constraints are specified. Design domain, optimization parameters, objective function and optimization constraints are defined. Topology optimization is run.
- The topologies are analyzed to see if it fulfills the requirements and if it is possible to realize in a concept.
- A topology is chosen and a concept is interpreted from it.

The procedure for setting up and performing a topology optimization using the Hyperworks software suite is described in the following steps:

- Acquire/create a FE model.
- Define loads and boundary conditions.
- Define design variables and constraints on the design variables.
- Define responses that will be used as objective or constraints.
- Formulate optimization objective.
- Define constraints on responses.

7.4 COMPONENT OPTIMIZATION OF TU FSAE 2014 VEHICLE

The Topology Optimization carried on various components of TU FSAE 2014 vehicle structure is as explained below:

7.4.1. Chassis Bulkhead

Topology Optimization was done on the rear bulkhead using Altair Hyperworks® Optistruct module to minimize weight and maximize stiffness which is manufactured from Aluminium 2014 T6 alloy. Use of rear bulkhead helps in easy engine removal and easy disassembly of Engine-drive train assembly. Lightweight bulkhead not only causes weight reduction to overall chassis structure but also aids in easy manual assembly & disassembly with main chassis.

7.4.1.1 Initial Model: The CAD and FE model of Bulkhead base model whose topology optimization needs to be carried out is as shown.

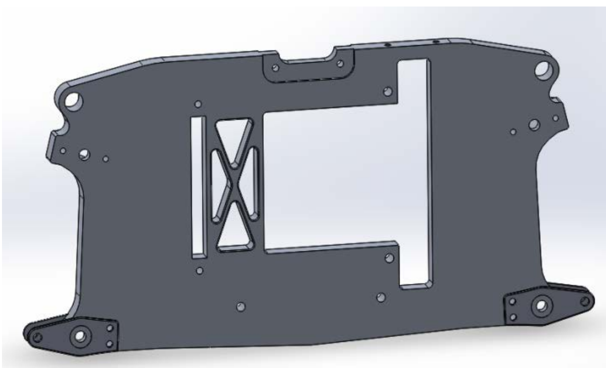

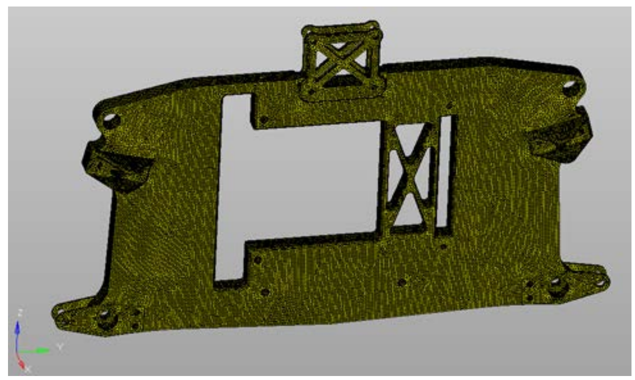

(a) CAD model (b) FE model

Fig 7.2: Chassis Bulkhead Base model

The design & non design space defined in the base model of Bulkhead during topology optimization setup and results obtained after optimization process are shown below:

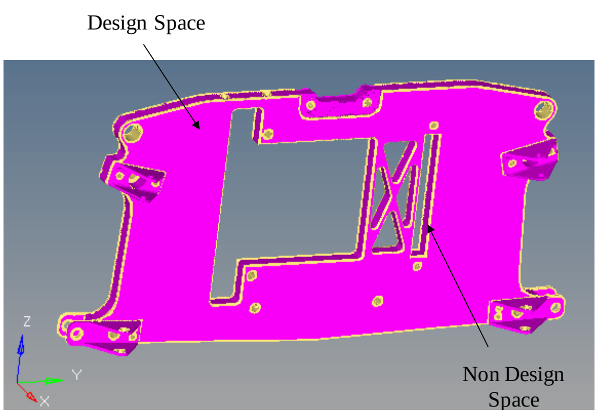

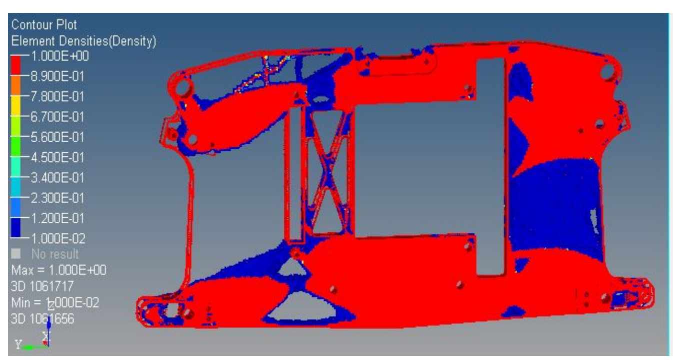

(a) Topology Optimization Set-up (b) Topology Optimization Contour

Fig 7.3: Chassis Bulkhead Topology Optimization (Base)

The design & non design space defined in the Final model of Bulkhead during topology optimization setup and results obtained after optimization process are shown below:

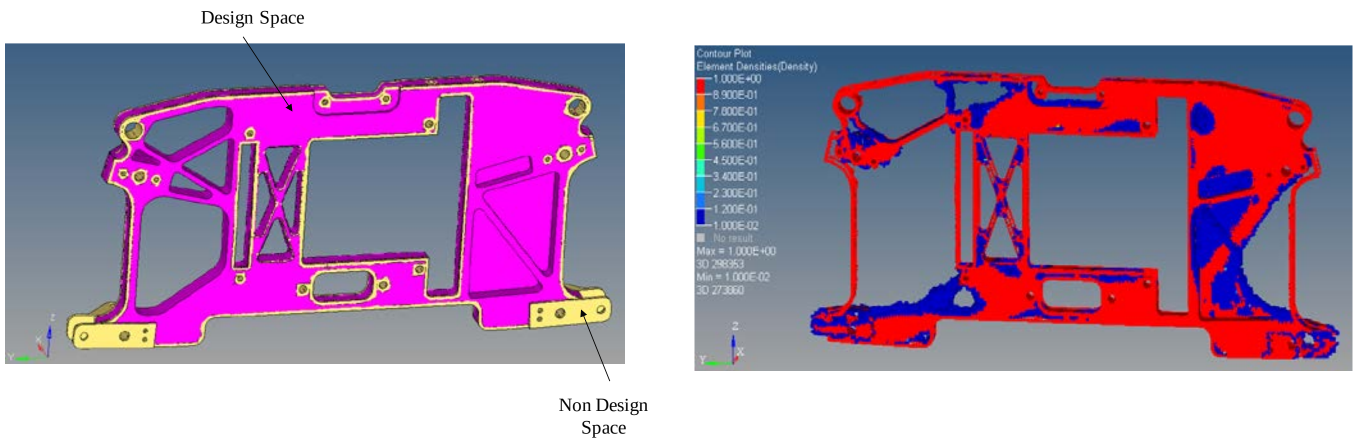

(a) Topology Optimization Set-up (b) Topology Optimization Contour

Fig 7.4: Chassis Bulkhead Topology Optimization (Final)

7.4.1.2 Final Model: The final optimized model obtained after considering both design & manufacturing constraints is as shown.

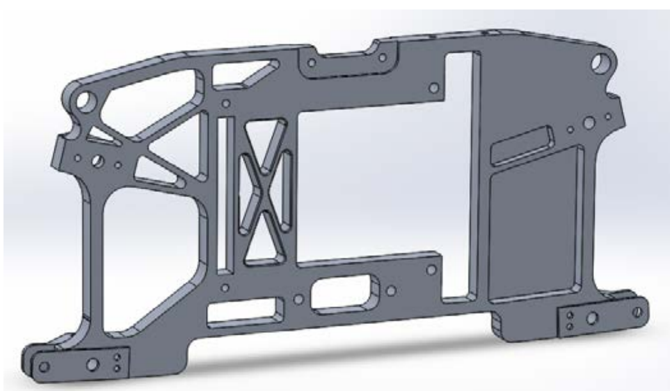

Fig 7.5: Chassis Bulkhead (Optimized model)

The mass saving as a result of Topology Optimization process is as shown in table 7.1.

Table 7.1: Chassis Bulkhead mass saving

Sr. No.	Component	Mass (kg)			
		Base model	Optimized model	Saving	% Saving
1	Bulkhead	4.2	2.6	1.6	38.1

7.4.1.3 Remarks

A mass saving of **1.6 kg** has been achieved through topology optimization of the Chassis Rear Bulkhead. This amounts to around 38% weight reduction over the base model.

7.4.2 Suspension Uprights

7.4.2.1 Front Upright

Initial Model: The CAD and FE model of Front Upright base model whose topology optimization needs to be carried out is shown below.

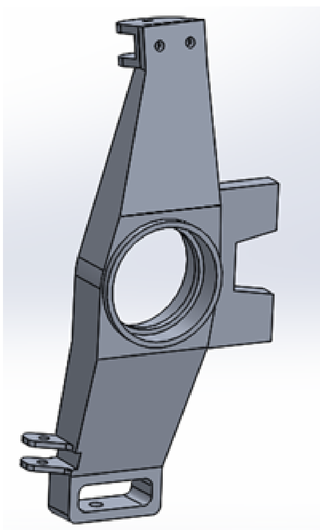

(a) CAD model

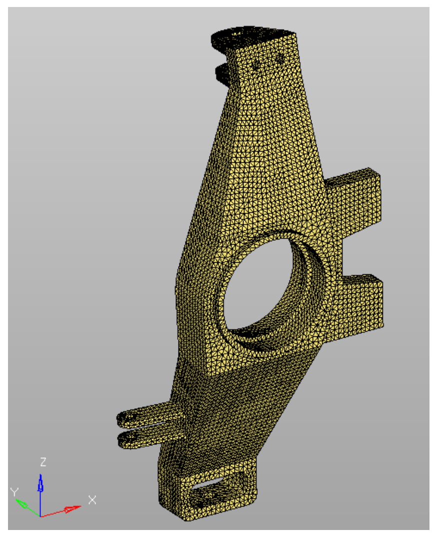

(b) FE model

Fig 7.6: Front Upright Base model

Optimization: For carrying out the topology optimization of Front upright, design and non design space was defined. The area colored pink was considered as the design space as shown in fig 7.7. The remaining portion was considered as the non design space.

The volume fraction was considered as the design constraint whose maximum value was taken as 0.3. The objective was to minimize the compliance so as to increase the stiffness.

The design & non design space defined in the base model of Front upright during topology optimization setup and results obtained after optimization process are as shown:

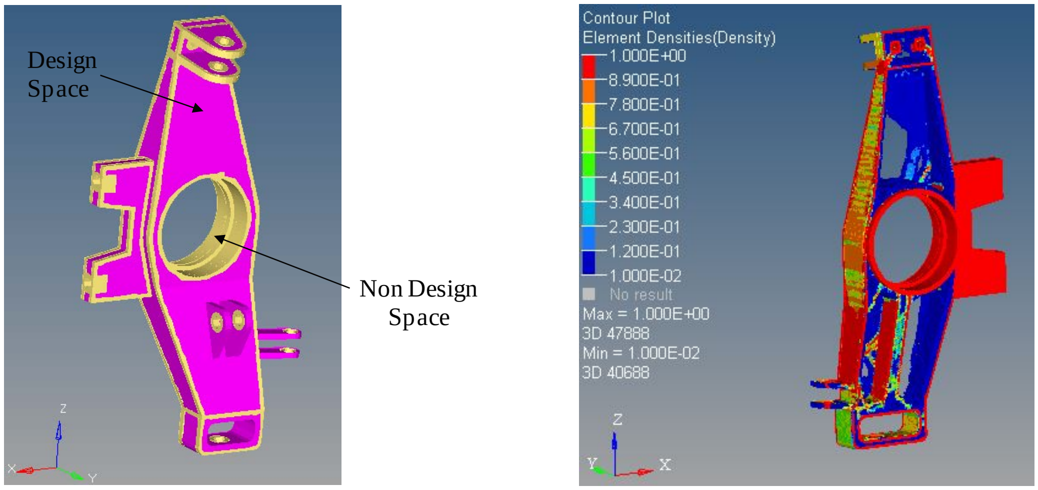

(a) Topology Optimization Set-up (b) Topology Optimization Contour

Fig 7.7: Front Upright Topology Optimization

<u>Final Model</u>:

The final optimized model of Front upright obtained after considering both design & manufacturing constraints is shown below.

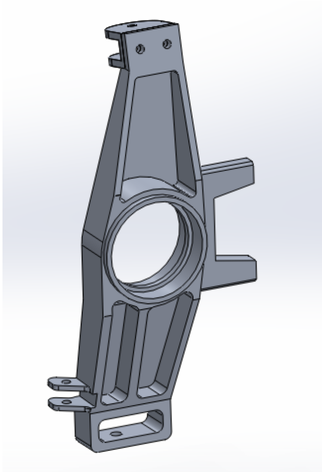

Fig 7.8: Front Upright (Optimized model)

7.4.2.2 Rear Upright

<u>Base Model</u>: The CAD and FE model of Rear Upright base model whose topology optimization needs to be carried out is shown below.

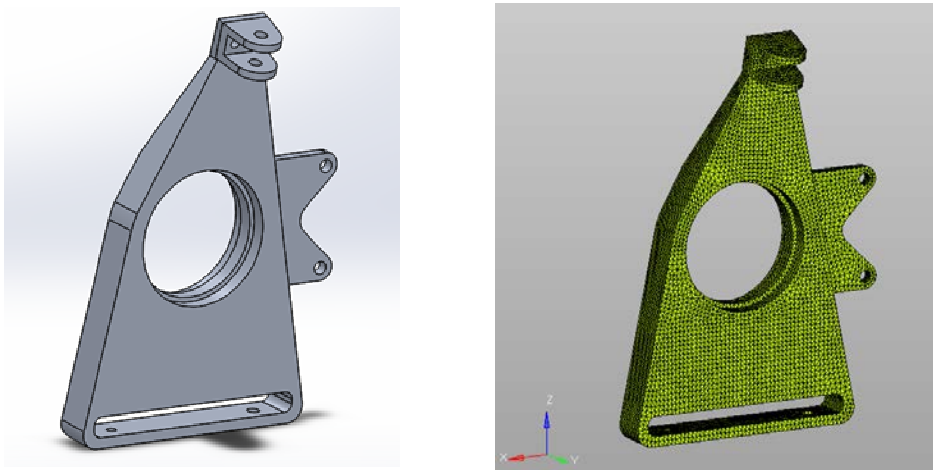

(a) CAD model (b) FE model

Fig 7.9: Rear Upright (Base model)

<u>Optimization</u>: For carrying out the topology optimization of Rear upright, design and non design space was defined. The area colored pink was considered as the design space as shown in fig 7.10. The remaining portion was considered as the non design space.

The volume fraction was considered as the design constraint whose maximum value was taken as 0.3. The objective was to minimize the compliance so as to increase the stiffness.

The design & non design space defined in base model of Rear upright during topology optimization setup and results obtained after optimization process are shown below:

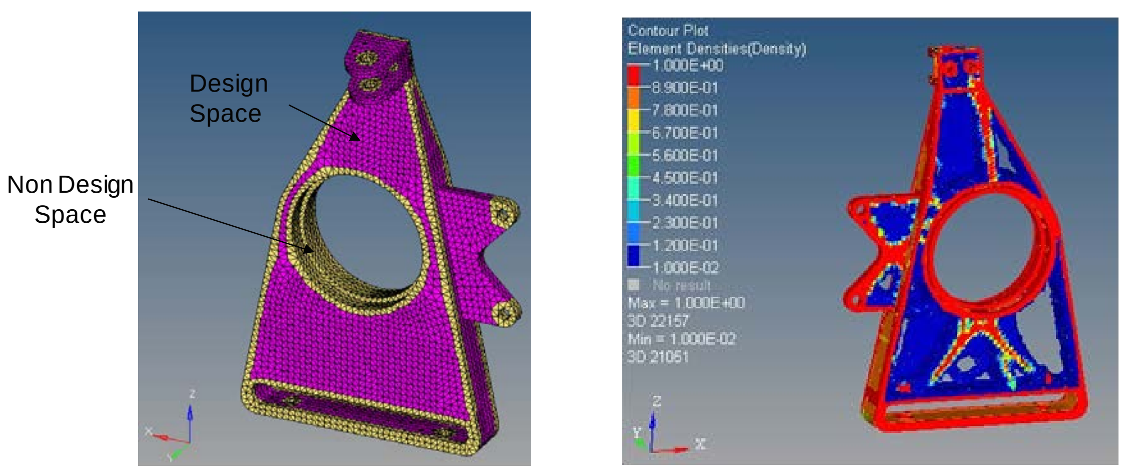

(a) Topology Optimization Set-up (b) Topology Optimization Contour

Fig 7.10: Rear Upright Topology Optimization (Base model)

Modified model 1: The CAD and FE model of Rear upright modified model 1 is shown below.

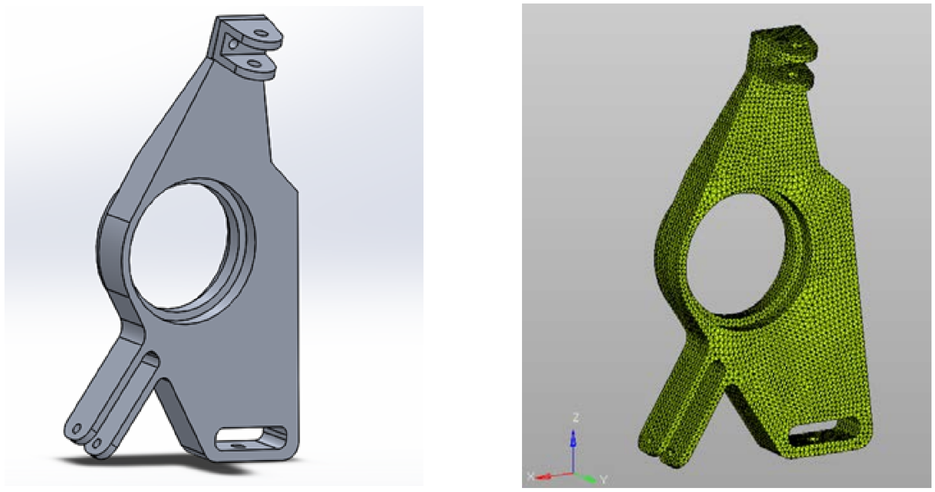

(a) CAD model (b) FE model

Fig 7.11: Rear Upright (Modified model 1)

The design & non design space defined in the modified model 1 of Rear upright during topology optimization setup and results obtained after optimization process are shown below:

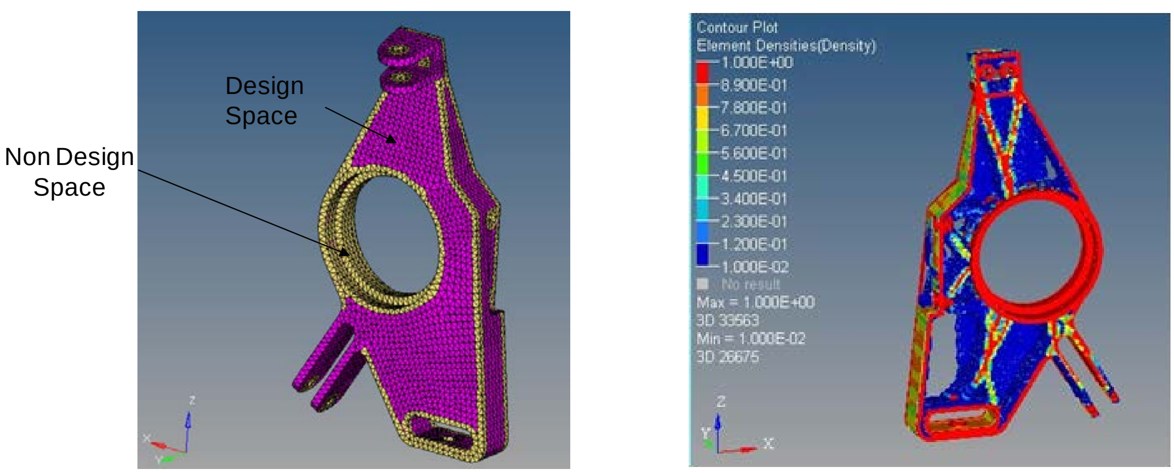

(a) Topology Optimization Set-up (b) Topology Optimization Contour

Fig 7.12: Rear Upright Topology Optimization (Modified model 1)

<u>Modified model 2</u>: The CAD and FE model of Rear upright modified model 2 is shown below.

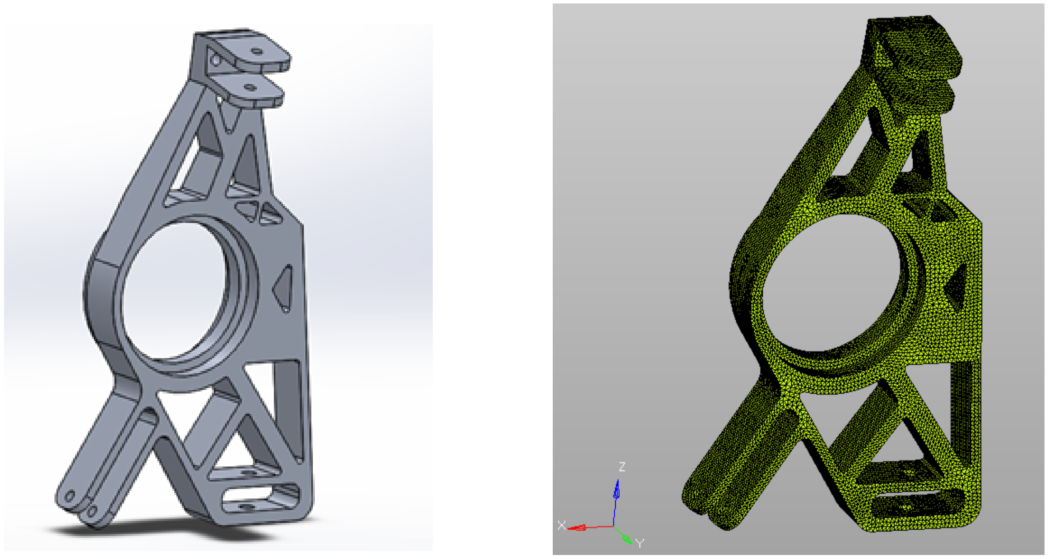

(a) CAD model (b) FE model

Fig 7.13: Rear Upright (Modified model 2)

The design & non design space defined in the modified model 2 of Rear upright during topology optimization setup and results obtained after optimization process are shown below:

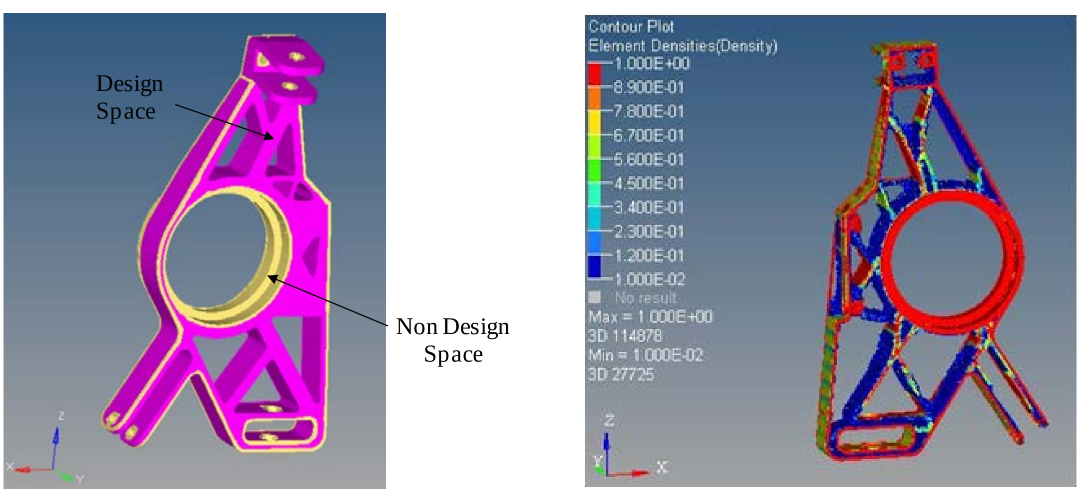

(a) Topology Optimization Set-up (b) Topology Optimization Contour

Fig 7.14: Rear Upright Topology Optimization (Modified model 2)

Final Model: The final optimized model of Rear upright obtained after considering both design & manufacturing constraints is shown below.

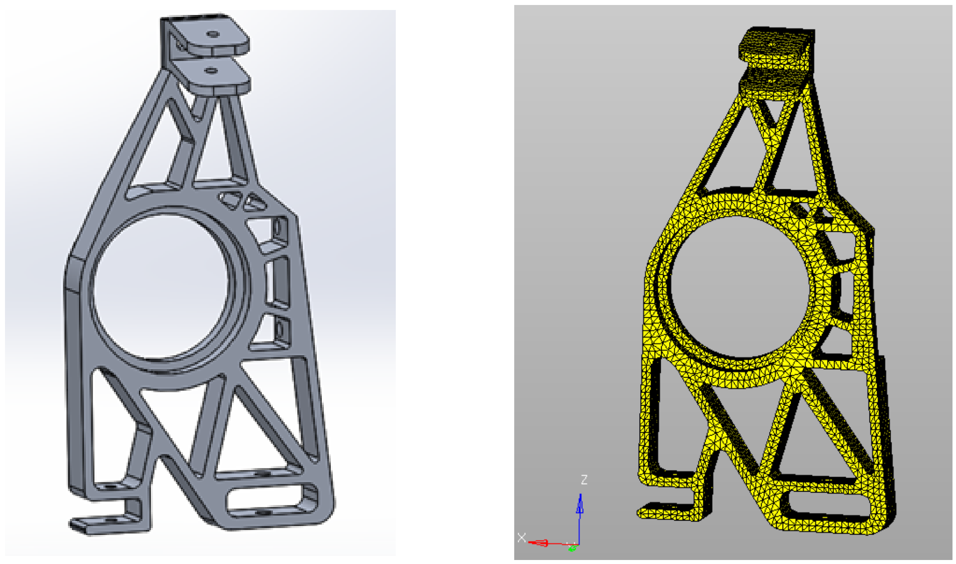

(a) CAD model (b) FE model

Fig 7.15: Rear Upright (Final model)

The design & non design space defined in Final model of Rear upright during topology optimization setup and results obtained after optimization process are shown below.

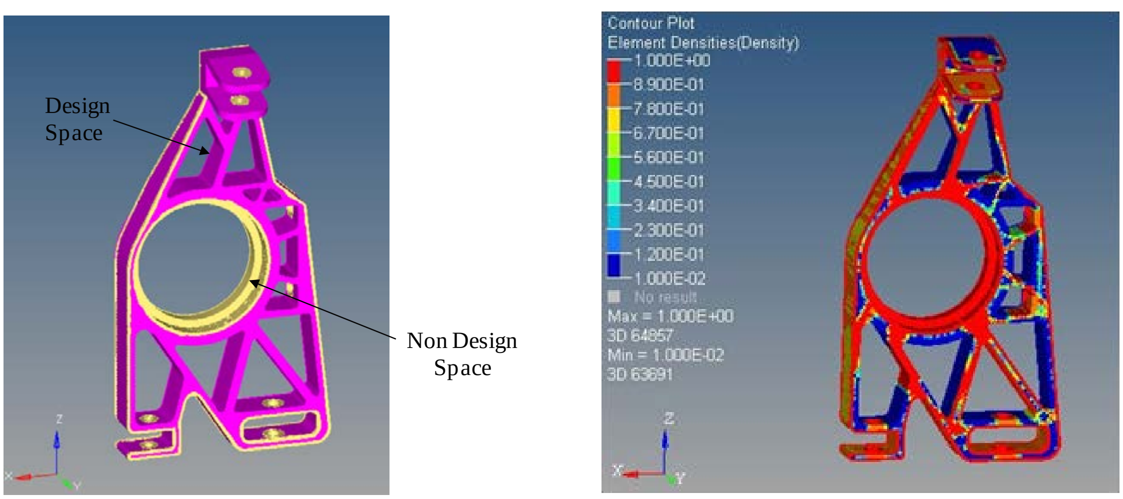

(a) Topology Optimization Set-up (b) Topology Optimization Contour

Fig 7.16: Rear Upright Topology Optimization (Final model)

The design of Rear Upright during various iterations of the optimization process is as shown below:

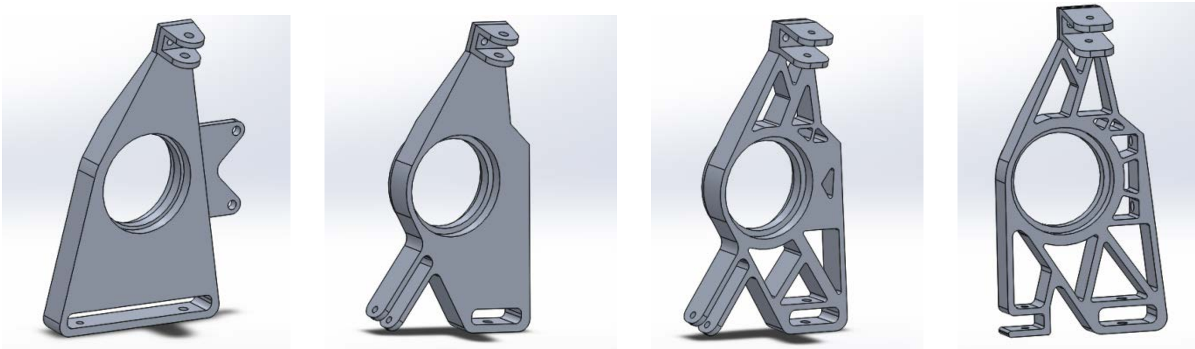

(a) Base model (b) Modified model 1 (c) Modified model 2 (d) Optimized model

Fig 7.17: Concept generation of Rear upright through topology optimization

The mass savings in Rear Upright during various iterations of the optimization process (w.r.t previous iteration & also cumulative value w.r.t Base model) is as shown below:

Table 7.2: Rear upright mass saving

Iteration	Model	Mass (kg)			
		Value	Saving	Cumulative Saving	% Cumulative Saving
1	Base	1.25	-	-	-
2	Modified 1	1.02	0.23	0.23	18.4
3	Modified 2	0.73	0.29	0.52	41.6
4	Optimized	0.66	0.07	0.59	47.2

The summary of mass savings in both Front & Rear Upright as a result of optimization is as shown below:

Table 7.3: Suspension Uprights mass saving

Sr. No.	Component	Mass (kg)			
		Base model	Optimized model	Saving	% Saving
1	Front Upright	1.15	0.69	0.46	40.0
2	Rear Upright	1.25	0.66	0.59	47.2
	Total	2.40	1.35	1.05	43.75

7.4.2.3 Remarks

Mass saving of 1.05 kg has been achieved through topology optimization of the Front & Rear Uprights. This amounts to around 44% weight reduction over the base models. At the vehicle level, a mass saving of **2.1 kg** (symmetric uprights for left & right) has been achieved through suspension upright weight reduction.

7.5 CONCLUSION

Topology Optimization carried out on various components of TU FSAE 2014 vehicle like Front & Rear suspension Uprights and Chassis Bulkhead (with input loads calculated from MBD analysis) has resulted in significant weight savings.

- A 44% reduction in mass of front & rear suspension Uprights with respect to base design has been achieved, resulting in overall mass savings of around **2.1 kg** on vehicle level.
- A 38% reduction in mass of the Chassis Bulkhead with respect to base design has been achieved, resulting in mass saving of around **1.6 kg**.

Thus, an overall weight saving of **3.7 kg** was achieved at the vehicle level through topology optimization technique/process which is quite significant for the FSAE vehicle.

CHAPTER 8

STRUCTURE FABRICATION

The fabrication work of TU FSAE 2014 vehicle structure started with the emblem manufacture of Team Fateh as shown below:

Fig 8.1: Team Fateh Emblem Manufacture (Thapar University)

The fabrication of various components of TU FSAE 2014 Vehicle structure viz. Chassis, Bulkhead & Suspension Uprights is as explained below:

8.1 TU FSAE 2014 CHASSIS

The fabrication of the TU FSAE 2014 chassis has been carried out by preparing fixtures to aid in preparing the chassis structure as per design.

The chassis fabrication process started with cutting the pipes according to required dimensions from the procured raw material. The profiling of the pipe ends was then carried out to allow for proper welding of pipes. The pipes were then connected by proper tacking at the joint ends through arc welding to form the basic structure. Metal Inert Gas (MIG) welding was then carried out to complete the pipe connectivity process. The various snapshots of the Jigs & Chassis for TU FSAE 2014 vehicle are shown below:

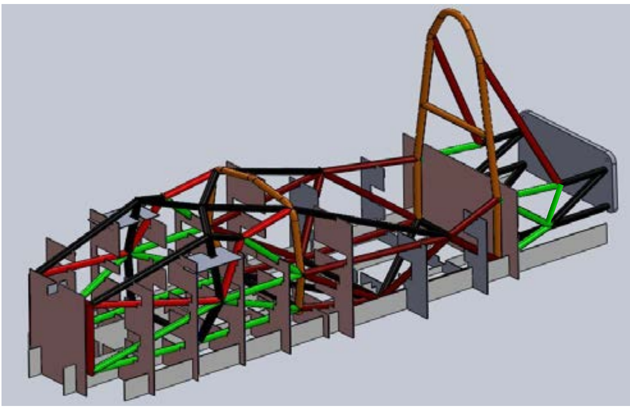

Fig 8.2: CAD model of Jigs

Fig 8.3: Fabricated model of Jigs

Fig 8.4: Front portion of TU FSAE 2014 Chassis supported on Jigs

Fig 8.5: Rear portion of TU FSAE 2014 Chassis supported on Jigs

TU FSAE 2014 Chassis Bulkhead

The manufacturing of the TU FSAE 2014 Chassis Bulkhead was carried out by the water jet cutting process followed by machining. The final machined component is shown below:

Fig 8.6: TU FSAE 2014 Chassis Bulkhead

Model Check: The Bulkhead was incorporated into the Chassis to make it a complete structure. The final structure was then checked for various dimensions (lengths & angles) to check for any deviation from the design.

Fig 8.7: Checking process in order to verify Chassis dimensions & angles

The completed front part of the TU FSAE 2014 Chassis and the Final structure including the Bulkhead is shown below:

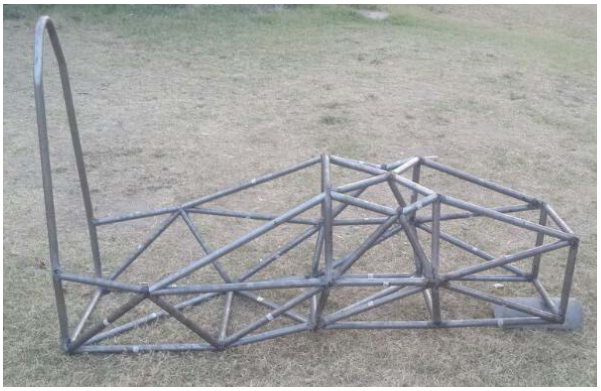

Fig 8.8: 2014 Chassis front part (completed) **Fig 8.9: Final completed 2014 Chassis with Bulkhead**

8.2 TU FSAE 2014 SUSPENSION UPRIGHTS

The manufacturing of the suspension uprights for TU FSAE 2014 vehicle has been carried out by preparing the billets. The billet is of cuboid shape with maximum dimensions (length, width & thickness) of the component (upright) plus a tolerance of 5 mm each side in order to account for manufacturing accuracy. The final machined components are shown below.

(a) Front Upright (b) Rear Upright

Fig 8.10: TU FSAE 2014 Suspension Uprights

8.3 TU FSAE 2014 FULL VEHICLE STRUCTURE

The TU FSAE 2014 Suspension & Chassis structure on wheels is shown as follows:

Fig 8.11: TU FSAE 2014 Suspension & Chassis structure (on wheels)

CHAPTER 9

CONCLUSION

The conclusion drawn from the Thesis project work carried out on TU 2011, 2012 & 2014 FSAE vehicle structures is presented below:

1. The MBD analysis (parallel wheel travel) of the Front & Rear suspension of TU FSAE 2012 & 2014 vehicles was carried out to calculate their respective roll centers.

   - The front roll center was observed to be lower than the rear roll center for both TU FSAE 2012 & 2014 vehicles. This is desired on the vehicle level as a whole for achieving the over steer characteristics for quick vehicle response & reduction in driver's effort during cornering.
   - The roll center movement due to vertical wheel travel is same for front and rear suspension of TU FSAE 2014 vehicle which is not the case in 2012 vehicle. Thus, the roll axis of 2014 vehicle is more stable than 2012 vehicle.
   - Further, the roll center variation with respect to vertical wheel travel of TU FSAE 2014 suspension was compared with that of 2012 suspension. Roll center movement was lesser in 2014 vehicle for both front & rear suspension resulting in better stability.

2. The FE analysis of TU FSAE 2011, 2012 & 2014 Chassis has been carried out for determining the chassis stiffness as well as normal modes.

   - The stiffness study shows that torsion, lateral & vertical bending stiffness & stiffness to weight ratio for TU FSAE 2014 chassis structure is significantly higher than that of 2011 & 2012 chassis structures.
   - Further, Torsion stiffness, being the most significant characteristic of FSAE chassis, has been analyzed at various sections along the length of the chassis and the same has been compared for 2011, 2012 & 2014 TU FSAE vehicles. It has been observed that the torsion stiffness of 2014 chassis is greater than that of 2011 & 2012 throughout the chassis length.

- The modal study shows the significant increase in natural frequency of first normal mode of 2014 chassis than that of 2011 & 2012 chassis reducing the possibility of resonance due to input excitations. Further, the torsion mode frequency in 2014 chassis has also been significantly improved over 2011 & 2012 chassis.

3. Topology Optimization carried out on various components of TU FSAE 2014 vehicle like Front & Rear suspension Uprights and Chassis Bulkhead (with input loads calculated from MBD analysis) has resulted in significant weight savings.

   - A 44% reduction in mass of front & rear suspension Uprights with respect to base design has been achieved, resulting in overall mass savings of around **2.1 kg** on vehicle level.
   - A 38% reduction in mass of the Chassis Bulkhead with respect to base design has been achieved, resulting in mass saving of around **1.6 kg**.

   Thus, an overall weight saving of **3.7 kg** was achieved at the vehicle level through topology optimization technique/process which is quite significant for the FSAE vehicle.

4. Finally, the Fabrication of the final design (Chassis, Bulkhead & Suspension Uprights) has been carried out and presented as part of TU FSAE 2014 vehicle structure development.

REFERENCES

[1] Edmund F. Gaffney III and Anthony R. Salinas, "***Introduction to Formula SAE® Suspension and Frame Design***", SAE Technical paper 971584.

[2] Lonny L. Thompson, Srikanth Raju and E. Harry Law, "***Design of a Winston Cup Chassis for Torsional Stiffness***", SAE Technical paper 983053.

[3] William B. Riley and Albert R. George, "***Design, Analysis and Testing of a Formula SAE Car Chassis***", SAE Technical paper 2002-01-3300.

[4] Badih A. Jawad and Brian D. Polega, "***Design of Formula SAE Suspension Components***", SAE Technical paper 2002-01-3308.

[5] Badih A. Jawad and Jason Baumann, "***Design of Formula SAE Suspension***", SAE Technical paper 2002-01-3310.

[6] Lucas V. Fornace, "***Weight Reduction Techniques Applied to Formula SAE Vehicle Design: An Investigation in Topology Optimization***", Master's Thesis Project, 2006, University of California, San Diego.

[7] R Andrew Jen Wong, "***Design and Optimization of Upright Assemblies for Formula SAE Racecar***", Bachelor's Thesis project, March 2007, University of Toronto, Canada.

[8] Derek Silsby and Francis Song, "***Optimization of Front Lower Arm***", Bachelor's Thesis project, August 2008, National University in Daegu, South Korea.

[9] Abrams, Ryan, "***Formula SAE Race Car Analysis: Simulation & Testing of the Engine as a Structural Member***", FISITA Technical paper F2008-SC-005, The University of Western Ontario, Canada.

[10] Lane Thomas Borg, "***An Approach to Using Finite Element Models to Predict Suspension Member Loads in a Formula SAE Vehicle***", Master's Thesis project, May 2009, Virginia Polytechnic Institute and State University, U.S.

[11] C. Ozturk, "***Design and Development of the URE06 Rear Suspension***", Internship Project Report, November 2009, Technical University Eindhoven, Netherlands.

[12] Anton Olason, Daniel Tidman, "***Methodology for Topology and Shape Optimization in the Design Process***", Master's Thesis Project, 2010, Chalmers University of Technology, Goteborg, Sweden.

[13] Jock Allen Farrington, "***Redesign of an FSAE Race Car's Steering and Suspension System***", Bachelor's Thesis Project, October 2011, University of Southern Queensland, Australia.

[14] Brendan. J. Waterman, "***Design and Construction of a Space-frame Chassis***", Master's Thesis Project, November 2011, The University of Western Australia.

[15] William Davis, Krysten Carney, Jonathan Leith, Anton Kirschner and David Piccioli, "***Design and Optimization of a Formula SAE Racecar***", Bachelor's Thesis Project, 2012, Worcester Polytechnic Institute, U.S.

[16] Liman Jiang, Guoquan Wang, Guoqing Gong and Ruiqian Zhang, "***Lightweight Design for a FSC Car based on Modal and Stiffness Analysis***", FISITA Technical paper F2012-E09-012.

[17] P.K. Ajeet Babu and M.R. Saraf, "***Design, Analysis and Testing of the primary structure of a race car for SUPRA SAEINDIA Competition***", SAE Technical paper 2012-0028-0016.

[18] Jacob I. Salter, "***Design, Analysis and Manufacture of 2011 REV Formula SAE Vehicle Chassis***", Master's Thesis Project, October 2012, The University of Western Australia.

[19] Syed Naveed Hasan, "***Design and Optimization of 2012 Formula SAE Chassis with Finite Element Analysis for CSULB***", Master's Thesis Project, December 2012, California State University, Long Beach, U.S.

[20] Liew Zhen Hui, "***Design, Analysis and Experimental Verification of Tubular Spaceframe Chassis for FSAE Application***", Master's Thesis Project, 2012, National University of Singapore.

[21] 2011 Formula SAE® rules, SAE International.

[22] 2012 Formula SAE® rules, SAE International.

[23] 2014 Formula SAE® rules, SAE International.

[24] Carroll Smith, "***Tune to Win: The art and science of racecar development and tuning***", Aero Publishers, Inc, Fallbrook, CA, USA, 1978, ISBN 0-87938-071-3.

[25] Thomas D. Gillespie, "***Fundamentals of Vehicle Dynamics***", SAE International, Warrendale, PA, Society of Automotive Engineers, 1992, ISBN 1-56091-199-9.

[26] W.F. Milliken and D.L. Milliken, "***Race Car Vehicle Dynamics***", Warrendale, Pennsylvania, Society of Automotive Engineers, 1995, ISBN 1-56091-526-9.

[27] Nitin S. Gokhale, "***Practical Finite Element Analysis***", Finite to Infinite, India, 2008, ISBN 978-81-906195-0-9.

[28] Altair Engineering Inc. Optistruct 11.0 Help & User Guide.

[29] MSC software documentation 2011 & User Guide.

[30] Formula Student Germany, www.formulastudent.de (12th February, 2014 at 05:30 pm).

[31] Formula Student India, www.formulastudent.in (25th April, 2014 at 11:30 am).

[32] Team Fateh, www.teamfateh.com (23rd March, 2014 at 02:10 pm).

ANNEXURE

TU FSAE CHASSIS 2014

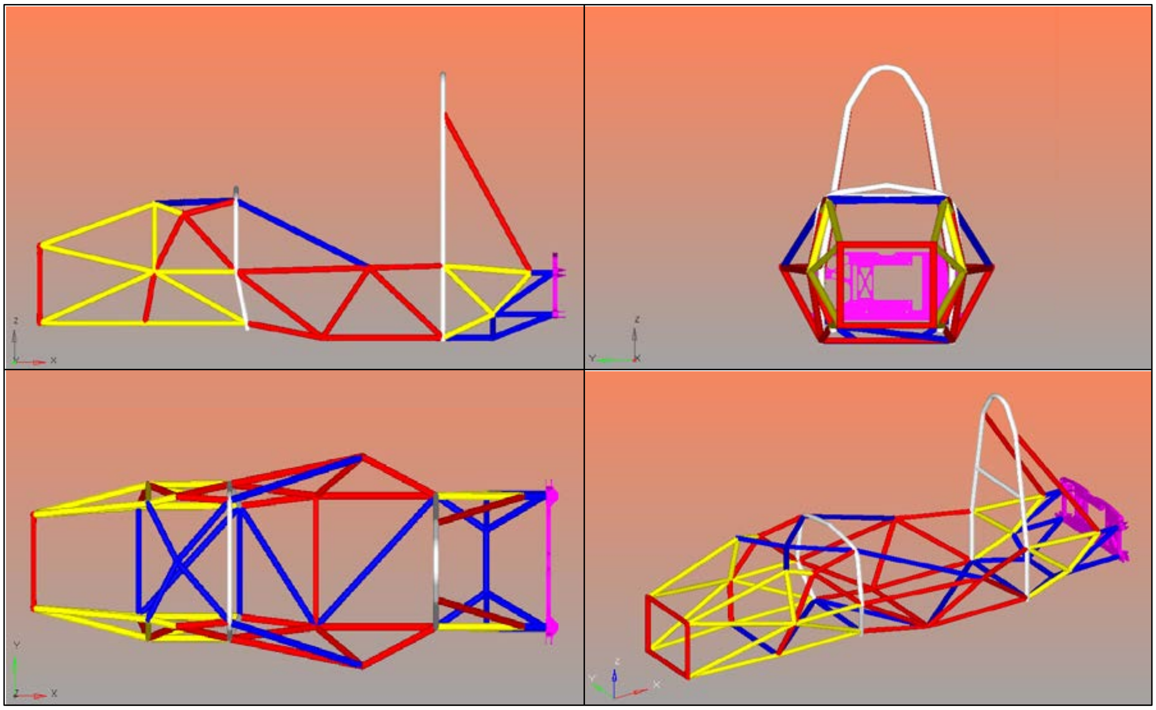

TU FSAE Chassis 2014 Views

TU FSAE 2014 FULL VEHICLE MODEL

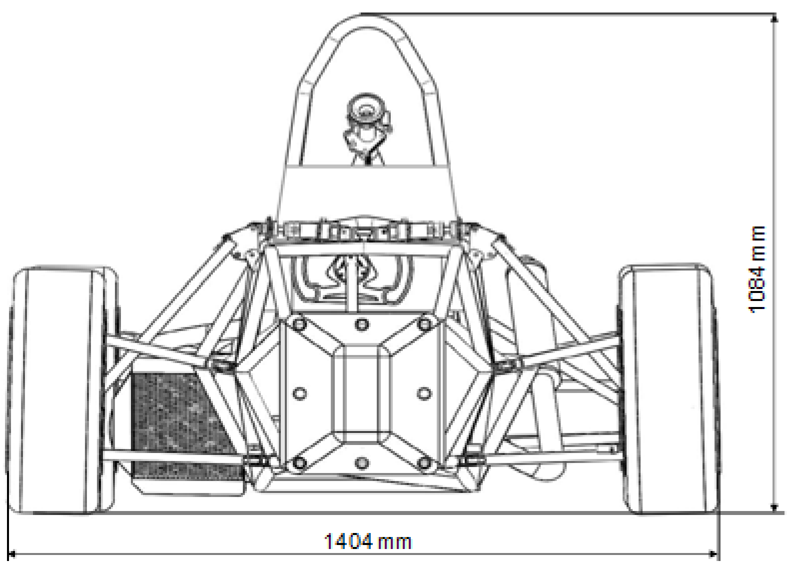

Front View

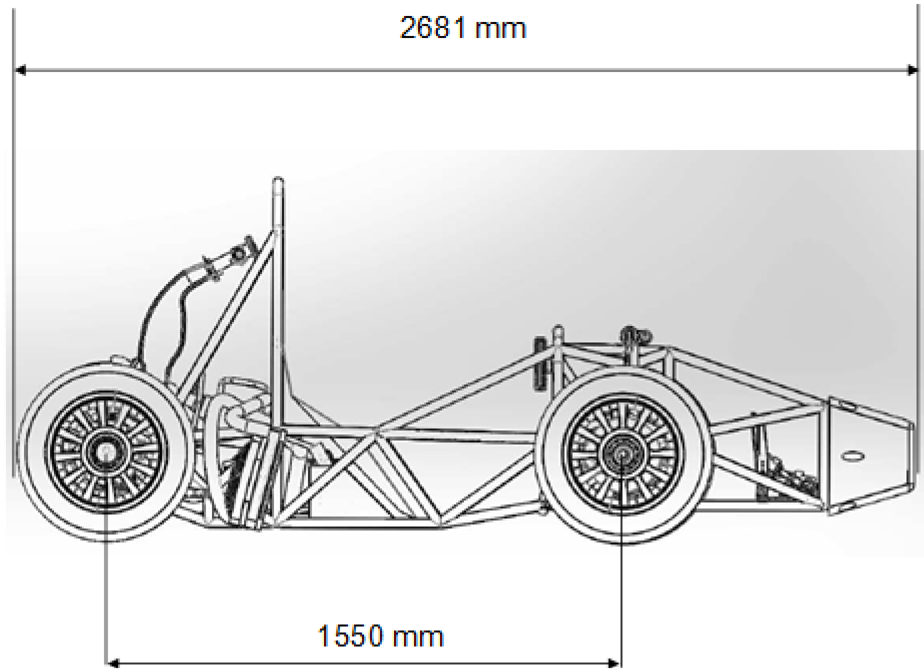

Side View

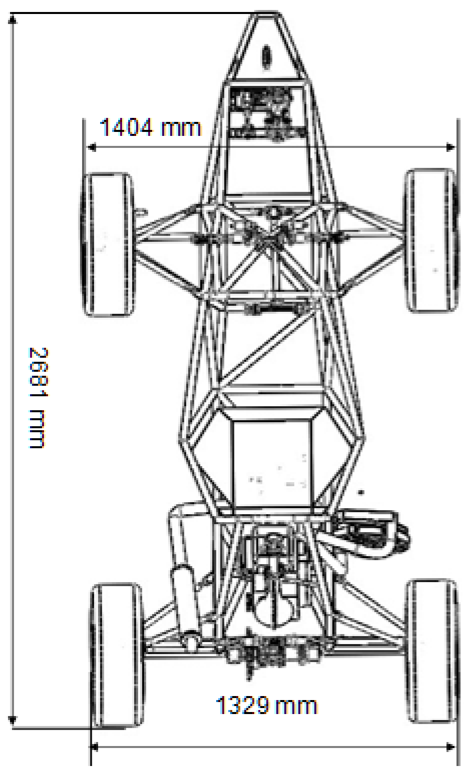

Top View

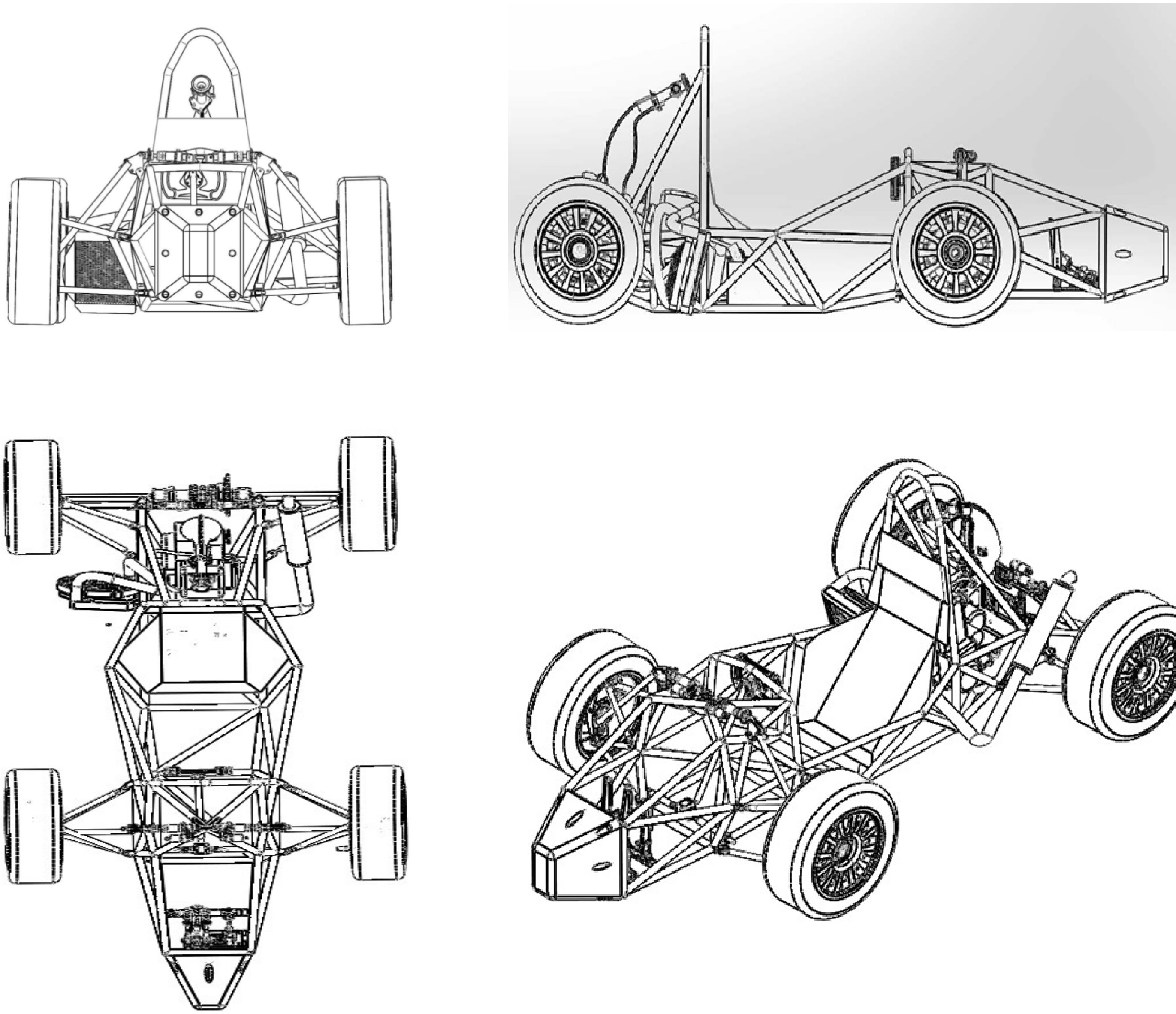

TU FSAE 2014 Full Vehicle Model Views